University of Stavanger

Faculty of Science and Technology

MASTER'S THESIS

Study program/ Specialization: Master of Science in Petroleum Engineering Reservoir Engineering	Spring semester, 2010 Open access
Writer: Dmitry Shchekotov	…… (Author's signature)
Faculty supervisor: Rune Wiggo Time Laboratory supervisor: Hermonja Andrianifaliana Rabenjafimanantsoa	
Title of thesis: Dynamics of multiphase dispersed systems in rotating annulus	
Credits (ECTS): 30	
Key words: multiphase dispersed system, rotating annulus, fluid dynamics	Pages: …… + enclosure: …… Stavanger, …….. Date/year

Dynamics of Multiphase Dispersed Systems in Rotating Annulus

By: Dmitry Shchekotov
Petroleum Engineering
Reservoir Engineering

University of Stavanger
Faculty of Science and Technology
2010

Acknowledgements

This project has been performed at the two-phase flow laboratory, University of Stavanger, Norway.

I would like to thank my supervisor, Rune Wiggo Time, for providing interesting subject. I am grateful for his guidance and support, for providing valuable background information, for advice and explanations, for patience throughout the duration of this project enabled me to develop an understanding of the subject. I also would like to thank Rune Wiggo Time for meetings where every student presented his own project and progress in investigation. It was a great opportunity to learn new information, and know about projects which other students were doing.

I owe my deepest gratitude to my laboratory supervisor Hermonja Andrianifaliana Rabenjafimanantsoa. While working towards this thesis I got valuable help from Benja with experimental setup, laboratory instruments and reagents, coordination and making new contacts with UiS staff. He provided nice environment conditions at the laboratory to improve my work efficiency. He was interested in thesis progress and gave advice how to do things better. He shared his experience how to write thesis, what software to use for solving problems. I also would like to thank Hermonja Andrianifaliana Rabenjafimanantsoa for literature he provided to learn more about investigated subject.

I would like to thank Udo Zimmermann and Ola Risvik for help with particle investigation.

I am heartily thankful to Sivert Bakken Drangeid, Kim André Nesse Vorland, Inger Johanne Munthe-Kaas Olsen and Svein Myhren for help with laboratory equipment and chemicals.

I would like to thank Barbara Maria Wrobel for help with software operating.

Lastly, I offer my regards and blessings to my friends who have done experiments and written their project in the same laboratory. Barbro Ramstad, Marit Irene Anti, Nils Oskar Berg Njå, Petter Andre Strømme thank you for your help and making a good, positive environment in the laboratory.

Dmitry Shchekotov

Abstract

An investigation of multiphase dispersed system dynamics in rotating annulus is described. The investigation was based on measuring rheological constant (viscosity) of two-phase flowing system. The flow was obtained between two cylinders of the Couette viscometer OFITE Model 900 with rotating outer cylinder. Rheological constant was measured at 20^0 C for different dispersed systems with liquid continuous phase and liquid/solid dispersed phase: water – oil Marcol 82, diluted alcohol – oil Bayol 35, glycerol – glass beads, salt water – glass beads. Optimal properties of liquids (density, viscosity, surface tension) and particles (size, shape, density) were obtained during investigation. Dispersed systems studied were different and had different viscosities. At least three measurement repetitions were done for each dispersed system and five viscosity/shear stress points have been taken per each RPM. Using Matlab software the program was written to analyse experimental data and obtain average value of viscosity/shear stress for each RPM. The less range in viscosity measurement for every dispersed system studied was observed at 600 RPM. The viscosities measured in the experiments have been compared to different viscosity models of dispersed system: Einstein, Batchelor, Frankel and Acirvos, Chong, Kitano, Mooney, Krieger and Dougherty.

List of figures

List of tables

TABLE OF CONTENTS

1 INTRODUCTION

Dispersed systems are heterogeneous systems containing two or more phases with strong interface. One phase usually forms a continuous dispersed medium; another one (or several) is suspended in the dispersed medium as solid particles, droplets or bubbles, that is dispersed phase.

There are many areas in science, technology and nature where dispersed systems present. For instance: oil which contains dispersed asphaltenes or paraffin particles; rocks, soils, plant and animal tissues; high-technical materials (filled plastics, composite materials) with an extremely high strength, drilling fluids. Dispersed materials and their mixtures can be used for different mechanical purposes, such as mixing, pressing, transportation through pipelines, batching. It can also be affected by prolonged static loads and high surge loads. Emulsions are used in food, pharmaceutical, cosmetics, and chemical industries, oil industry. That is why, it is important to have knowledge about rheological properties of the dispersed system [1].

Rheology is the science of deformation and flow of matter. It describes mainly the material properties of fluid and semi-solid materials. Rheology determines the measure (rheological constants) of material properties and defines would the material be a solid, liquid, paste or something else. In other words, it finds out the law which fits for all materials affected by a simple force, which is deformation. Rheology of dispersed systems is the study of a narrow class of materials – dispersed systems. In this paper the investigation of dispersed systems with a liquid medium (suspensions and emulsions) is represented.

Rheological properties of a dispersed system depend on the composition of a dispersed medium and characteristics of a dispersed phase, a lifetime of the system, a method of its preparation and a background. Rheological constants of a dispersed medium give an insight about fundamental properties of dispersed particles, about a size of the forces between particles, and a structure of the system [2].

Using Couette viscometer it is possible to learn more about rheological properties of dispersed system and observe the behaviour of multiphase mixture in rotating annulus. That is why it is important to investigate the dynamics of multiphase dispersed systems in the rotating annulus to find out how it affects on dispersed system properties.

1.1 Objectives of the project

The objective of this project is to investigate the dynamics of multiphase dispersed system in rotating annulus, to study rheology of the dispersed system and provide viscosity models that can be used for estimating viscosity of dispersed system.

The project is prepared to give an understanding of dispersed system, rheology, viscometry, fluid dynamics. Different methods and instruments have been used during the investigation for measuring rheology, physical properties of fluids and solids represented in the thesis. The different parts discussed in this paper are dispersed systems, rheology of the dispersed systems and dynamics of fluids, experiments, results and discussion.

Chapter 2 gives an introduction to dispersed systems, their types and characteristics. It describes fundamental rheology laws, different viscosity models and studies have been done before. The chapter includes information about forces which present in dispersed system and equations to

evaluate them. The principle of viscometry and description of the Couette viscometer are also included in this chapter.

Experimental methods, materials and equipment are represented in Chapter 3. It includes descriptions of measuring instruments, operation principles, and procedure of the experiments and characteristics of the materials which have been used in investigation.

Chapter 4 contains results obtained in the experiments and discussion. Results were compared to viscosity correlations discussed in Chapter 2.

Conclusion and recommendation are represented in Chapter 5.

Additional data are attached in Appendixes. Appendix A contains size distributions of particles tested during experiments. Glycerol and water mixture properties are represented in Appendix B. Rheological constants measured in the experiments are shown in Appendix C. Matlab script used for analyzing the experimental data is written in Appendix D.

Video and photos of experiments are available on CD attached to the project.

2 DISPERSED SYSTEMS: RHEOLOGY AND FLUID DYNAMICS

2.1 Characteristics of dispersed system

The main characteristic of the dispersed system is the dispersion, *D*, or specific surface *S*. The dispersion is inversely proportional to a cross-sectional dimension of a particle and it is determined as

$$D = \frac{1}{a}, \tag{2.1}$$

where *a* is the cross-sectional dimension (*a* is a diameter for a spherical particle, and *a* is an edge length for a cubic particle).

The cross-sectional dimension, *a*, is used only for spherical and cubic particles. If the shape of a particle is different from the sphere, the size of the particle depends on measured direction. To simplify calculations sometimes the particle shape is assumed to be spherical.

The specific surface is a quantity which measures the phase interface per unit volume or mass of dispersed phase. The specific surface of a dispersed system is determined as [3]

$$S = \frac{S_{1,2}}{V} = \frac{S_{1,2}}{m}, \tag{2.2}$$

where $S_{1,2}$ is the interface between phase 1 and phase 2 (phase interface),

V is the total volume of a dispersed phase,

$m = V \cdot \rho$ is the total mass of a dispersed phase,

ρ is the density of a dispersed phase material.

Since particles are uniform spheres this ratio equals

$$S = \frac{S_{1,2}}{\rho \cdot V} = \frac{4 \cdot \pi \cdot r^2}{\rho \cdot \frac{4}{3} \cdot \pi \cdot r^3} = \frac{6}{\rho \cdot d},$$

where *r* is the radius of a sphere,

d is the diameter of a sphere,

$p = 6$ is the shape factor for a spherical particle.

2.1.1 Polydispersity

The dispersed phase of a dispersed system is usually represented by particles of different size. This dispersed system is called polydisperse system. There are rare cases in which the distribution of dimensions is of negligible width. Dispersed systems with the particles of the same size are called monodisperse systems and can be made in special conditions. To describe a polydisperse system a statistical approach is required.

Having measured diameters of polydisperse spherical particles it is necessary to present the system in terms of the measured data. Statistical approach is valid if a fairly large number of observations are provided; therefore it is convenient to tabulate the measurements. The table should include classification of the data. Classification represents sorting of the observed quantities into 10 categories called classes. At least 10 categories results are required to describe the system without a loss of details. The frequency distribution of the sample is the number of particles in each class. The Table 3.3 shows the class range, midpoint of the interval, number of particles, fraction based on the sample of 475 particles.

Usually a frequency distribution is graphically represented by the histogram, a bar graph in which the class ranges are plotted as the abscissa and the number of particles in the class is proportional to the height of the bar [3].

2.1.2 Sedimentation

Consider the gravitational forces which act on a particle of volume, *V*, and density, ρ_2, which is submerged in a fluid of density, ρ_1. This situation is represented in Figure 2.1.

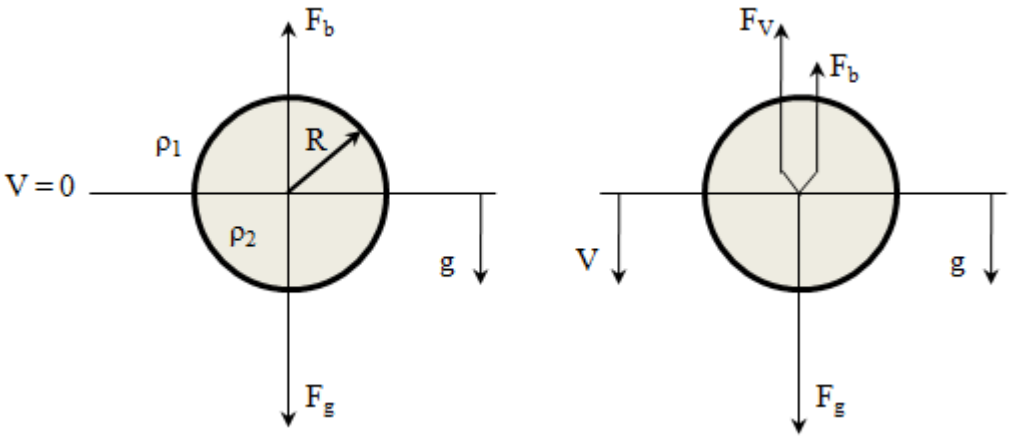

Figure 2.1 *The forces acting on a spherical particle due to (a) gravity alone and (b) gravity and the viscosity of the medium ($\rho_2 > \rho_1$) [3]*

Assume the gravity force, F_g, is operating on the particle in the downwards direction and it is positive. The buoyant force, F_b, acts in the contrary direction. Difference between these forces results in the acceleration of the particle gives a net force:

$$F_{net} = F_g - F_b = V \cdot (\rho_2 - \rho_1) \cdot g \,. \tag{2.3}$$

The sedimentation occurs when the net force, F_{net}, has the same sign as gravity g, i.e. $\rho_2 > \rho_1$, and this force pulls the particle downward. If $\rho_2 < \rho_1$, the particles move upward and this process is called “creaming”. Increasing in the particle net velocity leads to increasing in the viscous force, F_v, which opposes particle motion. If the particle is in balance by the forces acting on it, the acceleration is equal to zero, and the stationary state velocity is achieved. For small velocities under stationary conditions the force of resistance is proportional to the stationary state velocity υ:

$$F_V = f \cdot \upsilon \,, \tag{2.4}$$

where f is the proportionally constant, or friction factor.

This Eq. (**2.4**) fits for any particle geometry. For the sedimentation process the stationary state velocity is positive and for the creaming it is negative.

Taking into account the stationary state conditions and the net force of gravity equals to the viscous force, Eq. (**2.3**) and Eq. (**2.4**) can be equated to give

$$V \cdot (\rho_2 - \rho_1) \cdot g = f \cdot \upsilon . \tag{2.5}$$

This equation can be rewritten as

$$m \cdot \left(1 - \frac{\rho_1}{\rho_2}\right) \cdot g = f \cdot \upsilon , \tag{2.6}$$

where $m = V \cdot \rho_2$ is the mass of the particle.

Following features can be listed for this equation [3]:

1. It is independent of the particle size.

2. It assumes that the bulk density of the pure components applies to the settling units (i.e., no salvation).

3. It permits the evaluation of υ for a situation in which $\frac{m}{f}$ is known.

4. It permits the evaluation of $\frac{m}{f}$ in a situation where υ is known.

For some systems the stationary sedimentation velocity of a particle is an experimentally accessible number. The $\frac{m}{f}$ value is small for low velocity.

According to Eq. (**2.5**) the sedimentation velocity increases if the density difference between the particle and the medium increases. Then sedimentation velocity will decrease if the density of the settling unit will be closer to that of the solvent. The mass of dispersed material is unaffected by the salvation and that is why the reduced sedimentation velocity can be explained by increasing in the value of the fraction factor.

2.2 Fundamental rheology laws

Consider a parallelepiped which is deformed by the tangent force, *F*, to determine the shear stress. The force is acting on the upper face of the parallelepiped with the area, *S*, and the lower face is fixed. Choose a block inside the parallelepiped with faces paralleled to the XY-plane. Schematically this situation is represented in Figure 2.2.

The deformation, γ, of the parallelepiped or any block inside the parallelepiped can be determined as

$$\gamma = \frac{l}{L} = \frac{dx}{dz}. \tag{2.7}$$

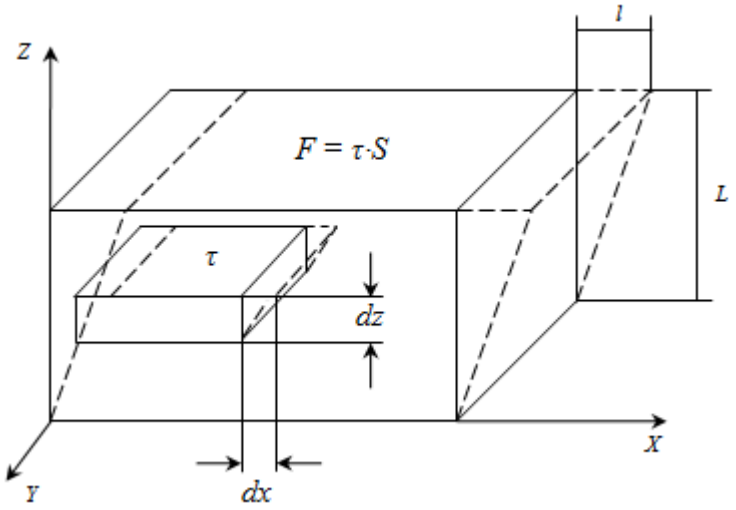

Figure 2.2 *Simple shear [4]*

Consequently, the shear stress, τ, is constant in the parallelepiped at any plane which is parallel to the XY-plane and defined as

$$\tau = \frac{F}{S}. \tag{2.8}$$

The rate of shear, $\dot{\gamma}$, for this case is determined as

$$\dot{\gamma} = \frac{d\gamma}{dt}. \tag{2.9}$$

Rewrite previous expression in form

$$\dot{\gamma} = \frac{d}{dz} \cdot \left(\frac{dx}{dt} \right) = \frac{du}{dz}, \tag{2.10}$$

where u is the flow rate.

The shear stress, τ, is proportional to the shear rate, $\dot{\gamma}$, for liquids and the Newton's law is written as [4]

$$\tau = \eta \cdot \dot{\gamma}, \tag{2.11}$$

where η is the viscosity of liquid.

Combining Eq. (**2.8**) and Eq. (**2.11**) obtain following

$$\frac{F}{S} = \eta \cdot \dot{\gamma}. \tag{2.12}$$

Note that $\frac{du}{dz}$ has units time^{-1}. Dimension form of Eq. (**2.12**) is defined as

mass length time^{-2} = η time^{-1}.

Consequently, the viscosity, η, has dimensions mass length^{-1} time^{-1}, or in SI units kg m^{-1} s^{-1}. Also viscosity can be expressed in the poise, P (10 P = 1 kg m^{-1} s^{-1}) [3].

Multiply the left-hand side (LHS) of the Eq. (**2.12**) by $\frac{d}{dz}\cdot\left(\frac{dx}{dt}\right)$ and right-hand side (RHS) by $\dot{\gamma}$ which are equal, according to Eq. (**2.10**), and write it as

$$\frac{d}{A\cdot dz}\cdot\left(\frac{F\cdot dx}{dt}\right)=\eta\cdot\dot{\gamma}^2, \tag{2.13}$$

where a force times an increment of distance $F\cdot dx$ equals an increment of energy dE,

an area times an increment of distance $A\cdot dz$ equals an increment of volume dV,

the $\frac{dE}{dV}$ quantity measures the energy dissipated per unit volume, by assuming the force measures viscous resistance to flow,

the $\frac{dE}{dV\cdot dt}$ gives the rate of energy dissipation per unit volume.

Consequently, Eq. (**2.13**) shows that the volume rate of energy dissipation is proportional to the square of the velocity gradient with the viscosity of the fluid as the factor of proportionality and can be written as equation [3]

$$\dot{q}=\eta\cdot\dot{\gamma}^2, \tag{2.14}$$

where $\dot{q}$ is the volume rate of energy dissipation.

Eq. (**2.11**) and Eq. (**2.14**) equivalently define the viscosity of a fluid.

2.3 Emulsions

Emulsions are colloidal dispersions in which two immiscible liquids constitute the dispersed and continuous phases. One of the liquids is usually water, and amphipatic molecules are often present as emulsifying agents, components which impart some degree of durability to the preparation [3].

The formation and stability of emulsions:

- Most emulsions are formed as a result of a complex process in which large blobs of the dispersed phase are eventually ground down to small drops. Basically process consists of drops becoming elongated under shearing forces, necking, and finally separating into smaller drops. Adsorption of amphipatic molecules leads to lowering the interfacial tension and increase in the interfacial viscosity.
- When the individual drops are coming together an emulsion “is breaking”. If water is the continuous phase and the emulsifier is ionic, then it is the ion atmospheres of the approaching particles that make the first contact.
- The droplets might coalesce into a single geometrical unit, if they can aggregate into a single kinetic unit. The thin film of a continuous phase ruptures and it causes droplets separation in an aggregate. Surface tension and surface viscosity are certainly pertinent to the coalescence process [3].

Their size and distribution of droplets are the most important parameters that affect stability, rheology, chemical reactivity, and physiological efficiency of any emulsion. Monodisperse emulsions have the improved stability and facilitated control of their properties and therefore received a great deal of attention [5].

2.4 Suspensions

Suspensions are dispersed systems consisting of a fluid and solid particles which represent dispersed medium and dispersed phase, respectively. For many years the rheology of suspensions has been the subject of serious research. It is related to a wide range of industrial applications. Cement, paint, printing inks, coal slurries, drilling muds and many proprietory products like medicines, liquid abrasive cleaners and foodstuffs represent suspensions.

The general plot viscosity against shear rate for all suspensions is represented schematically in Figure 2.3. At low shear rate the first Newtonian plateau is followed by the region which is governed by power-law shear-thinning and then by a flattening-out to the upper (second) Newtonian plateau. Viscosity of solid particle suspensions can be increased at some point, usually in this upper Newtonian region, given the appropriate conditions. There are situations when the first Newtonian plateau is so high and cannot be measured. In such cases an apparent yield stress often describes the low-shear rate behaviour [6].

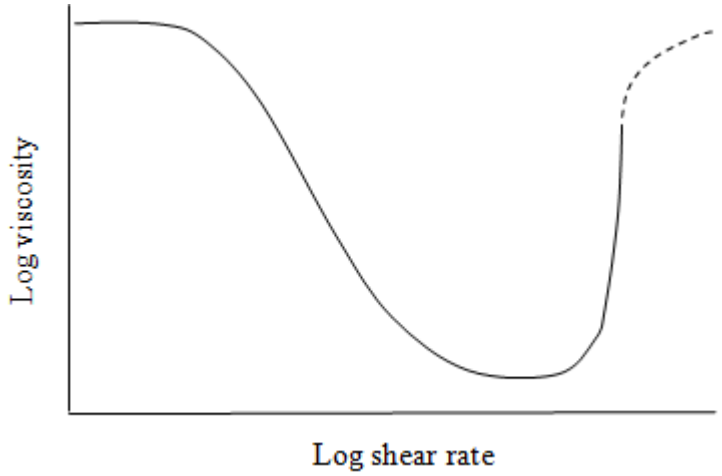

Figure 2.3 *Schematic plot of the flow curve of a concentrated suspension [6]*

Consider the factor controlling the details of the general flow curve. The fraction of space of the total suspension that is occupied by the suspended material is the relevant measure of the amount of material suspended in the liquid and it is called the phase volume φ. Phase volume is determined as volume-per-volume fraction, and not the weight-per-weight fraction that is often used to obtain concentration. The fact that rheology depends to a great extent on the hydrodynamic forces acting on the surface of particles or particle aggregates, generally irrespective of the particle density, makes phase volume so important. Phase volume is defined as [6]

$$\varphi = \frac{V_{d.p.}}{V_s}, \tag{2.15}$$

where $V_{d.p.}$ is the volume of dispersed phase,

V_s is the volume of suspension.

2.5 Forces in suspension

There are three kinds of forces in flowing suspensions. All of them coexist to various degrees. First, there are forces of colloidal origin that arise from interactions between the particles. The fluid properties, for instance, polarisability, but not viscosity, control these. An overall repulsion or attraction between the particles is caused by these forces. Repulsion is caused by electrostatic charges or entropic repulsion of polymeric or surfactant material present on the particle surfaces. London-van der Waals attraction between the particles leads to attraction arises. It also emerges from electrostatic attraction between unlike charges on deferent parts of the particle (e.g. edge/face attraction between clay particles). The particles tend to flocculate if the total force is an attraction, and they remain separate (i.e. dispersed or deflocculated) when overall repulsion prevails [6].

Flocculation is the process whereby small particles clump together like a bunch of grapes (a floc) but do not fuse into a new particle. In flocculation the surface is not reduced, although certain surface site is sometimes blocked at the points, where the smaller particles touch [3].

The rate of decrease of each colloidal force is different from the surface of the particle. That is why it is quite difficult to estimate the overall result of the combination of a number of these forces acting together. The single and combined forces are represented in Figure 2.4.

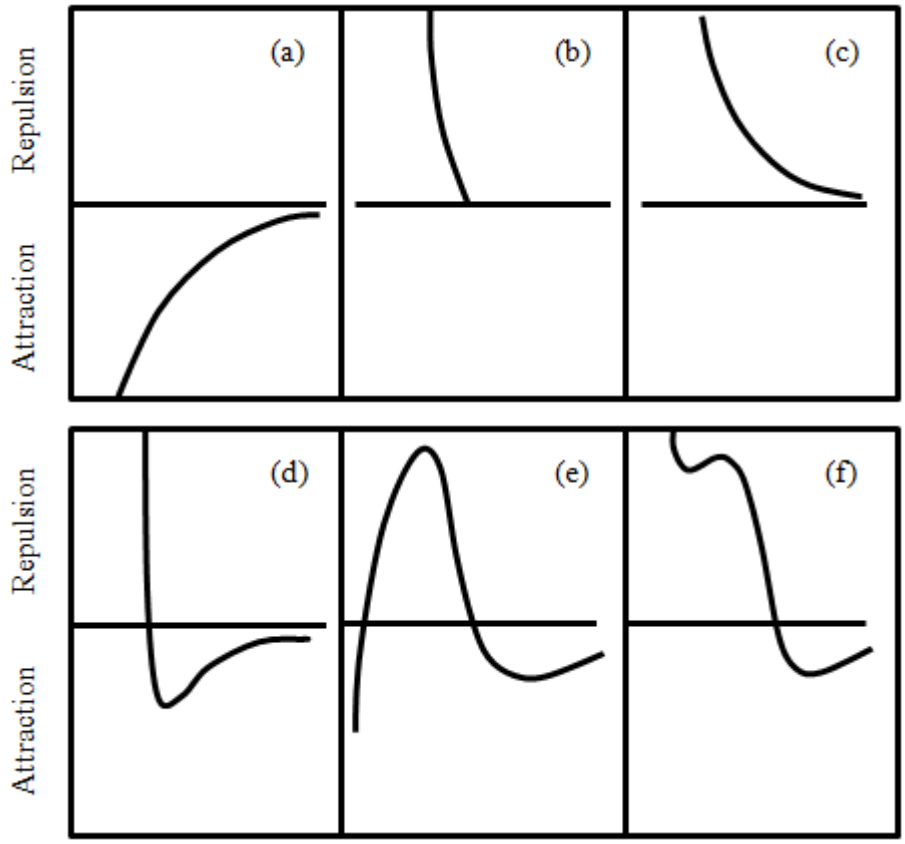

Figure 2.4 *Examples of the typical interaction forces between a pair of sub-micron particles: (a) van der Waals attraction (omnipresent); (b) Steric repulsion due to adsorbed macromolecules; (c) Electrostatic repulsion due to the presence of like charges on the particles and a dielectric medium; (d) A combination of (a) and (b); (e) A combination of (a) and (c); (f) A combination of (a), (b) and (c) [6]*

Secondly, the Brownian (thermal) randomizing force must be taken into account. The form of the radial distribution function, for particles of all shapes, is affected by this constant randomization (i.e. observation of the spatial arrangement of particles from the centre of any one

particle), whereas spatial orientation for non-spherical particles, is also being randomized. The Brownian force is strongly size-dependent and it ensures that the particles are in constant movement and any description of the spatial distribution of the particles is a time average. The Brownian randomizing force can be neglected for particle size more than 5 μm.

Thirdly, the viscous forces acting on the particles must be considered. There is a local velocity difference between the particle and the surrounding fluid. The viscous forces are proportional to this local velocity difference. Hence these affect the viscosity of the continuous phase which then scales all such interactions and consequently the suspension viscosity. For this reason, "suspension viscosity" is usually defined as the viscosity relative to that of the continuous phase [6].

2.5.1 Attractive forces

The general force between two particles in any suspension medium is London-van der Waals attraction. It is compared to van der Waals forces which act on a real gas to condensate it and form a liquid.

The attraction between two molecules, for instance water, which have a permanent dipole moment, is quite strong because the dipoles tend to align themselves, on average. More time is spent on orientations of molecules which are attractive rather than those which are repulsive. The free energy of the system decreases as a consequent. Molecules without permanent dipole are able to attract one another due to London dispersion interaction. This happens when a temporary dipole, produced by distribution of the fluctuating electron around one atom or molecule, induces a dipole in a neighbouring atom or molecule. The induced dipole is always directed such that the two atoms attract one another.

For example, an atom of argon has a perfectly symmetric electronic charge distribution around the central nucleus, when average over time. Nevertheless, on a short timescale, the electron motions produce a temporary dipole which fluctuates in magnitude and direction at frequencies of the order of optical frequencies (10^{14} s^{-1}). The field generated by that dipole can affect the electrons in a neighbouring atom so that they tend to fluctuate to some extent in unison with one another. Since the dipoles are aligned in the same direction, they attract one another [7]. Two atoms of argon are schematically represented in Figure 2.5.

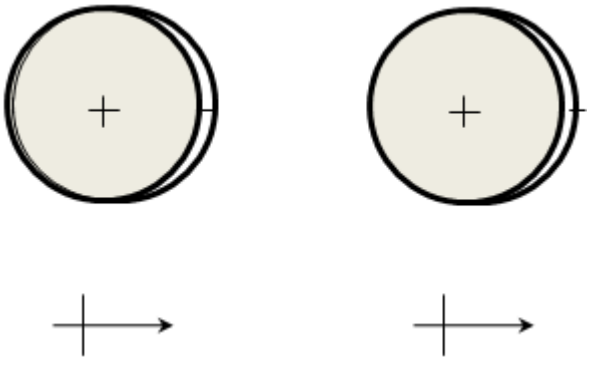

Figure 2.5 *Electronic charge distribution, dipole effect [7]*

The range of the force is very small (the order of nanometre or less) when this process occurs between two atoms or molecules. But when two colloidal particles are close to each other the atoms of one particle are on a distance able to interact with all of the atoms in the other particle and these effects are to some degree additive. The very important consequence of this partial additivity is that the force tends to be able to affect on a much longer distance. The name of this

force is “long-range van der Waals force” or Hamaker force. It is called after the theoretician who first investigated it.

2.5.2 Attraction between two colloidal particles

To determine the equations for the van der Waals forces between particles Hamaker used the additivity concept proposed by London. According to the additivity concept the force can be calculated based on the interaction between individual atoms making up the particles. The non-retarded energy of interaction between two particles of volumes V_1 and V_2 containing q_1 and q_2 atoms per cm^3 is written as [7]

$$E = -\int_{V_1} dV_1 \int_{V_2} \frac{q_1 \cdot q_2 \cdot \lambda_{1,2}}{H^6} dV_2 \,, \tag{2.16}$$

where $\lambda_{1,2}$ is the London's constant, whose value depends on the atomic numbers of the two interacting atoms,

H is the distance between two particles.

The van der Waals force can be determined as

$$F_{VDW} = \frac{\partial E}{\partial H}. \tag{2.17}$$

Combine Eq. (**2.16**) and Eq. (**2.17**) to determine the van der Waals force for two spheres of radii R_1 and R_2

$$F_{VDW} = \frac{A \cdot R}{12 \cdot H^2}, \tag{2.18}$$

where R is the reduced radius and defined as

$$R = \frac{2 \cdot R_1 \cdot R_2}{R_1 + R_2}. \tag{2.19}$$

And A is the Hamaker’s coefficient (or constant) and defined as

$$A = \pi^2 \cdot q_1 \cdot q_2 \cdot \lambda_{1,2}. \tag{2.20}$$

Eq. (**2.20**) was obtained for particles immersed in a vacuum. But if the particles are immersed in a medium like water, by using a general thermodynamic argument, it is necessary to replace A for the solid by a new value which reflects properties of both the solid and the dispersion medium. The dispersed medium reduces the magnitude of the attraction but do not affect the distance dependence. Assume that a particle of substance 1 interacts with a particle of substance 2 through a medium 3. The Hamaker’s coefficient for this situation is approximately equals to [7]

$$A_{123} \approx \left(A_{11}^{1/2} - A_{33}^{1/2}\right) \cdot \left(A_{22}^{1/2} - A_{33}^{1/2}\right), \tag{2.21}$$

where, for instance, subscript 11 refers to two particles of substance 1 interacting through a vacuum.

The A value is positive for particles interacting across a medium.

The potential energy of interaction between a sphere of radius R_1 and a sphere of radius R_2 with a centre-to-centre distance ($H = R_1 + R_2$) and in the limit when $H << R$ is integrated as

$$V_A(H) = -\frac{A_{12} \cdot R}{12 \cdot H} \cdot \left[1 + \frac{H}{R} \cdot \left(1 - \frac{R}{2 \cdot (R_1 + R_2)} \right) + 2 \cdot \frac{H}{R} \cdot \ln\left(\frac{H}{R} \right) + ... \right]. \quad (2.22)$$

This equation can be simplified for two equal spheres separated by a small distance in a form

$$V_A(H) = -\frac{A \cdot R}{12 \cdot H}. \quad (2.23)$$

2.6 Particle structures

Structuring depends on potential energy of interaction between particles. The relation between repulsion and attraction forces determines the structure and properties of dispersed system [6].

Rheological properties of a dispersed system depend on particle movement, which determined by particle concentration, shape of particles and attraction between particles. In shear flow neighbour layers of liquid with particles move with different velocities υ_1 and υ_2 toward each other. This situation is schematically represented in Figure 2.6.

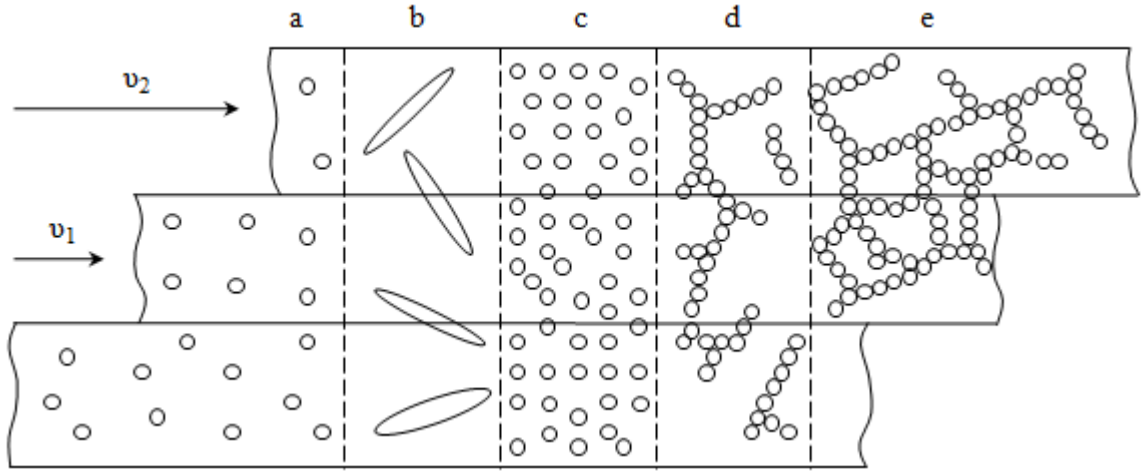

Figure 2.6 *Flow of different structures [1]*

At low volume fraction spherical particles move with the same velocity as the flow layer where they are distributed. There is no influence of this layer on slip and particle transport in neighbour layers (Figure 2.6, a). Particles with oblong shape penetrate to a neighbour layers and cling to the particles within these layers. Average velocity of such particles is different from velocity of the flow layer where they are dispersed (Figure 2.6, b).

The velocity difference causes more friction which is determined as

$$\tau = n_1 \cdot b_1 \cdot \eta_0 \cdot \Delta\upsilon, \quad (2.24)$$

where n_1 is the number of particles in the flow layer,

b_1 is the friction factor of particle,

η_0 is the viscosity of dispersed medium,

$\Delta\upsilon$ is the velocity difference.

The friction factor of spherical particle can be defined as

$$b_1 = 6 \cdot \pi \cdot \eta_0 \cdot a, \tag{2.25}$$

where *a* is the radius of a spherical particle.

At high volume fraction (Figure 2.6, c) there is interaction between particles of neighbour layers and therefore friction between layers is increased.

If particles have tendency to adhere to each other the aggregates (flocs) appear even at low volume fraction (Figure 2.6, d). The effect of flocs on a dispersed system is similar to the effect of oblong particles. However, the friction coefficient, b_1, changes (decreases) when the aggregates are disrupted due to aggregates collision and penetration in neighbour layers. It causes non-proportional dependence of shear stress and shear rate and consequently, leads to non-Newtonian properties of dispersed system appearing. High friction between layers creates a skeleton of particles, which are adhered to each other (Figure 2.6, e). At low shear rate the skeleton can prevent flow layers to move. Only when shear rate is high enough to destroy the skeleton the layer movement is possible. Hence, rheological properties mostly depend on attraction (adhering) between particles, which prevents free particle transport.

2.7 Wall effects

The local microstructure changes when a structured liquid is placed next to the wall and it causes difficulties arise in smooth-walled viscometers. The spatial concentration of particles deep in the bulk of the sample, well away from the wall, is random for a simple suspension of smooth spherical particles. However, right at the wall, the concentration of particles is equal to zero. It means there is rapidly rising of concentration as one moves away from the wall (see Figure 2.7). It takes about five particles diameters for this whole process from zero to average concentration. The consequence is that the material close to the wall is essentially different from the bulk, however worse than this is the effective lubricating layer near the wall where concentration of the particles is first zero, and is small even up to half a particle diameter. Wall depletion is the name of the phenomenon of lower concentration next to the wall, but it is popularly known as slip [6].

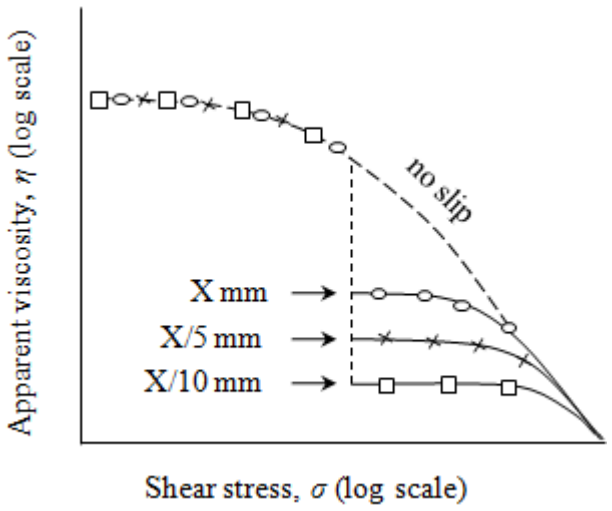

Figure 2.7 *Slip effect as a function of concentric-cylinder gap [6]*

The effect depends on size of particles, and here particle size for flocculated suspensions means floc size, which depends on shear-rate. Consequently, at low shear rate flocs are biggest, and therefore for flocculated systems where this problem is mostly seen, wall slip is a low shear rate phenomenon.

2.8 Viscosity models of dispersed system

The main problem of rheology is finding the relation between shear stress, τ, and shear rate, $\dot{\gamma}$. One of the solutions is based on the additive property of energy dissipation in different parts of the dispersed system. Energy dissipation is the work of the external force, τ, converted into heat, raising the temperature of a system, and the reason of friction appearing due to deformation. The relation between the energy dissipation and the shear rate is called a dissipation function. The dissipation function, $\dot{q}$, is defined as

$$\dot{q} = \eta \cdot \dot{\gamma}^2 . \tag{2.26}$$

This formula essentially represents the Newton's law. Using the dissipation function shear stress, τ, can be determined as [7]

$$\tau = \frac{\dot{q}}{\dot{\gamma}} = \eta \cdot \dot{\gamma} , \tag{2.27}$$

where η is the rheological constant (viscosity),

$\dot{\gamma}$ is the shear rate.

Knowing the expression for dissipation function Eq. (**2.27**), it is possible to determine the deformation law, because this relation defines the resistance of a fluid which is being deformed. This method is used in the Einstein model.

A large number of viscosity equations and correlations relating viscosity to dispersed phase volume fraction have been described in the literature. To determine the viscosity of a dispersed system it is necessary to obtain a number of factors [8]:

- Volume fraction of dispersed phase,
- Viscosity of the continuous phase,
- Shear rate (if non-Newtonian),
- Temperature,
- Average droplet (particle) size and size distribution,
- Viscosity of the dispersed phase (for liquids),
- Presence of solids in addition to dispersed liquid phase.

2.8.1 Einstein model

Consider dispersed system where interaction between particles is negligible. The rheological properties of this system are determined by behaviour of a single particle in the flow and energy dissipation can be found by summation of energy loss on all particles in the system. In shear flow a spherical particle is in translational motion with the velocity, v, which is equal to the velocity of liquid phase in the plane with the particle centre. The particle is shown in Figure 2.8.

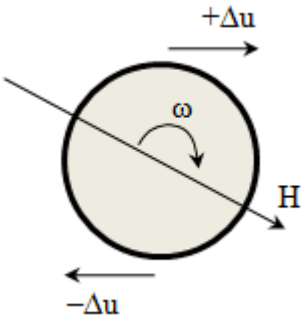

Figure 2.8 *Particle motion in a shear flow [1]*

Also the particle is in rotation with the approximate velocity $\frac{1}{2}\dot{\gamma}$. The reason is the flow velocity difference, $\pm\upsilon = \dot{\gamma}\cdot a$, in the planes which are on the distance from the particle center equals to its radius.

When the particle is in translational motion its centre is not moving towards the flow which is in the same plane as the particle centre. Energy attenuation is caused by only rotational motion due to friction between particle surfaces and dispersed medium. The particle of volume, *V*, which is rotating with rotational speed, ω, in the dispersed medium with the viscosity, η_0, is affected by the torque of friction forces determined as

$$M_{\omega} = p\cdot V\cdot\eta_0\cdot\omega, \tag{2.28}$$

where *p* is the shape factor of a particle.

The energy loss on the particle rotation is determined as

$$M_{\omega} = p\cdot V\cdot\eta_0\cdot\omega^2 \text{ or } \dot{q} = \frac{1}{4}\cdot p\cdot V\cdot\eta_0\cdot\gamma^2. \tag{2.29}$$

Set particle concentration, *n*, in suspension and define the energy dissipation for all particles as

$$\dot{q}_p = \frac{1}{4}\cdot p\cdot n\cdot V\cdot\eta_0\cdot\gamma^2 = \frac{1}{4}\cdot p\cdot\varphi\cdot\eta_0\cdot\gamma^2, \tag{2.30}$$

where $\varphi = n\cdot V$ is the volume fraction.

Energy dissipation in dispersed medium is equal to $\eta_0\cdot\dot{\gamma}^2$ and consequently total energy dissipation in suspension is determined as

$$\dot{q}_t = \eta_0\cdot\gamma^2 + \frac{1}{4}\cdot p\cdot V\cdot\eta_0\cdot\gamma^2. \tag{2.31}$$

Shear stress for the suspension is defined as

$$\tau = \frac{\dot{q}_t}{\dot{\gamma}} = \eta_0\cdot\left(1+\left(\frac{p}{4}\right)\cdot\varphi\right)\cdot\dot{\gamma}. \tag{2.32}$$

Determine the viscosity of suspension if the shape factor $p = 6$ for spherical particles as

$$\eta = \frac{\tau}{\dot{\gamma}} = \eta_0 \cdot (1 + 1.5 \cdot \varphi). \tag{2.33}$$

More precise solution was obtained by Einstein. He showed that single particles increased the viscosity of a liquid as a simple function of their phase volume, according to the formula

$$\eta = \eta_0 \cdot (1 + 2.5 \cdot \varphi), \tag{2.34}$$

where η is the viscosity of a suspension,

η_o is the viscosity of a suspending medium.

From Eq. (**2.34**) the viscosity of a dispersed system does not depend on particle size and particle position, because the theory neglects the effects of other particles. According to Einstein model this dispersed system is Newtonian fluid. The model was obtained by solving hydrodynamic problem. That is why, it is appropriate for the particle size bigger than molecule size.

2.8.2 Modified Einstein model

In 1911, Einstein modified his early theoretical errors and established a complete Einstein's viscosity law, that is

$$\eta_r = \frac{\eta}{\eta_0} = (1 + \varphi) \cdot (1 + \varphi + \varphi^2 + ...)^2, \tag{2.35}$$

where η_r is the relative viscosity of a dispersed system.

Since the theory neglects the effects of other particles there is no effect of particle size or of particle position in the Eq. (2.36). Interactions between particles make situation more complicated. The higher-order terms in φ should be used to take in account the presence of other particles. This theory is suited for extensional flow and the relative position of the particles can be accounting for analytically.

According to Batchelor (1977) the viscosity in this case determined as

$$\eta = \eta_0 \cdot (1 + 2.5 \cdot \varphi + 6.2 \cdot \varphi^2), \tag{2.36}$$

where the viscosities must now to be interpreted as extensional viscosities. The (uniaxial) extensional viscosity is a function of the extensional strain rate, just as the shear viscosity is a function of shear rate.

For shear flows many experiments have been done to find the term multiplying φ^2, but the range of values so obtained is large (varying from about 5 to 15).

Many reviews written and great deal of work has been done on dilute suspensions. The range of phase volume does not exceed 10% for dilute suspension theory, and this accounts for no more than a 40% increase in viscosity over the continuous phase.

2.8.3 Maximum packing fraction, influence on viscosity

The best way to determine the influence of particle concentration on the viscosity of the concentrated suspensions is to use relation with the maximum packing fraction. Adding more

and more particles into suspensions leads to a situation, when suspensions "jam up". It gives continuous three-dimensional contact throughout the suspension and makes flow impossible, i.e. the viscosity tends to infinity. This happens at the particular phase volume which value depends on the arrangement of the particles and it is called the maximum packing fraction φ_m. Table 2.1 represents examples of φ_m. The range of maximum packing fraction is from approximately 0.5 to 0.75 even for monodisperse spheres [6].

Table 2.1 *The maximum packing fraction of various arrangements of monodisperse spheres [6]*

Arrangement	Maximum packing fraction
Simple cubic	0.52
Minimum thermodynamically stable configuration	0.548
Hexagonally packed sheets just touching	0.605
Random close packing	0.637
Body-centred cubic packing	0.68
Face-centred cubic/ hexagonal close packed	0.74

The maximum packing fraction is very sensitive to particle-size distribution and particle shape. The smaller particles fit into the gaps between the bigger ones when there is a wide particle-size range. On the other hand, lower φ_m is obtained because of poorer space-filling by nonspherical particles. The flocs themselves are not close-packed and that is why particle flocculation can also lead to a low maximum packing fraction. The ratio φ/φ_m is a relevant normalized concentration according to above consideration [6].

2.8.4 Concentrated Newtonian suspensions

It is difficult to analyse from a theoretical point of view the situation for concentrated suspensions, where higher-order terms than φ^2 is expected to be important. To solve this problem is only possible by simulating the situation using computer modelling or alternatively introducing a technique for averaging the influence of neighbouring particles [6].

Ball and Richmond (1980) proposed a theory, based on an averaging technique. They essentially started from the assumption that the sum of the effects of particles added sequentially is equal to the effect of all the particles in a concentrated suspension. The Einstein equation can be defined in a differential form

$$d\eta = \left(\frac{5\cdot\eta}{2}\right)d\varphi, \tag{2.37}$$

where $d\eta$ is the increment of viscosity on the addition of a small increment of phase volume $d\varphi$ to a suspension of viscosity η.

Integrate the phase volume between 0 and φ for which the viscosity is η_0 and η respectively, to obtain the viscosity of the final suspension. Then

$$\eta = \eta_0 \cdot \exp\left(\frac{5\cdot\varphi}{2}\right). \tag{2.38}$$

Ball and Richmond point out that the correlations between spheres due to their finite size are neglected. This means that a particle requires more space than its volume $d\varphi$ due to packing

difficulties when it is added to a relatively concentrated suspension. Replace $d\varphi$ by $\frac{d\varphi}{1-K\cdot\varphi}$, where K accounts for the so-called "crowding" effect. Integration now gives [6]

$$\eta = \eta_0 \cdot (1 - K \cdot \varphi)^{-\frac{5}{2 \cdot K}}. \tag{2.39}$$

According to this equation the viscosity becomes infinite when $\varphi = \frac{1}{K}$. Therefore, it is possible to identify $\frac{1}{K}$ with the maximum packing fraction φ_m. The expression obtained by Ball and Richmond's is effectively identical to that of Krieger and Dougherty (1959). The point of Krieger and Dougherty's theory is that the intrinsic viscosity [η], in the general case, could replace the $\frac{5}{2}$ factor. The intrinsic viscosity for an ideal dilute suspension of spherical particles is equal to value of $\frac{5}{2}$. To account particles of any shape it is required to replace [η] by [q].

The Krieger-Dougherty equation is defined as

$$\eta = \eta_0 \cdot \left(1 - \frac{\varphi}{\varphi_m}\right)^{-[\eta]\cdot\varphi_m}, \tag{2.40}$$

where [η] is the dimensionless intrinsic viscosity, since the phase volume is also dimensionless.

Mooney (1951) derived an expression for the relative viscosity of dispersions of monodisperse spheres as

$$\ln\frac{\eta}{\eta_0} = \frac{2.5\cdot\varphi}{1-\frac{\varphi}{\varphi_m}}. \tag{2.41}$$

The test of experimental data showed that equation is valid for volume fractions (φ) less than 0,5.

Frankel and Acirvos (1967) supposed that viscosity of the system increases due to energy losses resulting from the relatively racking of particles to the low viscosity medium. By averaging the energy loss of each particle-pair in the medium (even with high particle concentration), the final formula for relative viscosity was written as [9]

$$\eta = \eta_0 \cdot \frac{9}{8} \cdot \left[\frac{(\varphi/\varphi_m)^{\frac{1}{3}}}{1-(\varphi/\varphi_m)^{\frac{1}{3}}}\right]. \tag{2.42}$$

Chong (1971) obtained empirical formula for relative viscosity as [9]

$$\eta = \eta_0 \cdot \left[1 + 7{,}5 \cdot \left(\frac{\varphi/\varphi_m}{1-\varphi/\varphi_m}\right)\right]^2. \tag{2.43}$$

More universal formula was suggested by Kitano (1980) and that is [9]

$$\eta_r = \left[1 - \varphi / \varphi_m\right]^{-2}. \tag{2.44}$$

For small φ Eq. (**2.43**) and Eq. (**2.44**) both reduce to the Einstein equation (Eq. (**2.34**)).

Obtained from the empirical use of Eq. (**2.44**) the values of φ_m are strongly dependent on the particle-size distribution. Hence, if polydispersity increases (i.e. the spread of sizes), φ_m also increases. Figure 2.9 represents the viscosities of mixtures of large and small particles plotted as a function of the total phase volume. The particle-size ratio is 5:1. P→ Q shows the fiftyfold reduction in viscosity when a 60% *V*/*V* suspension is changed from a mono- to a bimodal (50/50) mixture. P → S illustrates the 15% increase in phase volume possible for the same viscosity when a suspension is changed from mono- to bimodal [6].

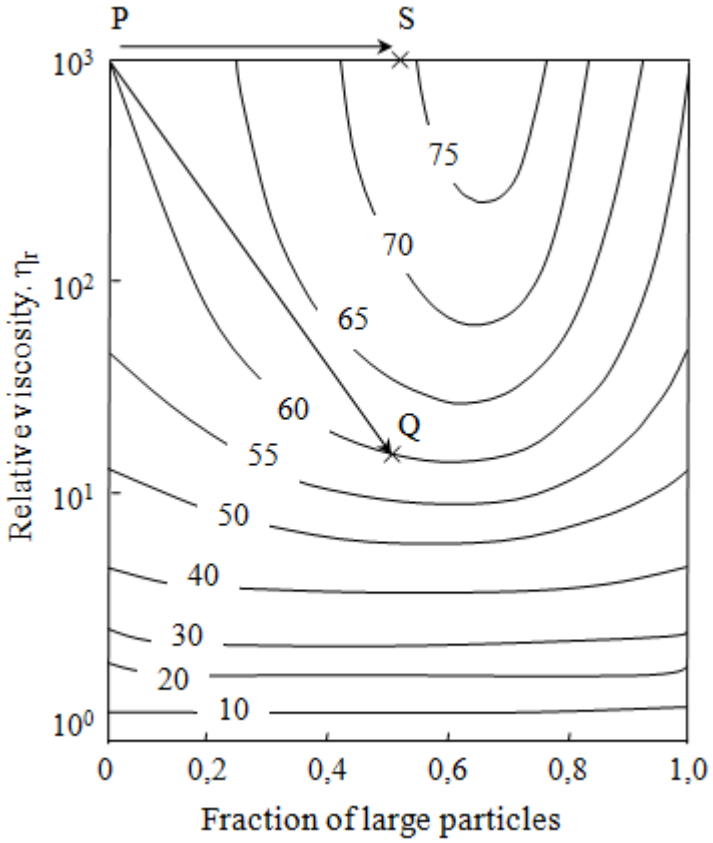

Figure 2.9 *Effect of binary particle-size fraction on suspension viscosity, with total % phase volume as parameter. The particle-size ratio is 5:1 [6]*

About a fraction of 0.6 of large particles the high reduction in viscosity is observed, which is known as the Farris effect. At a total phase volume of more than 50% the effect is very large.

The viscosity can be reduced by mixing particle sizes whilst maintaining the phase volume to be constant. It allows also increasing the phase volume whilst maintaining the same viscosity. Similar effects are shown for tertiary mixtures in Figure 2.10. Contours show values of the relative viscosity at 65% total solids (from the theoretical relationship of Farris (1968)) [6].

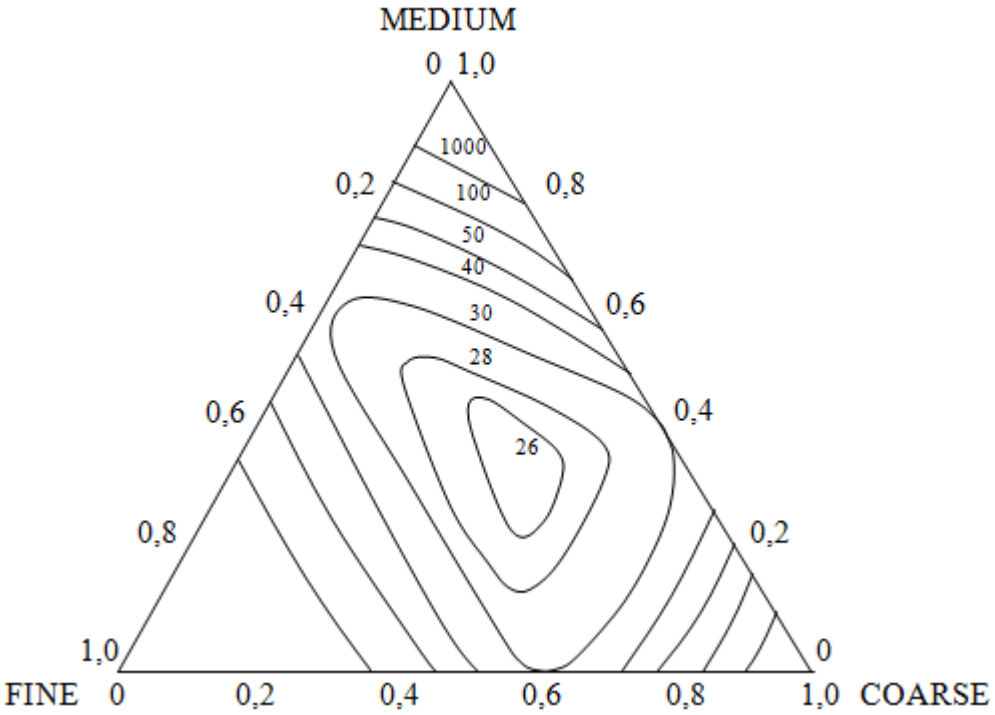

Figure 2.10 *Effect of particle-size distribution on trimodal suspension viscosity [6]*

In this example it is shown that the minimum relative viscosity is approximately equal 25 for the optimum tertiary mixture and is over 30 for the binary mixture. Using Eq. 2.44 all these effects can be predicted by assuming, for example, that the continuous phase is thickened by small particles and this phase is then thickened by the next-size-up particles. The result viscosity for a binary mixture is determined as

$$\eta = \eta_0 \cdot \left(1 - \frac{\varphi_1}{\varphi_{m1}}\right)^{-[\eta_1]\varphi_{m1}} \cdot \left(1 - \frac{\varphi_2}{\varphi_{m2}}\right)^{-[\eta_2]\varphi_{m2}} . \qquad (2.45)$$

A continuous distribution of particle sizes often fit some empirical mathematical expression for most suspensions of industrial interest. Nevertheless information is not available in the rheological literature on how the parameters of such a fit control φ_m. Therefore φ_m has to be found by nonlinear curve fitting and each system has to be measured. When φ_m is determined for any practical suspension, this parameter can be used to observe the effect on viscosity if the dispersed phase concentration or the continuous phase viscosity were changed [6].

Spherical particles influence on the viscosity of suspensions. However, the intrinsic viscosity and maximum packing fraction and hence the concentration/viscosity relationship are effected by particle asymmetry. A number of studies have shown that viscosity increases for the same phase volume when there is any deviation from spherical particles. Figure 2.11 represents this point.

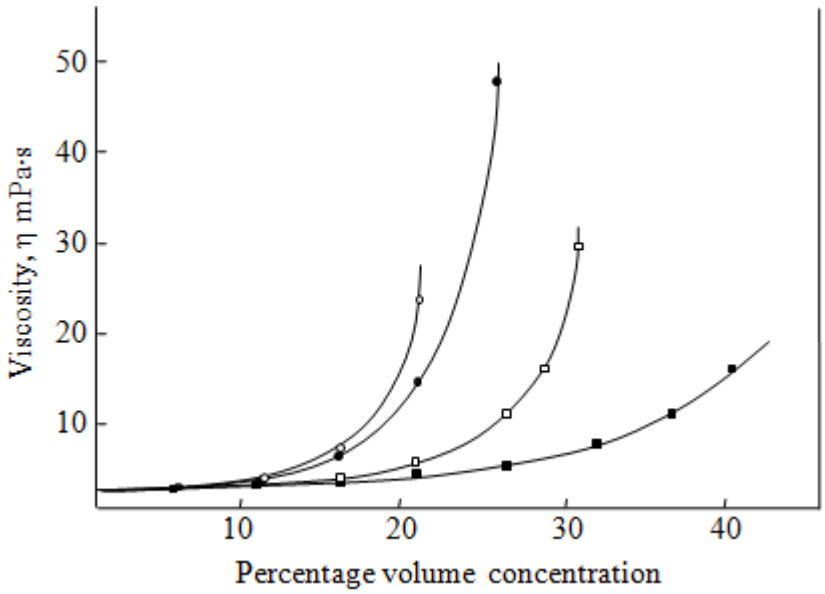

Figure 2.11 *Viscosity dependence of differently shaped particles in water on concentration at a shear rate of 300 s^{-1}*
(■) spheres, (□) grains, (●) plates, (○) rods [6]

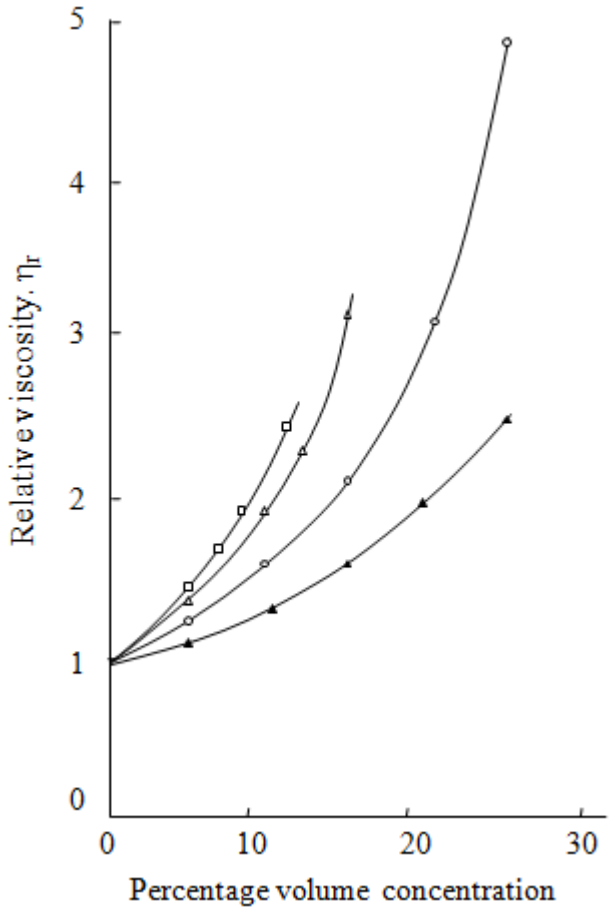

Figure 2.12 *Relative viscosity dependence of glass fibre suspensions of various length/diameter ratios.*
(▲) spheres, L/D = 7 (○), L/D = 14 (△), L/D = 21 (□) [6]

According to the theory, at least as far as it goes for dilute suspensions, rods have a greater effect than discs in increasing the viscosity. Simple empiricisms for the effect of very large axial ratio on the intrinsic viscosity [η] were provided by Barnes (1981). These are

discs: $[TJ] = 3$ (axial ratio)/10,

rods: $[TJ] = 7\ [(\text{axial ratio})^{5/3}]/100$. (2.46)

The values of $[\eta]$ and φ_m are represented in Table 2.2 and were obtained by fitting the results of a number of experimental investigations on suspensions of asymmetric particles using Eq. (**2.44**). It is shown that increasing asymmetry leads to higher $[\eta]$ and lower φ_m, but the product of the two terms changes little. This fact allows estimating of the viscosity of a wide variety of suspensions. The values of $[\eta]$ are qualitatively in line with the predictions of Eq. (**2.46**).

Table 2.2 *The values of [η] and φ_m for a number of suspensions of asymmetric particles, obtained by fitting experimental data to Eq. (***2.46**) *[6]*

System	$[\eta]$	φ_m	$[\eta] \cdot \varphi_m$
Spheres (submicron)	2.7	0.71	1.92
Spheres (40 pm)	3.28	0.61	2.00
Ground gypsum	3.25	0.69	2.24
Titanium dioxide	5.0	0.55	2.77
Laterite	9.0	0.35	3.15
Glass rods (30x700 pm)	9.25	0.268	2.48
Glass plates (100x400 pm)	9.87	0.382	3.77
Quarts grains (53-76 pm)	5.8	0.371	2.15
Glass fibers:			
axial ratio-7	3.8	0.374	1.42
axial ratio-14	5.03	0.26	1.31
axial ratio-21	6.0	0.233	1.40

2.9 Concentric cylinder viscometer

The Couette viscometer is shown in Figure 2.13 and it consists of two coaxial cylinders (bob and rotor). The fluid to be measured is filling the space (gap) between two cylinders. The bob is held in place by a torsion wire and outer cylinder is rotated at a constant rate (ω rad s^{-1}).

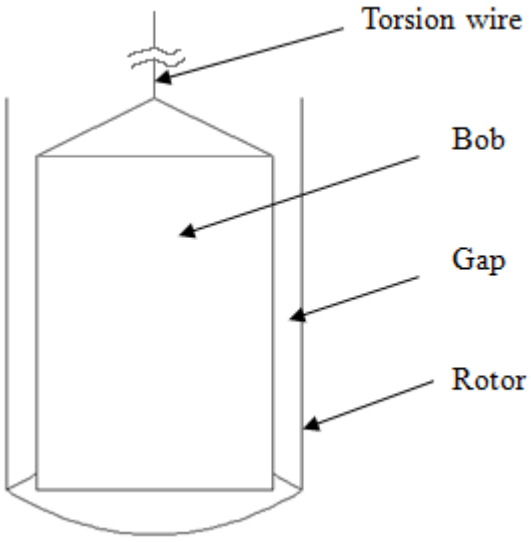

Figure 2.13 *A sketch of a Couette viscometer*

The inner cylinder (bob) is twisting against the torsion wire by viscous drag of the liquid against the surface. When the restoring torque in the wire is equal to the torque applied by the moving fluid it stops to turn [7].

When the bob stops twisting the flow velocity of the fluid at the inner wall equals zero, $\upsilon(r) = 0$, and at the outer wall is determined as

$$\upsilon(r) = \Omega \cdot R_0 , \tag{2.47}$$

where R_0 is the radius of the outer cylinder.

Correcting for the fact that some of the rotational motion is a rigid body motion which is not shearing the liquid at all that is the reason why the shear rate is not equal to $\frac{d\upsilon(r)}{dr}$. It can be measured by ω, which varies across the gap from 0 to Ω. The shear rate is given by equation

$$\dot{\gamma} = \frac{d\upsilon}{dr} - \omega = \frac{d\upsilon}{dr} - \frac{\upsilon}{r} = r\left(\frac{d\omega}{dr}\right). \tag{2.48}$$

The stress on each cylinder of fluid is determined as

$$S = \eta \cdot \left(\frac{d\upsilon}{dr} - \frac{\upsilon}{r}\right). \tag{2.49}$$

The stress impacts a torque to the cylinder defined as

$$\text{force x radius = stress x area of surface x radius = } 2 \cdot \pi \cdot r^2 \cdot L \cdot S , \tag{2.50}$$

where L is the length of the cylinder.

A torque is a twisting force, the size of which is measured by the product of the force and the distance from the centre about which the twisting motion is being applied [7]. On every cylinder of fluid the torque is the same and is also the same as the torque Ti on the inner cylinder

$$T_i = 2 \cdot \pi \cdot r^2 \cdot \eta \cdot \left(\frac{d\upsilon}{dr} - \frac{\upsilon}{r}\right) \cdot L . \tag{2.51}$$

Integrating this expression with respect to r obtain

$$\upsilon_i = \frac{T_i \cdot r}{4 \cdot \pi \cdot \eta \cdot L} \cdot \left(\frac{1}{R^2} - \frac{1}{r^2}\right), \tag{2.52}$$

where R_i is the radius of the inner cylinder.

On the outer cylinder, υ must be equal to $\Omega \cdot R_0$. Substitute these values in previous equation and obtain torque

$$T_i = \left(\frac{4 \cdot \pi \cdot L \cdot R_i^2 \cdot R_o^2}{R_o^2 - R_i^2}\right) \cdot \eta \cdot \Omega = C \cdot \eta \cdot \Omega , \tag{2.53}$$

where C is a constant.

The torque generated in the wire is proportional to the angle, θ. Wire has been twisted and proportionality is determined as

$$T_i = k \cdot \theta \,, \tag{2.54}$$

where k is another instrument constant which can be determined using a liquid of known viscosity.

The plot of Ω versus θ should be linear with a slope of $\frac{C \cdot \eta}{k}$. The ratio $\frac{C}{k}$ can be obtained from the slope and used for evaluation of η for other liquids from similar plots [7].

The shear rate in the gap between the cylinders can be defined as

$$\dot{\gamma} = \frac{T_i}{2 \cdot \pi \cdot \eta \cdot L \cdot r^2} \,. \tag{2.55}$$

It means for a viscometer in which radius of outer cylinder is twice bigger than radius of inner cylinder there will be a fourfold variation in shear rate across the gap. For investigating the flow of colloidal suspensions where the viscosity is often a function of shear rate such a device would not be appropriated. That would make η be a function of the radius and the above analysis than is invalid. Taking account of a varying viscosity in the gap, it is possible to modify the analysis by keeping the gap width, d, as small as possible. The shear rate is then approximately constant and is determined as

$$\dot{\gamma} = \frac{\Omega \cdot R}{d} \,. \tag{2.56}$$

The radius of commercial viscometers is usually several centimeters and a gap width is 1 mm or less. Often these viscometers have an inner cylinder rotating, due to reasons of convenience, and it gives rise to instabilities for liquids of low viscosity like water, even at low speeds. It is necessary to make an end-correction because the flow regime in the annulus between the cylinders of the Couette viscometer is different from the flow in the bottom [7].

There are two general types of instruments. Some maintain a known speed of rotation (that is a constant shear rate) and have some kind of strain gauge which allows determining the shear stress. Others determine the consequent rotational speed by applying a constant stress. To the behaviour at small deformations the instruments of the second type are usually more sensitive. Both kinds can display the results either as a meter reading or a digital readout and can be electronically automated [7].

2.10 Forces affecting on a particle in a shear flow

In equilibrium position, the forces acting on the bubble, particle – buoyancy, viscous drag, added mass, inertial (or pressure gradient) force and lift – exactly balance each other.

2.10.1 Governing equations for a rigid particle in a flowing liquid. Drag force

An investigating of the terminal falling velocity of particles in stationary and moving fluid flows is needed in a wide range of process engineering applications, for instance liquid – solid separations, fluidization and transportation of solids, falling ball viscometry, drilling applications. The size, shape, and density of particles, its orientation, properties of the liquid medium (density, rheology), size and shape of the fall vessels, and whether the liquid is

stationary or moving, that are variables which influence on the terminal falling velocity of particle [10].

A rigid spherical particle of diameter *d*, which is schematically represented in Figure 2.14, is moving relative to an incompressible fluid of infinite extent with a steady velocity υ.

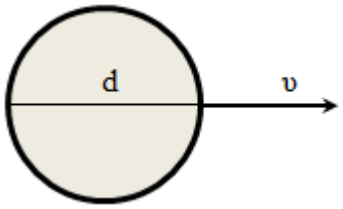

Figure 2.14 *A rigid particle moving in a liquid [10]*

Consider the symmetrical two-dimensional flow. The velocity vector, υ, has φ-component which is equal to zero, and there is no variation of flow variables with φ; hence, one can be written

$$\begin{aligned} \upsilon_{\mathrm{r}} &= \upsilon_r(r,\theta), \\ \upsilon_\theta &= \upsilon_\theta(r,\theta), \\ \upsilon_\varphi &= 0. \end{aligned} \tag{2.57}$$

Introduce a stream function, ψ, determined as

$$\begin{aligned} \upsilon_r &= -\frac{1}{r^2 \cdot \sin\theta} \cdot \frac{\partial \psi}{\partial \theta}, \\ \upsilon_\theta &= -\frac{1}{r \cdot \sin\theta} \cdot \frac{\partial \psi}{\partial \theta}. \end{aligned} \tag{2.58}$$

The conservation of mass and the Newton's second law of motion are two fundamental physical laws, which govern the steady motion of a sphere in an incompressible fluid under isothermal conditions. So-called continuity and momentum equations obtained from these laws to an infinitesimal control volume of a fluid are, respectively, written as [10]

$$\begin{aligned} \nabla \cdot \upsilon &= 0, \\ \rho \upsilon \cdot \nabla \upsilon &= -\nabla p + \nabla \cdot \left\{ \mu \cdot \left(\nabla V + (\nabla V)^T \right) \right\}, \end{aligned} \tag{2.59}$$

where *p* is the nongravitational pressure.

For this flow problem it is necessary to set the appropriate boundary conditions which are no-slip at the sphere surface, and the free stream velocity far away from the sphere. Assume a reference frame fixed to the particle with the origin at its center and write these boundaries as:

At $r = R$,

$$\begin{aligned} \upsilon_r &= 0, \\ \upsilon_\theta &= 0. \end{aligned} \tag{2.60}$$

At $r \to \infty$

$$\upsilon_r = \upsilon \cdot \cos\theta\,,$$
$$\upsilon_\theta = -\upsilon \cdot \sin\theta\,. \tag{2.61}$$

To define the problem completely a rheological equation of state has to be written in addition to the field equations and the boundary conditions (Eq. (**2.59**) – Eq. (**2.61**)) to relate the components of the extra stress tensor to that of the rate of deformation tensor for the fluid. This leads to the viscosity term appearing in the momentum equation (Eq. (**2.60**)) to be shown in terms of the relevant velocity components and their gradients.

This will enable the viscosity term appearing in the momentum Eq. (**2.59**) to be expressed in terms of the relevant velocity components and their gradients. However, it is possible to make some progress without choosing an equation of state at this stage. There are two unknowns the velocity and pressure fields (υ and p) in the equation. To solve the problem for these two unknowns Eq. 2.60 with the boundary conditions (Eq. (**2.60**) – Eq. (**2.61**)) are sufficient [10].

Knowing the pressure and velocity fields, the drag force acting on a moving particle can be estimated as

$$F_D = \int_0^{2\pi}\int_0^{\pi} \left(-\,p_{r=R} \cdot \cos\theta\right) \cdot R^2 \sin\theta d\theta d\varphi + \int_0^{2\pi}\int_0^{\pi} \left(\tau_{r\theta}\big|_{r=R} \sin\theta\right) \cdot R^2 \sin\theta d\theta d\varphi\,. \tag{2.62}$$

The two components are known as the form or pressure and the friction drag are represented, respectively, on the RHS of Eq. (**2.62**).

Reynolds number is determined as

$$\mathrm{Re} = \frac{\rho \cdot \upsilon \cdot d}{\mu_{ref}}\,. \tag{2.63}$$

For developing a general formulation applicable to the flow of time-independent fluids a reference viscosity, μ_{ref}, has been introduced here. Rewrite the drag force in dimensionless form by introducing a drag coefficient C_D as

$$C_D = \frac{8 \cdot F_D}{\pi \cdot d^2 \cdot \rho \cdot \upsilon^2}\,. \tag{2.64}$$

The simplest realistic class of materials is represented by the Newtonian fluid and Stokes was the first who considered the hydrodynamic behavior of rigid spheres in Newtonian media in 1851. The rheological equation of state for an incompressible fluid can be written as [10]

$$\tau_{ij} = 2 \cdot \mu \cdot \varepsilon_{ij}\,,\ i, j = r, \theta, \varphi\,, \tag{2.65}$$

where ε_{ij} represents the components of the rate of deformation tensor.

In a spherical coordinate system these are related to the two nonzero components of the velocity vector ($\upsilon_r, \upsilon_\theta$) as following

$$\varepsilon_{rr} = \frac{\partial \upsilon_r}{\partial r},\ \varepsilon_{\theta\theta} = \left(\frac{1}{r}\cdot\frac{\partial \upsilon_\theta}{\partial \theta} + \frac{\upsilon_r}{r}\right),\ \varepsilon_{\varphi\varphi} = \left(\frac{\upsilon_r + \upsilon_\theta \cdot \cot\theta}{r}\right),$$

$$\varepsilon_{r\theta} = \varepsilon_{\theta r} = \frac{1}{2}\cdot\left(r\cdot\frac{\partial}{\partial r}\cdot\left(\frac{\upsilon_\theta}{r}\right) + \frac{1}{r}\cdot\frac{\partial \upsilon_r}{\partial \theta}\right), \tag{2.66}$$

$$\varepsilon_{r\varphi} = \varepsilon_{\varphi r} = \varepsilon_{\theta\varphi} = \varepsilon_{\varphi\theta} = 0.$$

Rewrite the momentum equation in terms of ψ^* using equations and obtain

$$E^4 \cdot \psi^* = \frac{\mathrm{Re}}{2}\left[\frac{\partial \psi^*}{\partial \theta}\cdot\frac{\partial}{\partial r^*}\cdot\left(\frac{E^2\cdot\psi^*}{r^{*2}\cdot\sin^2\theta}\right) - \frac{\partial \psi^*}{\partial r^*}\cdot\frac{\partial}{\partial \theta}\cdot\left(\frac{E^2\cdot\psi^*}{r^{*2}\cdot\sin^2\theta}\right)\right]\cdot\sin\theta, \tag{2.67}$$

where

$$E^2 \equiv \frac{\partial^2}{\partial r^{*2}} + \frac{\sin\theta}{r^{*2}}\cdot\left(\frac{1}{\sin\theta}\cdot\frac{\partial}{\partial \theta}\right). \tag{2.68}$$

The reference viscosity, μ_{ref}, is equal to μ, the Newtonian viscosity in this case, and this leads to the regular definition of the Reynolds number.

Only approximate solutions are available for the Eq. (**2.67**). Due to its highly nonlinear form the general solution is impossible. For instance, the nonlinear inertial terms can be dropped by using creeping flow approximation and Eq. (**2.67**) can be reduced to the form

$$E^4 \cdot \psi^* = 0. \tag{2.69}$$

Stokes obtained a solution for the fourth-order partial differential equation in 1851, and the resulting expression for the so-called Stokes drag is defined as

$$F_D = 6\cdot\pi\cdot\mu\cdot R\cdot\upsilon. \tag{2.70}$$

From pressure and friction the individual contributions arising are $2\cdot\pi\cdot\mu\cdot R\cdot\upsilon$ and $4\cdot\pi\cdot\mu\cdot R\cdot\upsilon$, respectively. Eq. (**2.71**) is determined in a more familiar form as [10]

$$C_D = \frac{24}{\mathrm{Re}}. \tag{2.71}$$

2.10.2 Steady-state drag force

The “steady-state” drag is the drag force which acts on the particle or droplet in a uniform pressure field when there is no acceleration of the relative velocity between the particle and the conveying fluid. The force is quantified by the drag coefficient through the equation [10]

$$F_D = \frac{1}{2}\cdot\rho_c\cdot C_D\cdot A\cdot|u-\upsilon|\cdot(u-\upsilon), \tag{2.72}$$

where ρ_c is the density of the continuous (conveying) phase,

A is the representative area of the droplet (particle),

u is the velocity of the continuous phase,

υ is the particle or droplet velocity.

An extension of Stokes analysis is the Hadamard-Rybczynski drag law for a spherical fluid particle in which the shear stress on the surface induces an inertial motion. In this case drag coefficient is determined as [10]

$$C_D = \frac{24}{\mathrm{Re}} \cdot \left(\frac{1 + \frac{2}{3} \cdot \overline{\mu}}{1 + \overline{\mu}} \right), \tag{2.73}$$

where $\overline{\mu}$ is the ratio of the viscosity of the carrier phase to that of the fluid sphere. For a droplet in air, $\overline{\mu} \to 0$ and Stokes law is recovered. For a bubble in a liquid, $\overline{\mu} \to \infty$ so the drag coefficient becomes 16/Re.

Drag coefficient also was obtained by Oseen (1910) and by Ingebo (1956).

2.10.3 Pressure gradient and buoyancy force

The effect of the local pressure gradient gives rise to a force in the direction of the pressure gradient. The net pressure force acting on a particle is given by [11]

$$F_p = \int_{cs} - pndS \,. \tag{2.74}$$

Applying the divergence theorem gives

$$F_p = \int_{c\upsilon} - \nabla p dV \,. \tag{2.75}$$

By assuming the pressure gradient is constant over the volume of the particle one has

$$F_p = -\nabla p \cdot V_d \,, \tag{2.76}$$

where V_d is the particle volume.

The pressure gradient produced by hydrostatic pressure is

$$\nabla p = -\rho_c \cdot g \cdot \vec{e}_z \,, \tag{2.77}$$

where z is in the direction opposed to gravity (upward). The corresponding pressure force is

$$F_p = \rho_c \cdot g \cdot V_d \,, \tag{2.78}$$

which states that the force is equal to the weight of the fluid displaced. This is known as Archimedes principle.

The equation of motion of a particle including buoyancy effects is

$$m \cdot \frac{d\upsilon}{dt} = 3 \cdot \pi \cdot \mu_c \cdot d \cdot f \cdot (u - \upsilon) + mg - \rho_c \cdot g \cdot V_d \,, \tag{2.79}$$

or

$$\frac{d\upsilon}{dt} = \frac{f}{\tau_\upsilon} \cdot (u - \upsilon) + g \cdot \left(1 - \frac{\rho_c}{\rho_d}\right). \tag{2.80}$$

The terminal velocity is affected by the buoyant force and it is given by

$$\upsilon_t = \frac{g \cdot \tau_\upsilon}{f} \cdot \left(1 - \frac{\rho_c}{\rho_d}\right) = \frac{g \cdot d^2 (\rho_d - \rho_c)}{18 \cdot f \cdot \mu_c}. \tag{2.81}$$

When $\rho_d = \rho_c$ the terminal velocity is zero and the particles are neutrally buoyant.

In a similar fashion, there is also a force on the particle due to the shear stress in the conveying fluid; namely,

$$F_\tau = \int_{cs} \tau_{ij} \cdot n dS . \tag{2.82}$$

Using the divergence theorem, the force can be expressed as

$$F_\tau = \int_{c\upsilon} \nabla \cdot \tau_{ij} dV . \tag{2.83}$$

And if the shear stress gradient is constant over the particle, the force becomes

$$F_\tau = \nabla \cdot \tau_{ij} V_d . \tag{2.84}$$

An estimate of the importance of the force due to the pressure gradient in the continuous phase is the order of the flow acceleration.

$$\frac{\partial p}{\partial x} \sim \rho_c \cdot \frac{Du_c}{Dt} . \tag{2.85}$$

Thus the ratio of the pressure force to the force to accelerate a particle is

$$\frac{V_d \dfrac{\partial p}{\partial x}}{m \dfrac{du_d}{dt}} \sim \frac{\rho_c}{\rho_d} \cdot \frac{Du_c}{Dt} \frac{dt}{du_d} . \tag{2.86}$$

If the accelerations of the two phases are of the same order, then the ratio of the pressure force to the acceleration is

$$\frac{V_d \dfrac{\partial p}{\partial x}}{m \dfrac{du_d}{dt}} \sim \frac{\rho_c}{\rho_d} . \tag{2.87}$$

In a gas-particle flow the ratio of material densities is generally of the order of 10^{-3} so the pressure gradient force can be neglected. Of course this is not true for a slurry flow. In a bubbly flow the buoyant force is the most important force controlling bubble motion.

2.10.4 Saffman lift force

Particle which is moving in a shear flow is represented in Figure 2.15. Lift forces appear due to particle rotation. Rotation may be caused by a velocity gradient or may be imposed from some other source such as particle contact and rebound from the surface [11].

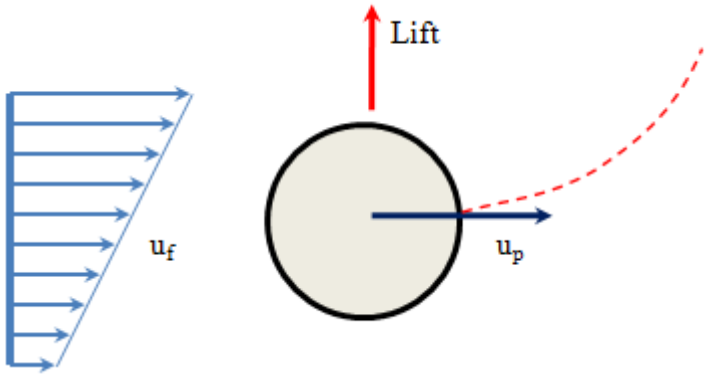

Figure 2.15 *Particle in a shear flow [11]*

Particle motion in shear flow depends on forces of different origin. One of these forces is a lift force caused by shear flow. A lift force acts on particles in a shear field perpendicular to the direction of flow. Inertia effects in the viscous flow around the particle make shear lift appearing. The analytical expression for the inertia shear lift was determined by Saffman as

$$F = F_S = C_S \cdot \rho \cdot \nu^{\frac{1}{2}} \cdot d^2 \cdot \left(u_f - u_p\right) \cdot \left|\frac{du_f}{dy}\right|^{\frac{1}{2}} \cdot \mathrm{sgn}\left(\frac{du_f}{dy}\right), \tag{2.88}$$

where C_S is the coefficient,
u_f is the fluid velocity at the location of mass centre of the particle,
u_p is the particle velocity,
d is the particle diameter,
ρ, ν are the fluid density and viscosity.

Coefficient C_S for smooth spherical particle in an incompressible fluid depends on translation motion Re_p and shear flow Re_s Reynolds numbers [10]:

$$\mathrm{Re}_p = \frac{\left|u_f - u_p\right| \cdot d}{\nu} << 1 \ , \ \mathrm{Re}_s = \frac{d^2}{\nu} \cdot \left|\frac{du}{dy}\right| << 1. \tag{2.89}$$

Using numerical integration of the relation $\varepsilon = \frac{\mathrm{Re}_p}{\mathrm{Re}_s} << 1$ Saffman determined the C_S coefficient as $C_S = 1{,}61$.

McLaughlin continued Saffman's work using arbitrary values of ε and showed the lift force decreasing with the ε decreasing. He also found out that shear force changes direction if ε increases and it is equal zero when $\varepsilon = 4{,}65$.

Dandy & Dwyer (1990) numerically solved the problem where rigid spherical particle is moving in a shear flow with Re_p = 0,1 – 100 and α = 0,005 – 0,4, where $\alpha = \frac{\mathrm{Re}_p}{2 \cdot \mathrm{Re}_s}$ is shear parameter. They established for small Re_p and α = const the dimensionless shear force (lift) coefficient

$$C_L = \frac{8 \cdot F}{\pi \cdot \rho \cdot d^2 \cdot \left(u_f - u_p\right)^2}. \tag{2.90}$$

And it is proportional to $\mathrm{Re}_p^{0,5}$, and for $\mathrm{Re}_p^{0,5} \approx 40$ it is approximately constant. When $F = F_S$ the lift coefficient is determined as

$$C_L = C_{LS} = 5{,}816 \cdot \sqrt{\frac{\alpha}{\mathrm{Re}_p}}. \tag{2.91}$$

Mei combined these studies and expressed lift coefficient as $C_L = C_{LS} \cdot k$ where

$$k = \begin{cases} \left(1 - 0{,}3314 \cdot \alpha^{0,5}\right) \cdot \exp\left(-0{,}1 \cdot \mathrm{Re}_p\right) + 0{,}3314 \cdot \alpha^{0,5}, \; for \; \mathrm{Re}_p \le 40 \\ 0{,}0524 \cdot \sqrt{\alpha \cdot \mathrm{Re}_p}, \; for \; \mathrm{Re}_p > 40 \end{cases}. \tag{2.92}$$

For large and small α McLaughlin obtained expressions:

$$k = \begin{cases} 1 - 0{,}287 \cdot \alpha^{-2}, \; for \alpha >> 1 \\ -140 \cdot \alpha^5 \cdot \ln\left(\alpha^{-2}\right), \; for \alpha << 1 \end{cases}. \tag{2.93}$$

And for $\mathrm{Re}_p << 1$ and $\alpha \le 3$ Asmolov empirical formula

$$k = \left(1 + 0{,}581 \cdot \alpha^2 - 0{,}439 \cdot \alpha^3 + 0{,}203 \cdot \alpha^4\right)^{-1}. \tag{2.94}$$

2.10.5 Magnus lift force

The Magnus force is the lift developed due to rotation of the particle as shown in Figure 2.16 the lift is caused by a pressure differential between both sides of the particle resulting from the velocity differential due to rotation. The rotation may be caused by sources other than the velocity gradient [11].

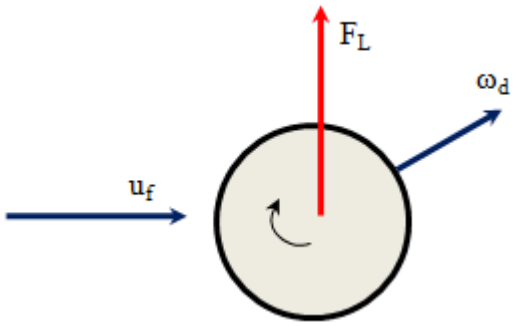

Figure 2.16 *Magnus lift on a particle rotating in a fluid [11]*

The lift force derived by Rubinov and Keller (1961) for Reynolds numbers the order of unity is

$$F_{Mag} = \frac{\pi}{8} \cdot d^3 \cdot \rho \cdot \left[\left(\frac{1}{2} \nabla \times u_f - \omega_d \right) \times \left(u_f - u_p \right) \right]. \tag{2.95}$$

where $\frac{1}{2} \nabla \times u_f$ is the local fluid rotation,

ω_d is the particle rotation.

One notes that the lift would be zero if the particle rotation is equal to the local rotation of the fluid.

The lift produced by the Magnus force can be qualified by a lift coefficient in the form [11]

$$F_{Mag} = \frac{1}{2} \cdot \rho \cdot \left(u_f - u_p \right) \cdot C_{LR} \cdot A \cdot \left(\frac{\left(u_f - u_p \right) \times \omega_r}{\left| \omega_d - \frac{1}{2} \nabla \times u_f \right|} \right). \tag{2.96}$$

where A is the projected area of the particle,
C_{LR} is the lift coefficient due to rotation,
ω_r is the relative spin of the particle with respect to the fluid

$$\omega_r = \omega_d - \frac{1}{2} \nabla \times u_f . \tag{2.97}$$

The lift coefficient is determined as

$$C_{LR} = \frac{d \cdot \left| \omega_d \right|}{\left| u_f - u_p \right|}. \tag{2.98}$$

The nondimensional parameter used for spin rate is the ratio of the equatorial velocity to the particle-fluid relative velocity is written as

$$\Omega = \frac{\omega \cdot d}{2 \cdot \left| u_f - u_p \right|}. \tag{2.99}$$

It means the lift coefficient related to the spin parameter and due to particle spin in Stokes flows it increases linearly with the spin parameter

$$C_{LR} = 2 \cdot \Omega . \tag{2.100}$$

There have been numerous experiments to measure C_{LR}. These experiments (Macoll, 1928; Davis, 1929; Barkla and Auchterlonie, 1971; Tanaka et al., 1990) were conducted at Reynolds numbers exceeding $2 \cdot 10^3$ [11].

McLaughlin (1993) included the effects of presence of the wall in his analysis of the lift force. Cherukat and McLaughlin (1994) analyzed the lift force acting on spherical particles near a wall. Leighton and Acrivos (1985) obtain the expression for the lift on the spherical particles resting on a plane substrate. Experimental studies of lift force were performed for generally larger particles in the range of 100 to several hundred μm by Hall (1988) and by Mollinger and Nieuwstadt (1996).

3 EXPERIMENTS

3.1 Equipment and methods have been used

The experiments were carried out using rotating viscometer OFITE Model 900. PHYSICA Rheometer was used to compare measurements of different viscometers. To measure density of liquids Anton Paar density meter has been used. The density of particles was determined by AutoPyknometer and Le Chatelier method. Particle size, composition and distribution were obtained from Scanning electron microscope. Surface tension was measured with Du Nouy ring method.

3.1.1 OFITE Model 900 Viscometer

The experimental setup OFITE Model 900 Viscometer used in this study is shown in Figure 3.1. The bob has a radius of 34,5 mm and a height of 38 mm, and the outer cylinder which is connected to the rotor by thread has a radius of 37 mm. For visualization purpose the outer cylinder and a beaker where fluid is held are acrylic.

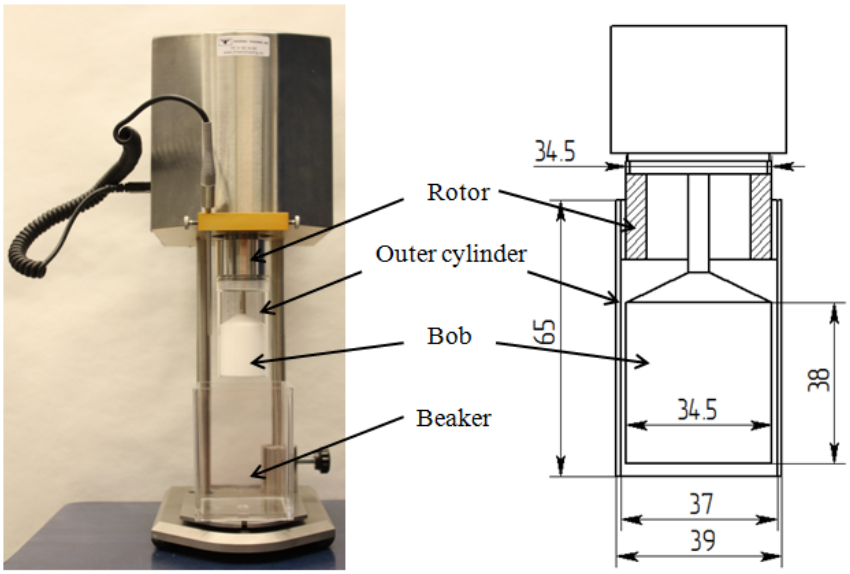

Figure 3.1 *OFITE Model 900 Viscometer*

The OFITE Model 900 Viscometer has following characteristics [12]:

- accurate readings;
- true Couette Coaxial Cylinder;
- motor speeds (RPM) (600, 300, 200, 100, 60, 30, 20, 10, 6, 3, 2, and 1);
- variable speed range - 0.006 – 1000;
- speed accuracy (RPM) - 0.001;
- shear rate range (sec-1) - 0.01 – 1700;
- shear stress range (dynes/cm2) - 0-1500;
- fully automated system provided with ORCADA™ software.

Diameter of the gap is calculated as

$$V_{gap} = \frac{\pi \cdot H}{4} \cdot \left(D^2 - d^2\right) = \frac{\pi \cdot 38}{4} \cdot \left(37^2 - 34.5^2\right) = 5334.82 mm^3 .$$

The ORCADA system for the model 900 is a combination of hardware and software modules. It monitors and controls instruments and equipment used in performing rheological tests on fluids. Data from the tests is collected, analyzed and saved in electronic format. The rheological test data includes the temperature of the sample, temperature of the heating system, viscosity of the sample, shear stress on the sample, shear rate of the sample and the RPM of the rotation system. Features included with the ORCADA system include calibration, archival of calibration results, saving system defaults, programming shear and temperature ramps, auto data analysis using Power Law and Bingham Plastic Models, printing test results and charts [13]. Rheological test builder is represented in Figure 3.2.

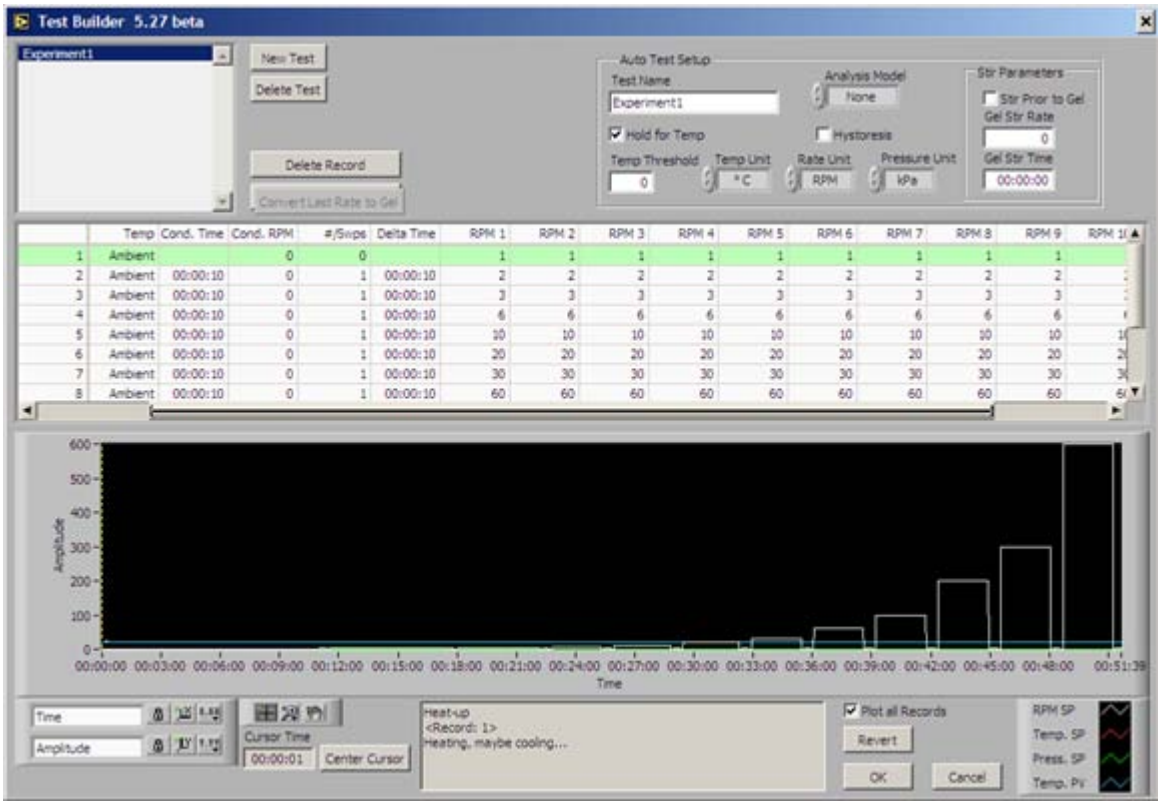

Figure 3.2 *Test builder of ORCADA system*

Calibration

The calibration is performed to determine the deviation between displayed shear stress (viscosity) values and reference values of shear stress (viscosity) standards. The instrument has been calibrated with calibration fluid provided by supplier. Similar results were obtained and it was decided to choose five measuring points as optimal number for each RPM.

3.1.2 PHYSICA Rheometer

The instrument was used to measure viscosity of dispersed systems to have a comparison with the results obtained with OFITE Model 900 Viscometer. PHYSICA Rheometer has inner cylinder rotating. Measured results were similar to results recorded with OFITE Model 900 Viscometer.

Characteristics of PHYSICA

- accurate readings;
- true Couette Coaxial Cylinder;

- shear rate (1.5 – 1021 s^{-1});
- shear rate range (s^{-1}) – 0 – 4.840;
- shear stress range (Pa) – 0 – 453;
- viscosity range (sec-1) – 0.001 – 748;
- fully automated system provided with US 200 software.

The US 200 Software by Physica Messtechnick GmbH has been developed for the control of the Physica instrumentation. It is used for the recording, evaluation and presentation of measurement data. The software allows the export and import of data to or from other programs [14].

Rheological test description

Rotational test has been used. At each shear rate ten values of shear stress (viscosity) were continiously measured during ten seconds of measuring time for each of values. The system was in rotation without pauses between each shear rate for stabilization.

- rotational test;
- shear rates ($\dot{\gamma}$) (1,5; 3,1; 5,1; 10,2; 51,1; 102; 153; 340; 511 and 1021 s^{-1});
- 10 values of viscosity (torque);
- measuring time is 10 seconds;
- no stabilization period between shear rates;
- constant temperature 20 ^{0}C.

3.1.3 Anton Paar - DMA 4500/5000 Density/Specific Gravity/Concentration Meter

The DMA 4500/5000 is an oscillation U-tube density meter which provides measurements with high accuracy in wide viscosity and temperature ranges. It secures stability and makes adjustments at temperatures other than 20^0 C.

The accuracy of the DMA 4500 is $1 \cdot 10^{-5}$ g/cm^3. Some software features like temperature scan and adjustment at high density or viscosity are not available in this instrument [15].

The DMA 4500/5000 features:

- accurate readings;
- measuring range is 0-3 g/cm^3;
- density accuracy is $1 \cdot 10^{-5}$ g/cm^3;
- temperature accuracy is $0{,}01^0$ C;
- measuring temperature is 0 – 90^0 C;
- pressure range is 0-10 bars;
- amount of sample in the measuring cell is approx. 1 ml;
- measuring time per sample is approx. 30 sec.

Checking Procedure, Adjustment and Calibration

The adjustment of the instrument is performed with air and bi-distilled water. The calibration is performed to determine the deviation between displayed density values and reference values of density standards.

Using degassed, bidistilled water the validity of adjustment must be checked before each series of measurements. An adjustment is accurate when the density reading of water and the true density at measuring temperature are equal.

Measurements

It is important to know density of liquids, it uses in calculation of lift and drag forces, Reynolds number and etc. Measurement of density and specific gravity includes viscosity correction for liquids of viscosity below 700 mPa·s. This method is suitable for highly accurate measurements of the true density of liquids. The instrument is represented in Figure 3.3.

Figure 3.3 *Anton Paar Density meter*

A sample has to be carefully prepared (homogeneous and free of gas bubbles) before it is filled into the instrument and a proper cleaning procedure for the measuring cell must be performed.

The syringe is attached slowly and continuously until a drop emerges from the other nozzle. Then the measuring cell is filled by the sample. The syringe remains in the filling position for leakage prevention. It is important that there are no gas bubbles in the measuring cell. An acoustic signal informs when the measurement is finished, and results are automatically converted (including temperature compensation where necessary) into concentration, specific gravity or other density-related units using the built-in conversion tables and functions.

Incorrect results might be obtained for suspensions or emulsions because of their tendency to separate in the measuring cell. The measuring time is reduced when a sample temperature similar to the measuring temperature of 20^0 C. Temperature of the sample introduced in the cell must be higher than the measuring temperature if bubbles appear in the sample during the temperature equilibrium or measurement. Another remedy may be put to the density meter at an angle by means of proper spacers below the right side of the instrument to allow the bubbles to escape (buoyancy).

At the outlet of the measuring cell a waste bottle must always be set and the samples need to be used together with the nozzles. This is in order to avoid glass breakage of the measuring cell [15].

3.1.4 Le Chatelier method

Le Chatelier bottle was used to measure the density of glass beads. To provide an accurate result the Le Chatelier bottle should be filled with water at room temperature up to the first level. The instrument is shown in Figure 3.4.

Figure 3.4 *Le Chatelier bottle*

After bottle is filled the initial volume of water, V_i and weight of the bottle, m_i are found. Afterwards a certain amount of the glass beads is carefully added into the bottle. Care must be taken so the bottle neck is not sealed. Usually it is convenient to fill the Le Chatelier bottle with glass beads up to the next reading level (about 20 ml). Then the volume, V_t and the weight of the bottle, m_t are found, and the specific density of the glass beads can be calculated [16]. This procedure is shown in Figure 3.5.

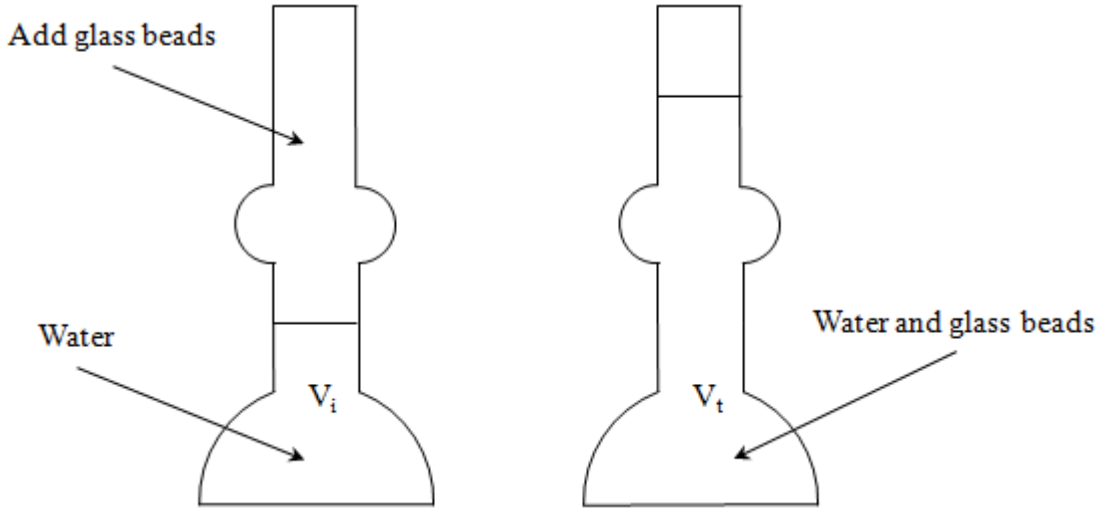

Figure 3.5 *Measuring procedure*

3.1.5 AutoPyknometer

The AccuPyc 1340 Pycnometer is fully automatic gas displacement pycnometer (see Figure 3.6). Analyses are started with a few keystrokes and after that, data are collected, calculations performed, and results displayed without further operator intervention. It is used in laboratory experiments to measure the sample volume, from which density can be determined, knowing the mass of a sample [16].

The basic technique of the AutoPyknometer is to compress identically two quantities of dry gas at the same temperature and pressure, but initially of unequal volume because of the space occupied by a sample. Since the compression of unequal volumes results in unequal pressure even at the same temperature, an adjustment is made in the volume of the lower pressure gas

while under compression to bring it to that of the higher. The compression of both gases is then removed and gas pressures are equalized.

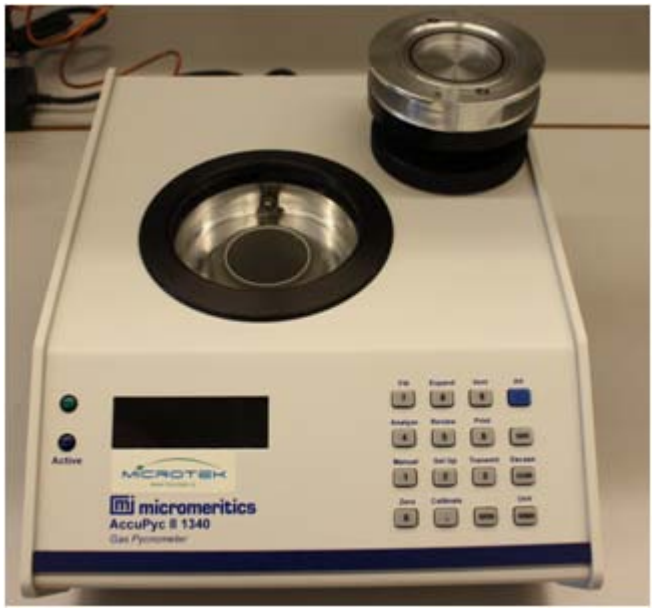

Figure 3.6 *AccuPyc 1340 Pycnometer*

Again, compression of both gases is applied with, probably, again unequal pressure resulting. The pressures will be more nearly equal than before, however, because of the volume adjustment that was made. Further volume adjustments are made and the decompression, equalization, and recompression repeated until final pressure equality is established [16].

The sum of volume adjustments to bring about final pressure equality is equal to the sample volume. This value is electronically divided by the sample weight to give the sample density.

Calibration

Instrument must be calibrated to laboratory atmospheric and environmental conditions. Calibration is used to determine the size of the cell and expansion chambers within the instrument and consists of a two-part procedure [17]:

- specifying calibration parameters;
- performing the calibration.

The standard is placed into the sample cup. At the thermal equilibrium volume of the standard is obtained. An inaccuracy can be recognized by a deviation of the volume reading of standard from the true volume of standard. After calibration, the cell and expansion chamber volumes are stored automatically.

Characteristics:

- temperature is stable between 15 – 35^0 C;
- humidity is 20 – 80 % relative, non-condensing;
- accurate to within 0,03 % of reading, plus 0,03 % of sample capacity;
- chamber volume is 100 cm^3, inner diameter is 4,62 cm, height is 6,17 cm.

3.1.6 Scanning electron microscope

It is important to know the particle shape, size distribution because viscosity models, attractive forces and forces affecting in moving system depend on it. Also dispersed system is classified according to size of dispersed phase.

The invention of the transmission electron microscope (TEM) and the scanning electron microscope (SEM) was most significant development in microscopy. To propose of particle shape early scientist relied on indirect evidence. Often they assumed that particles were roughly spherical if there was no indication of the contrary [7].

It is possible now to determine the shape of colloidal particles with very little uncertainty using the electron microscope. But the intense electron beam can cause melting of some of the softer polymers.

With the modern techniques scanning electron microscope (SEM) provides high quality images, which are interpreted by the eye as truly three-dimensional. In the SEM sample is held at an angle to the beam. The electron beam is focused to about 5 – 10 nm and deflected across the surface of the sample [7].

A collector grid in a sensitive detector draws the emitted low-velocity secondary electrons. In a cathode ray tube (CRT) the intensity of an electron beam is modulated by using the output from the detector. The surface of the CRT is scanned by the beam in synchronism with the scanning of the sample by the primary electron beam. A remarkable reconstructed image on the CRT is the result.

SEM has a big advantage because emitted at a low voltage the secondary electrons are easily deflected to the collector to follow curved paths. The striking realism of the three-dimensional image is obtained by collecting (though at lower intensity) the electrons emerged from parts of the surface that are out of the line of sight. A very large depth of field (300 – 500 times bigger than for a light microscope) allows remaining in focus many different levels of the object at the same time. That is why SEM can be used to examine the fine detail of quite large objects [7].

3.1.7 Du Noüy ring method

The instrument was used to measure surface tension between two liquids (oil – water and oil – diluted red ethanol).

To provide an accurate measurement the dish should be filled with fluids at room temperature. The more dense fluid fills the dish first. The ring submerges at 10 mm distance from top of the fluid. Then a lighter dense fluid is carefully added into the dish to prevent mixing of two liquids. The layer thickness of lighter fluid on the top of more dense fluid should be 10 mm. Adjust the ring to reference level at the scale and to be at the interface of two liquids. Then turning two wheels (dish table wheel and wheel of dial) and keeping the ring at reference level on the scale. In the moment when ring breaks the interface between two fluids the value from dial should be recorded.

Instrument for measuring surface tension is represented in Figure 3.7

Figure 3.7 *Du Noüy ring*

3.2 Materials and methods

3.2.1 Materials used in the experiments

Two different oils, Marcol 82 and Bayol 35, and glass beads were used as dispersed phase of multiphase system in the experiments. Deionized water, diluted red ethanol (80 % alcohol, 20 % water) and glycerol were used as continuous phase of multiphase system. To increase the density of water NaCl was used. Specification of materials, physical properties measured by instruments are given in Table 3.1.

Table 3.1 *Physical properties of materials measured at 20^0 C*

Name of material	Density, g/cm^3	Specific gravity	Viscosity, cP
Oil Marcol 82	0.8474	0.8489	27.28
Oil Bayol 35	0.790	0.791	2.2
Glycerol	1.223	1.225	109.48
Water	0.9914	0.9932	0.98
Salt water	1.1050	1.1070	1.42
Diluted red ethanol	0.8890	0.8906	1.9
Surface tension of Bayol 35 and diluted red ethanol is 4 – 4.2 mN/m, Marcol 82 and water is 42 – 42.2 mN/m			

Properties of oils Bayol 35 and Marcol 82 are represented in Table 3.2.

Table 3.2 *Properties of oils [18], [19], [20]*

Bayol 35	
Density [kg/m^3]	791
Colour, Saybolt	+ 30
Kinematic Viscosity, [cSt]	2,3 (from manufacturer)
Flash Point, TCC Closed Cup, [°C]	96
Appearance and odor	Clear colorless oil with a neutral odor
Density, [g/ml]	0,79
Viscosity [mm^2/S] [40°C]	2
Viscosity [Pa*s]	0,00099088
Vapour Pressure [kPa] [20°C]	Very low
Evaporation Rate	Very low
Solubility in water [20°C]	Insignificant
Flash Point Method	>75°C PMCC ASTM D-93
Marcol 82	
Form	Liquid
Colour	Colourless
Odour	Inodorous
Relative density [g/cm^3]	0.85
Flash Point	>182°C
Explosive limit	NEG: 0.9, ØEG: 7.0
Water solubility	Insignificant
Explosion limits [cSt, 40°C]	14.5

Glass beads

Particles from sample which has been used in the experiments are represented in Figure 3.8. Picture obtained from SEM.

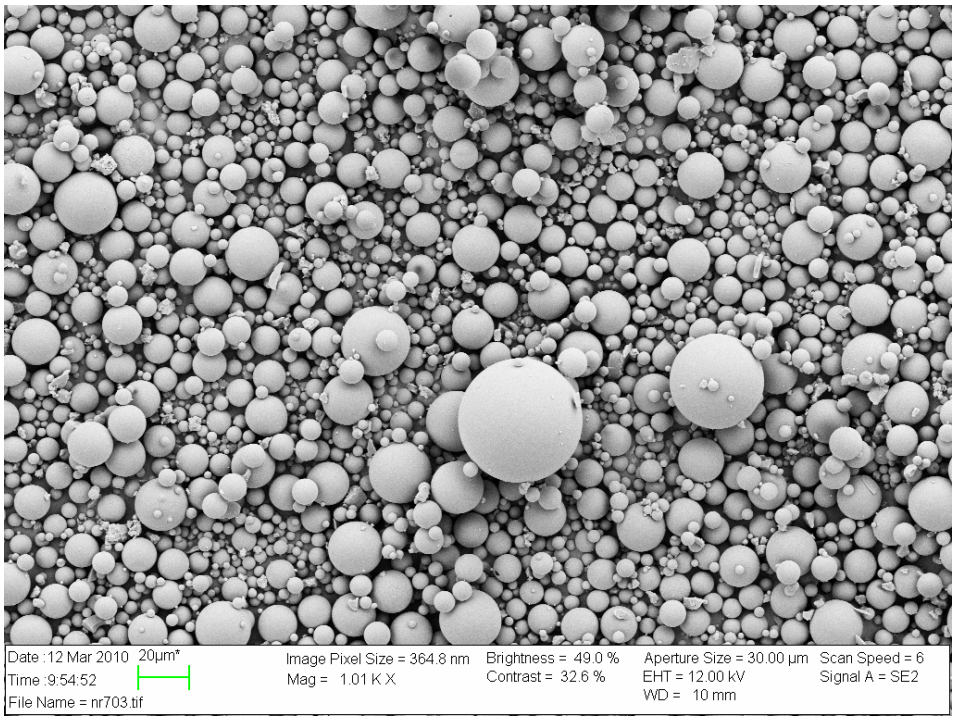

Figure 3.8 *Sample of particles*

Break the range up into 6 steps of 2 – 15 µm and record the number of particles in each class to determine the particle size distribution of the sample. Table 3.3 represents this procedure and the particle size distribution of the sample is plotted as a histogram in Figure 3.9

Table 3.3 *Particle size distribution:* $\sum n_i = 475 = N$, $\sum f_i = 1.00$, $f_i = \frac{n_i}{\sum n_i}$

Class range, µm	Mid-point of class range, d_i, µm	Number of particles, n_i	Fraction in this class, f_i	Total number with $d<d_i$	Cumulative per cent
1 – 2	1.5	70	0.147	70	14.7
3 – 4	3.5	115	0.242	185	24.2
5 – 6	5.5	150	0.316	335	31.6
7 – 8	7.5	48	0.101	383	10.1
9 – 11	10	36	0.076	419	7.6
12 – 14	11	23	0.049	442	4.9
15 – 17	16	13	0.027	455	2.7
18 – 20	19	11	0.023	466	2.3
21 – 34	27	7	0.015	473	1.5
35 – 50	42.5	2	0.004	475	0.4

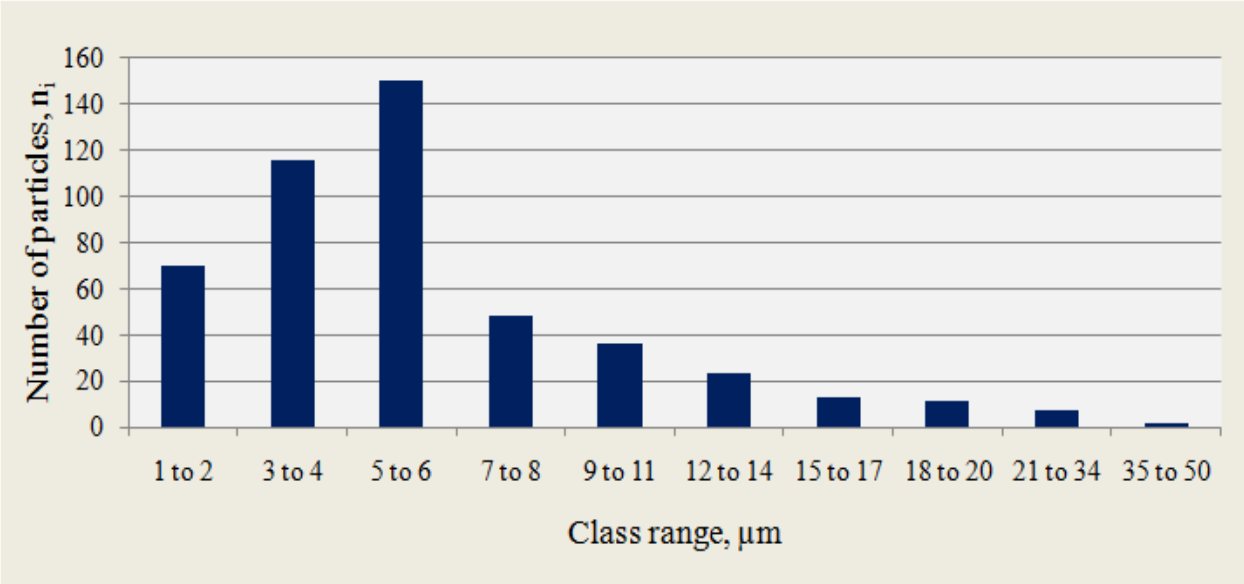

Figure 3.9 *Particle size distribution of the sample*

The mean and standard deviation [21]

The mean is the most important characteristic of a distribution. It measures the central tendency and the standard deviation. The spread of the data is measured by the standard deviation. The mean diameter is defined as

$$\bar{d} = \frac{\sum n_i \cdot d_i}{\sum n_i} = \frac{\sum n_i \cdot d_i}{N} = \sum f_i \cdot d_i \,, \tag{3.1}$$

where f_i is the fraction in class i (Table 3.3).

$\bar{d} = 6.308$ μm.

The standard deviation, σ, is defined as

$$\sigma = \left(\frac{\sum n_i \cdot \left(d_i - \bar{d}\right)^2}{N} \right)^{\frac{1}{2}} = \left(\sum f_i \cdot \left(d_i - \bar{d}\right)^2 \right)^{\frac{1}{2}}, \tag{3.2}$$

$\sigma = 5.088$ μm.

Calculate the average surface area of a sphere in this population and calculate the area of each size sphere in the distribution and average these areas [3].

The area of a sphere is determined as

$$A = \pi \cdot d^2, \tag{3.3}$$

where d is the diameter of a sphere.

Calculate the "average" area, $\bar{A}$, of a sphere using the average diameter $\bar{d} = 6.308$ μm:

$\bar{A} = \pi \cdot 6.308^2 = 125.007$ μm.

Applying the same formula to each class in Table 3.4, calculate the area of each size sphere. Also calculate the surface "average" diameter, $\bar{d}_s$, "average" volume, $\bar{V}$, and volume "average" diameter, $\bar{d}_V$, using equations:

$$\bar{d}_s = \left(\sum f_i \cdot d_i^2 \right)^{\frac{1}{2}},$$

$$\bar{V} = \frac{1}{6} \cdot \pi \cdot \sum f_i \cdot d_i^3, \tag{3.4}$$

$$\bar{d}_V = \left(\sum f_i \cdot d_i^3 \right)^{\frac{1}{3}}.$$

Table 3.4 *Calculation of the "average" area*

d_i, μm	A_i, μm^2	$n_i \cdot A_i$, μm^2	$f_i \cdot d_i^2$, μm^2	$f_i \cdot d_i^3$, μm^3
1.5	7,069	494,801	0,332	0,497
3.5	38,485	4425,719	2,966	10,380
5.5	95,033	14254,977	9,553	52,539
7.5	176,715	8482,300	5,684	42,631
10	314,159	11309,734	7,579	75,789
11	380,133	8743,052	5,859	64,448
16	804,248	10455,220	7,006	112,101
19	1134,115	12475,264	8,360	158,840
27	2290,221	16031,547	10,743	290,065
42.5	5674,502	11349,003	7,605	323,224
Sum		98021.618	65,687	1130,517

"Average area" $\overline{A} = \frac{\sum n_i \cdot A_i}{N} = 206.361\,\mu m^2$, "average" volume $\overline{V} = 591.937\ \mu m^3$,

surface "average" diameter $\overline{d}_s = 8.105\ \mu m^2$, volume "average" diameter $\overline{d}_V = 10.417\ \mu m^2$.

Density of the glass beads was determined using Le Chatelier bottle and AccuPyc 1340 Pycnometer. Data is represented in

Table 3.5 *Specific density of the particles of different size*

Le Chatelier bottle			AccuPyc 1340 Pycnometer		
Particle size less 20 micron					
Mass, g	Volume, cm^3	Density, g/cm^3	Mass, g	Volume, cm^3	Density, g/cm^3
48.44	20	2.422	94	38.917	2.415
Particle size less 10 micron					
Not available			24	35.1738	0.6823

Since the density of particles of size 20 micron is high it is difficult to keep them in suspension and smaller particles were used in the experiments. Calculate the dispersion ability, *D*, and specific surface *S* using Eq. (**2.1**) and Eq. (**2.2**).

$$D = \frac{1}{8.105} = 0.123 \cdot 10^6\ \frac{1}{\text{m}},$$

$$S = \frac{6 \cdot 0.123}{0.6823} = 1.082\ \frac{m^2}{\text{g}}.$$

3.2.2 Experimental methods

Liquid – liquid system

The experiments were carried out by an OFITE Model 900 Viscometer (see Figure 3.1). The experimental procedure for liquid - liquid system is following:

- measuring the rheological constant of continuous phase (at least three repetitions);
- adding certain amount of dispersed phase into the gap through the holes in the outer cylinder, by using syringe with the needle as it is shown in Figure 3.10;
- adjusting instrument that both continuous phase and dispersed phase are in the gap at measuring position;
- measuring the rheological constant of two-phase system (at least three repetitions).

Liquid – solid particle system

For liquid – solid particle system the experimental procedure is following:

- measuring the rheological constant of continuous phase (at least three repetitions);
- adding certain amount of dispersed phase (particles) into the beaker with continuous phase and mixing it to obtain dispersed system (particles are homogeneously distributed in the liquid volume);
- adjusting instrument at measuring position;
- measuring the rheological constant of two-phase system (at least three repetitions).

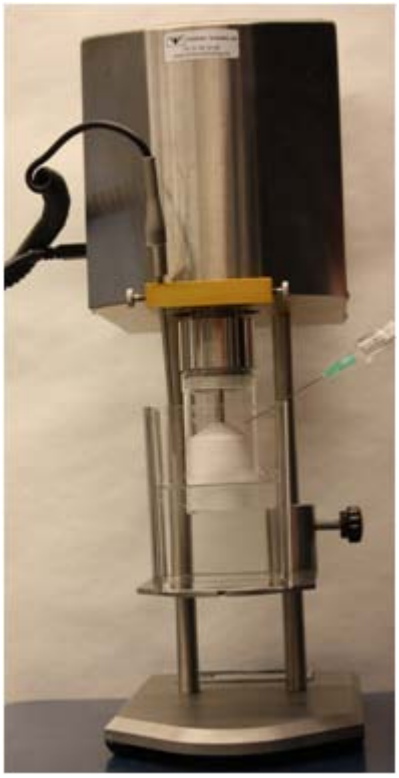

Figure 3.10 *Oil injection into the gap*

Rheological test description:

Rotational test has been used in the experiments. At each RPM five values of shear stress (viscosity) were continiously measured during 10 seconds of measuring time for each of values. The experiments were started at a low rotating speed and then increased in steps. At each step the velocity mainatined constant for 50 seconds, allowing the torque to stabilize. The break time (the system was not rotating) between every RPM was 10 seconds.

- rotational test, Newtonian fluid;
- motor speeds (RPM) (1, 2, 3, 6, 30, 60, 90, 200, 300, and 600);
- 5 values of shear stress (viscosity);
- measuring time is 10 seconds;
- break time is 10 seconds;
- constant temperature 20 ^{0}C.

4. RESULTS AND DISCUSSION

4.1 Water Oil Marcol 82 mixture

The summary of the experimental shear stress and viscosity data is represented in Table C. 1 (Appendix C – Measured Data of Multiphase Systems). The data at 1021 s^{-1} shear rate were chosen as optimal for discussion, because the accuracy of measurements is less at a lower shear rate. The experimental results used in comparison with the different correlations.

Shear stresses and viscosities recorded in the experiments at optimal shear rate for different concentration of oil are represented in Table 4.1. It is necessary to mention that concentration of oil in this case is the ratio between volume of oil presents in the gap and the total volume of the gap (the summary volume of oil and water in the gap).

Table 4.1 *Experimental data of oil and water mixture*

Concentration, %	0	28.12	56.23	84.35	100
Shear stress, Pa	1	9.9	19.4	26.46	27.86
Viscosity of suspension, cP	0.98	9.7	19	25.94	27.28

Shear stress increases with concentration of oil. The plot shear stress against concentration is illustrated in Figure 4.1.

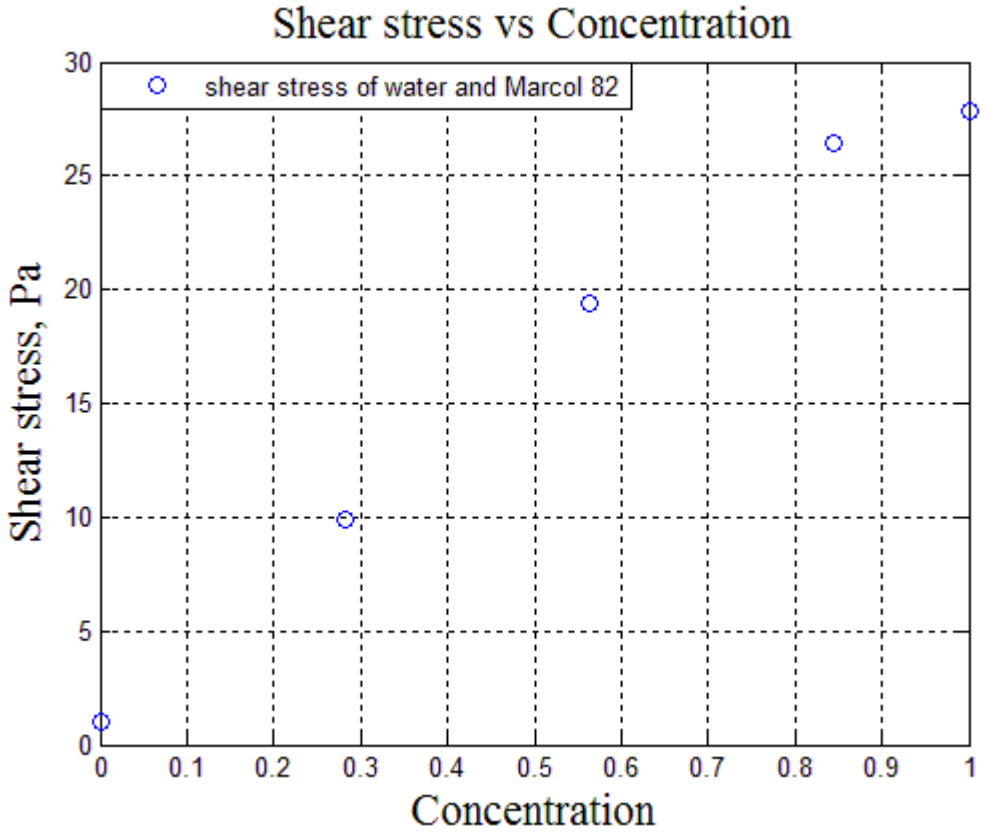

Figure 4.1 *Experimental shear stress data, showing shear stress as a function of oil concentration (28%, 56% and 84% of oil). Two shear stress points at concentrations of 0 and 1 correspond to shear stresses of water and oil Marcol 82, respectively*

It can be noticed from the Figure 4.1 that shear stress increases non-linearly with concentration of oil. It indicates the presence of one fluid in the volume of another fluid while rotational test.

Consider the gap filled by water and oil. Due to density difference oil as a lighter fluid is on the top of the gap and water occupies the lower part. The height of oil layer in the gap is h_o, and water layer is h_w. When the outer cylinder rotates at a constant rate (ω rad s^{-1}) bob twists against the torsion wire by viscous drag of two liquids against the surface. Torque applied by the moving oil is τ_o and by the moving water is τ_w. Schematically this situation is shown in Figure 4.2.

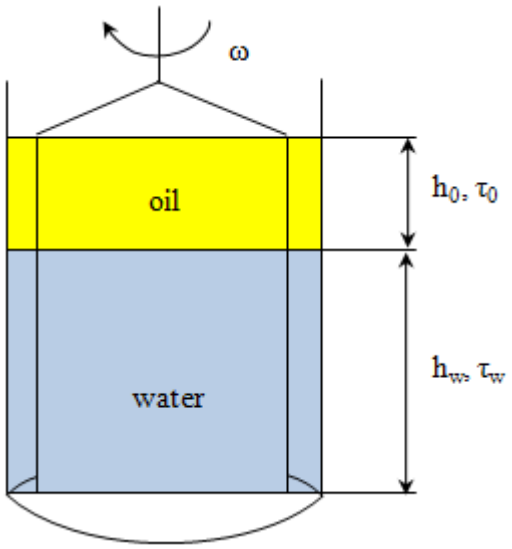

Figure 4.2 *Distribution of two fluids in the gap. Oil Marcol 82 occupies the upper part of the annulus and water is on the lower part*

Assume that oil and water were not mixed while rotation and stratified flow was observed in the gap. Total shear stress of the system then can be determined as

$$\tau = \frac{1}{H} \cdot \left(h_o \cdot \tau_o + h_w \cdot \tau_w \right), \tag{4.1}$$

where $H = h_o + h_w$ is the height of the bob.

Calculate the shear stress when concentration of oil in the gap is 28.12 % using Eq. 4.1:

$$\tau = \frac{1}{38} \cdot \left(10.69 \cdot 27{,}86 + 27.31 \cdot 1 \right) = 8{,}56 \text{ Pa}.$$

The result of calculations of shear stress for the rest volume concentrations is represented in Table 4.2.

Table 4.2 *Shear stress calculated for different concentration of oil in the gap*

Concentration of oil, %	28.12	56.23	84.35
Height of oil, mm	10.69	21.37	32.05
Height of water, mm	27.31	16.63	5.95
Shear stress, Pa	8.6	16.1	23.7

Compare experimental data with calculated results represented in Figure 4.3.

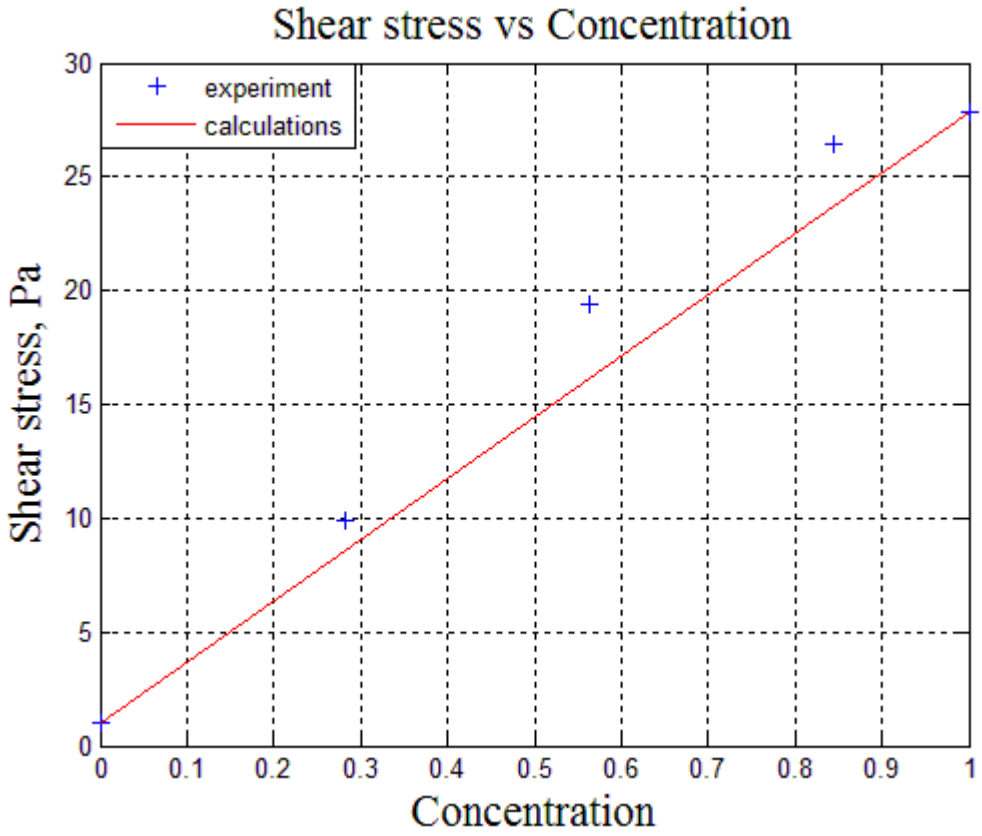

Figure 4.3 *Shear stress as a function of oil concentration. Experimental data are represented by the pluses and calculated data are shown by the line*

It can be seen from Figure 4.3 that experimental shear stress results are higher than shear stress calculated for the stratified flow in the gap. Mixing of oil and water can be explained by the lift force effect discussed in section 2.10, which appears in a shear flow. When outer cylinder begins to rotate the water layer in the gap starts to move faster than the oil layer and some amount of oil goes to the water phase due to lift force. High surface tension prevents oil phase moving into water phase.

Besides, the different volume fraction of oil (volume of oil in the water phase) for different concentration can be observed in Figure 4.3. So the highest volume fraction is seemed to be with oil concentration of 56.23 %.

4.2 Diluted red ethanol and oil Bayol 35 system

Working with red ethanol experiments were run with the original setup (metal bob, metal outer cylinder and glass beaker). Acrylic has poor resistance to many solvents and chemicals due to easily hydrolyzed ester groups and can be destroyed (swelling, cracks) [22].

A number of tests were made to obtain appropriate properties of the diluted red ethanol. Water and red ethanol were mixed in different proportions and after oil was added. Good mixing of diluted red ethanol and water even at low RPM was observed at proportion: 20% of water and 80% of red ethanol.

The experimental shear stresses and viscosities are represented in Table C. 2 – Table C. 8 *Oil Bayol 35 measured data - 3 repetitions* (Appendix C – Measured Data of Multiphase Systems). The data obtained at 1021 s^{-1} shear rate are represented in Table 4.3.

Table 4.3 *Viscosity and shear stress experimental data of diluted red ethanol and Bayol 35*

Concentration, %	0	18.74	37.49	56.23	74.98	93.72	100
Shear stress, Pa	1.9	2.2	2.2	2.2	2.2	2.2	2.2
Viscosity of suspension, cP	1.9	2.2	2.2	2.2	2.2	2.2	2.2

Viscosity of dispersed system against oil concentration in the gap is shown in Figure 4.4.

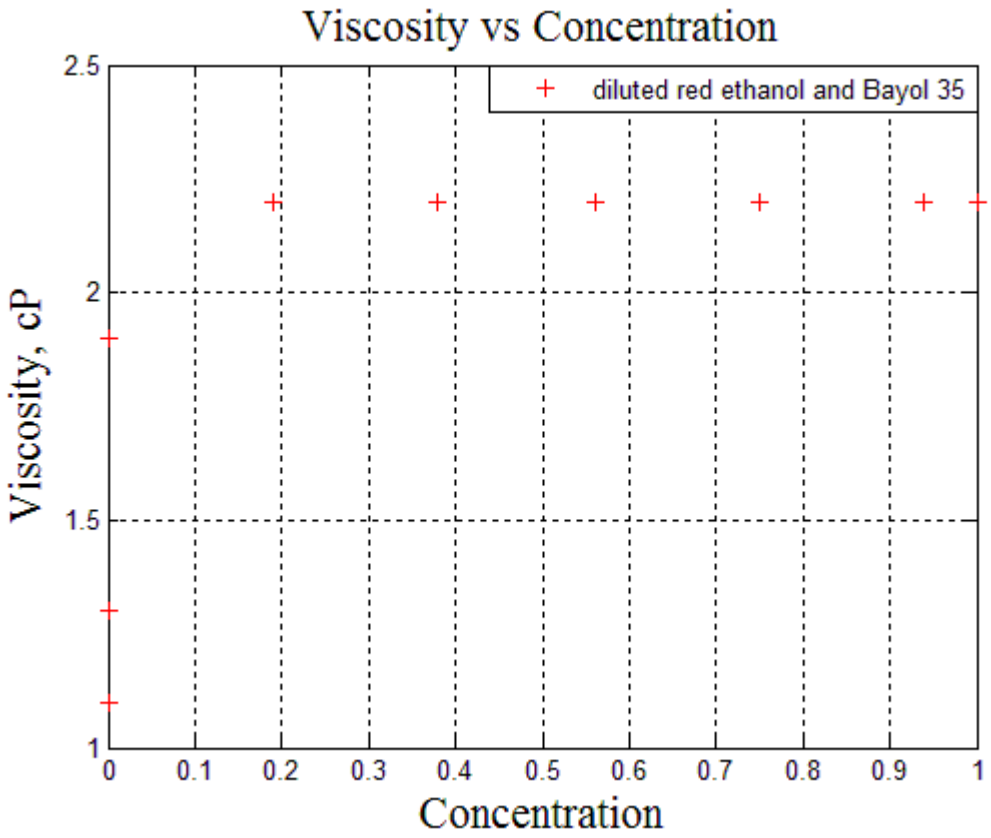

Figure 4.4 *Experimental viscosity of diluted red ethanol and oil Bayol 35 system as a function of oil concentration (19%, 37%, 56%, 75% and 94%). Three viscosity points from the lower to higher at concentration of 0 are represented viscosities of water, red ethanol and diluted red ethanol, respectively. The point at concentration of 1 corresponds to viscosity of oil Bayol 35*

From Table 4.3 and Figure 4.4 it can be seen that there is no difference in shear stress and viscosity for different concentration of oil. Also viscosity of dispersed system is constant.

Two points on the plot that are 1.1 cP and 1.3 cP correspond to viscosity of water and viscosity of alcohol respectively. The viscosity of diluted red ethanol (1.9 cP) is higher than viscosity of water or viscosity of red ethanol. It can be explained by the hydrogen bonding (attractive interaction of a hydrogen atom with an electronegative atom) between water and red ethanol molecules.

Figure 4.4 indicates that maximum viscosity of diluted red ethanol – Bayol 35 system is equal to viscosity of oil (2.2 cP) for minimum concentration of oil (18.74 %) has been used.

Consider the gap filled by diluted red ethanol. When certain amount of Bayol 35 is added into the gap the situation is following: oil is on top of the gap and diluted red ethanol is at the lower part. While rotation a strong mixing zone appears between oil and diluted red ethanol layers. Figure 4.5 schematically represents this situation.

Like in previous case this can be explained by the lift force effect between two liquids. But in this system more oil phase easily goes to diluted red ethanol phase. The reason is attractive forces (section 2.5.1) between molecules of Bayol 35 oil (lower viscosity) is less than attractive force of Marcol 82 oil (higher viscosity). Also surface tension between diluted red ethanol and Bayol 35 is less than surface tension between Marcol 82 and water. So, less energy (work) is necessary to break the molecular bonds (structure) and transfer certain amount of Bayol 35 than Marcol 82 into continuous phase.

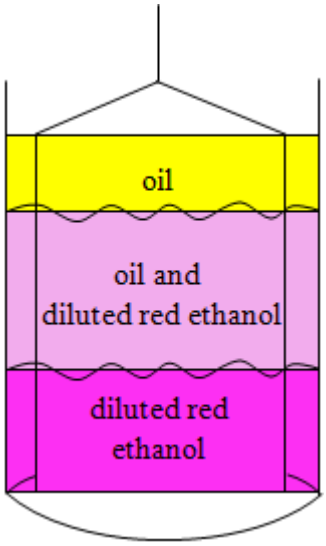

Figure 4.5 *Distribution of oil and red ethanol in the annulus during rotation. Oil Bayol 35 occupies the upper part of the gap, diluted red ethanol is on the lower part and certain amount of the oil presents in the diluted red ethanol phase*

Determine the volume fraction of oil for viscosity of the system of 2.2 cP using Eq. (**2.34**)

$2.2 = 1.9 \cdot (1+2.5 \cdot \varphi)$, consequently, $\varphi = 0.063$.

The data obtained for less volume fraction are shown in Table 4.4 and Figure 4.6.

Table 4.4 *Viscosity and shear stress experimental data of diluted red ethanol and Bayol 35*

Volume fraction, %	0	1.6	3.1	3.6	4.1	4.6	4.6
Shear stress, Pa	1.5	1.6	1.7	1.8	1.9	2.0	2.1
Viscosity of suspension, cP	1.5	1.6	1.7	1.8	1.9	2.0	2.1

Table 4.4 continued

Volume fraction, %	4.8	5.3	5.5	5.5	5.5	5.5	6.0
Shear stress, Pa	2.2	2.3	2.4	2.5	2.6	2.7	2.8
Viscosity of suspension, cP	2.2	2.3	2.5	2.6	2.7	2.8	2.9

It can be seen from Figure 4.6 and Table 4.4 that viscosity increases linearly with volume fraction in three regions marked with line.

Viscosities obtain in the experiments and calculation using different viscosity models discussed in section 2.8 are represented in Figure 4.7 and recorded in Table 4.5.

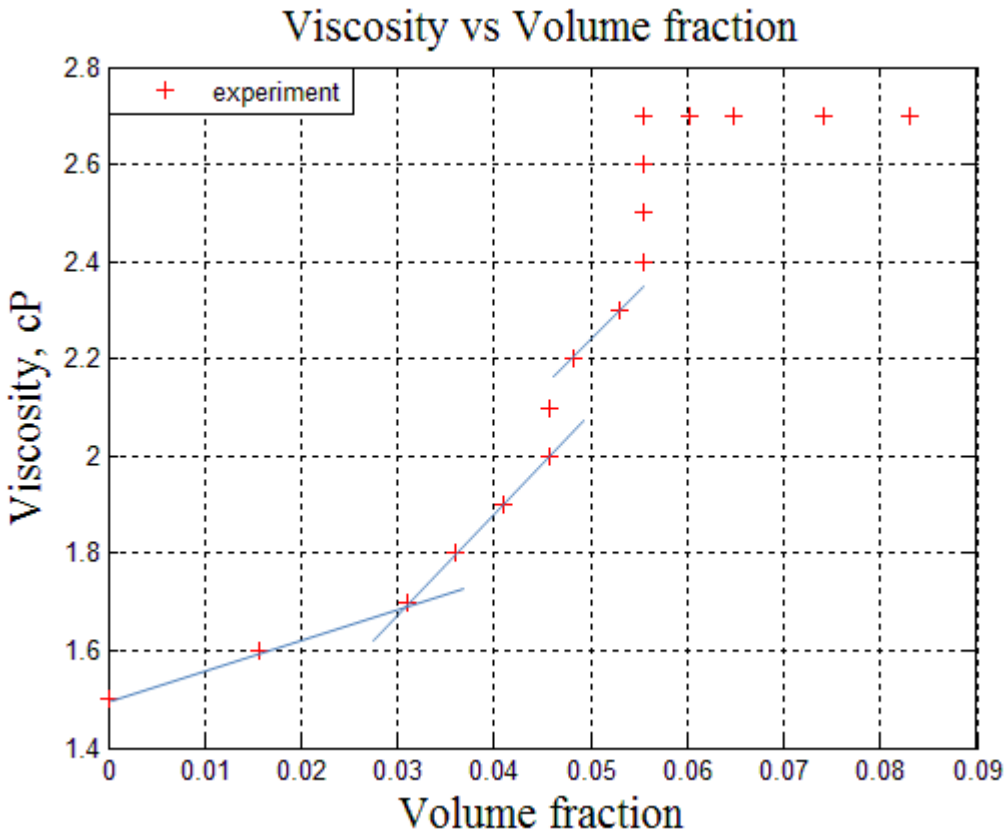

Figure 4.6 *Experimental viscosity of diluted red ethanol and oil Bayol 35 system as a function of oil volume fraction. Lines show linearity of the viscosity rising*

Table 4.5 *Viscosity data of diluted red ethanol and oil Bayol 35 system, calculated using different viscosity models*

φ	Einstein	Batchelor	Kitano	Mooney	Krieger-Dougherty	Chong
0.0157	1.56	1.56	1.57	1.56	1.57	2.03
0.0310	1.62	1.63	1.63	1.63	1.63	2.65
0.0360	1.63	1.65	1.66	1.65	1.66	2.87
0.0409	1.65	1.67	1.68	1.67	1.68	3.11
0.0458	1.67	1.69	1.70	1.69	1.70	3.35
0.0458	1.67	1.69	1.70	1.69	1.70	3.35
0.0482	1.68	1.70	1.72	1.71	1.72	3.48
0.0530	1.70	1.73	1.74	1.73	1.74	3.74
0.0554	1.71	1.74	1.75	1.74	1.75	3.87
0.0554	1.71	1.74	1.75	1.74	1.75	3.87
0.0554	1.71	1.74	1.75	1.74	1.75	3.87
0.0554	1.71	1.74	1.75	1.74	1.75	3.87
0.0554	1.71	1.74	1.75	1.74	1.75	3.87
0.0554	1.71	1.74	1.75	1.74	1.75	3.87

*Table 4.5*Table 4.9 *continued*

φ	Einstein	Batchelor	Kitano	Mooney	Krieger-Dougherty	Chong
0.0602	1.73	1.76	1.78	1.77	1.78	4.15
0.0648	1.74	1.78	1.80	1.79	1.80	4.44
0.0741	1.78	1.83	1.85	1.84	1.85	5.05
0.0831	1.81	1.88	1.90	1.90	1.90	5.70

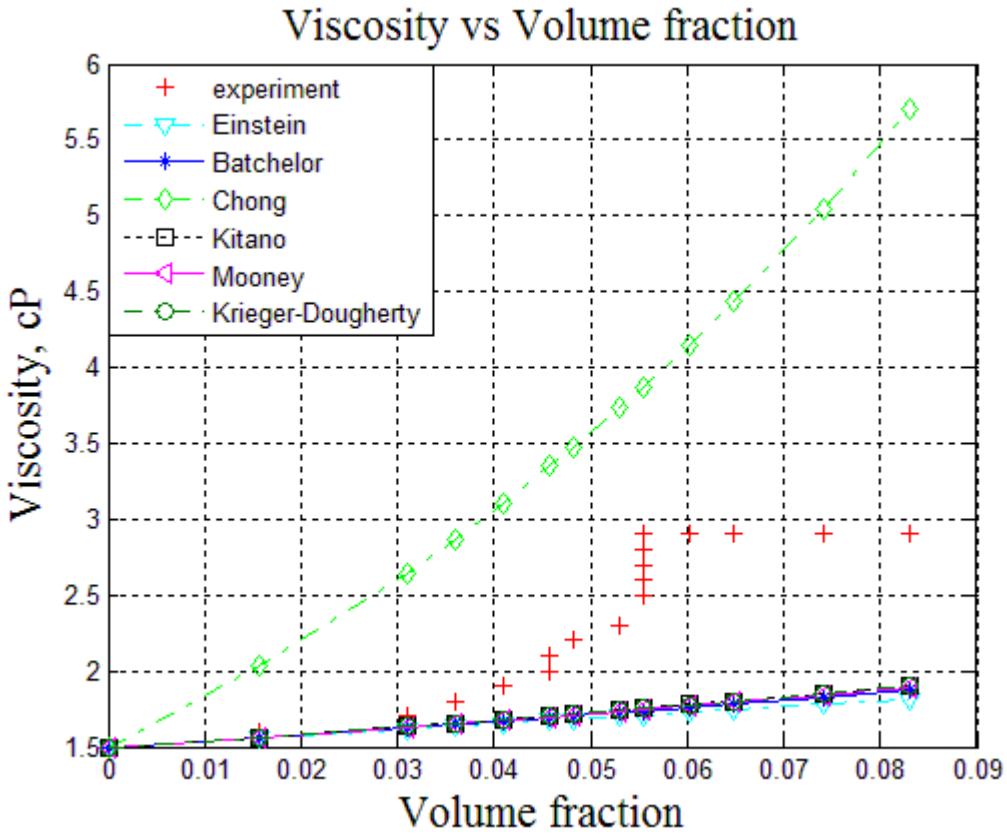

Figure 4.7 *Viscosity data of diluted red ethanol and oil Bayol 35 system as a function of oil volume fraction. Experimental data are represented by the pluses and calculated data are shown by the lines corresponded to different viscosity correlations*

4.3 Glycerol and spherical glass beads system

A number of tests have been done to obtain an appropriate suspension. Different sizes of particles, and glycerol diluted by water in different proportions were investigated. Properties of particles and diluted glycerol are represented in Appendix A - Particle Size Distributionand Appendix B – Properties of Glycerol and Water Mixture.

Dynamics of glycerol and spherical glass beads system in rotating annulus at 200 RPM is represented in Figure 4.8. The beginning of rotation is shown in Figure 4.8, a and the annulus after 30 seconds of rotation is represented in Figure 4.8, d.

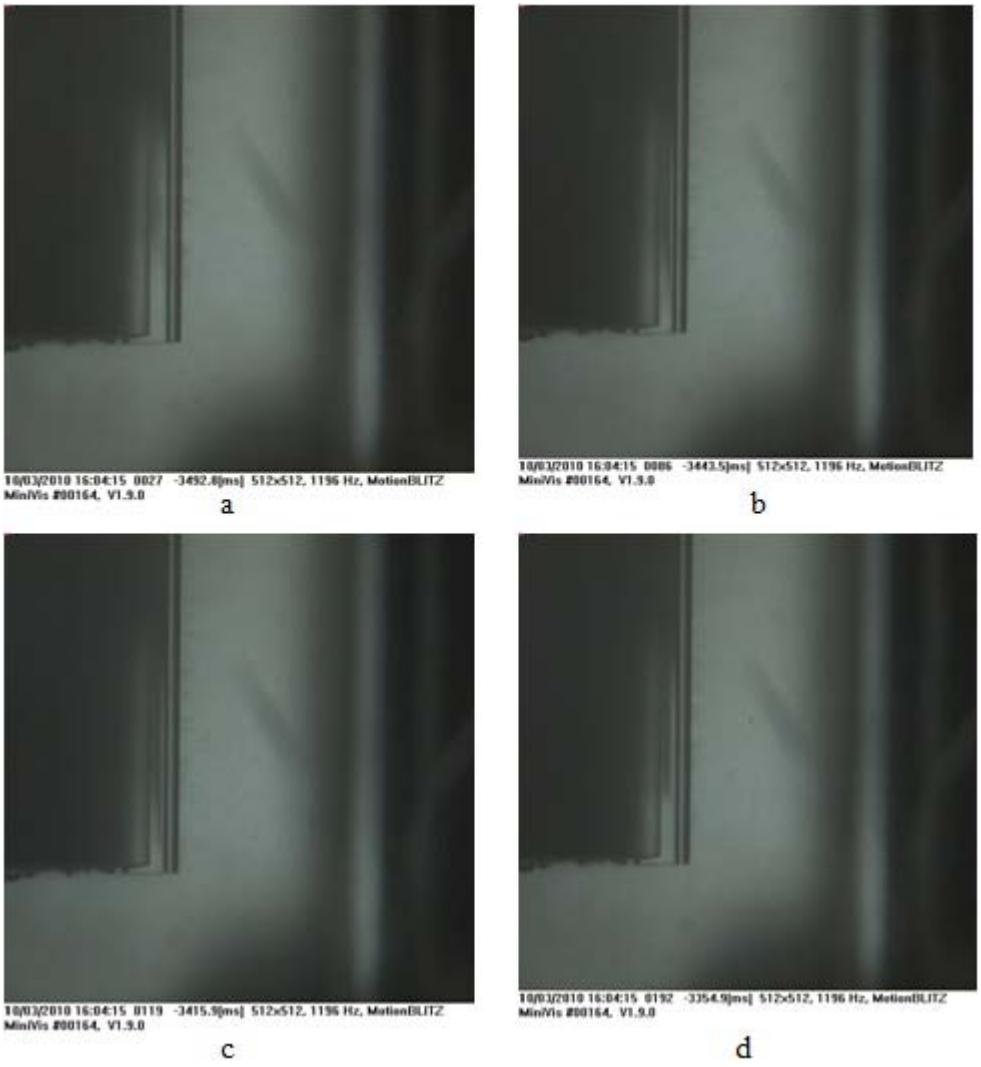

Figure 4.8 *Glycerol and glass beads dispersed system in rotating annulus at 200 RPM: a – start of rotation, b – after 12 seconds of rotation, c – after 20 seconds of rotation, d – after 30 seconds of rotation.*

The experimental shear stresses and viscosities data is represented in Table C. 9 – Table C. 16 (Appendix C – Measured Data of Multiphase Systems). The data obtained at 1021 s^{-1} shear rate are represented in Table 4.6.

Table 4.6 *Viscosity and shear stress data of glycerol and glass beads dispersed system at different volume fraction*

Volume fraction, %	0	0.3	0.6	0.9	1.2	1.5	1.8	2.1
Shear stress, Pa	111.82	114.28	123.8	130.24	131.68	141.32	158.4	150.84
Viscosity, cP	109.48	111.92	121.24	127.56	128.98	138.42	155.16	147.84

Figure 4.9 represents viscosity against volume fraction plot. It can be seen from Table 4.6 and Figure 4.9 that viscosity of dispersed system increases with volume fraction non-linearly. By plotting a trend line it is possible to observe four points lying on a line and four points out of it. The slope of the trend line can be determined as

$\eta = \eta_o \cdot (1 + k \cdot \varphi)$, using differentiation $\frac{\partial \eta}{\partial \phi} = \eta_o \cdot k$ find k as (4.2)

$$k = \frac{1}{\eta_o} \cdot \frac{\partial \eta}{\partial \phi} = \frac{1}{109.48} \cdot \frac{138.42 - 109.48}{0.015} = 17.62 .$$

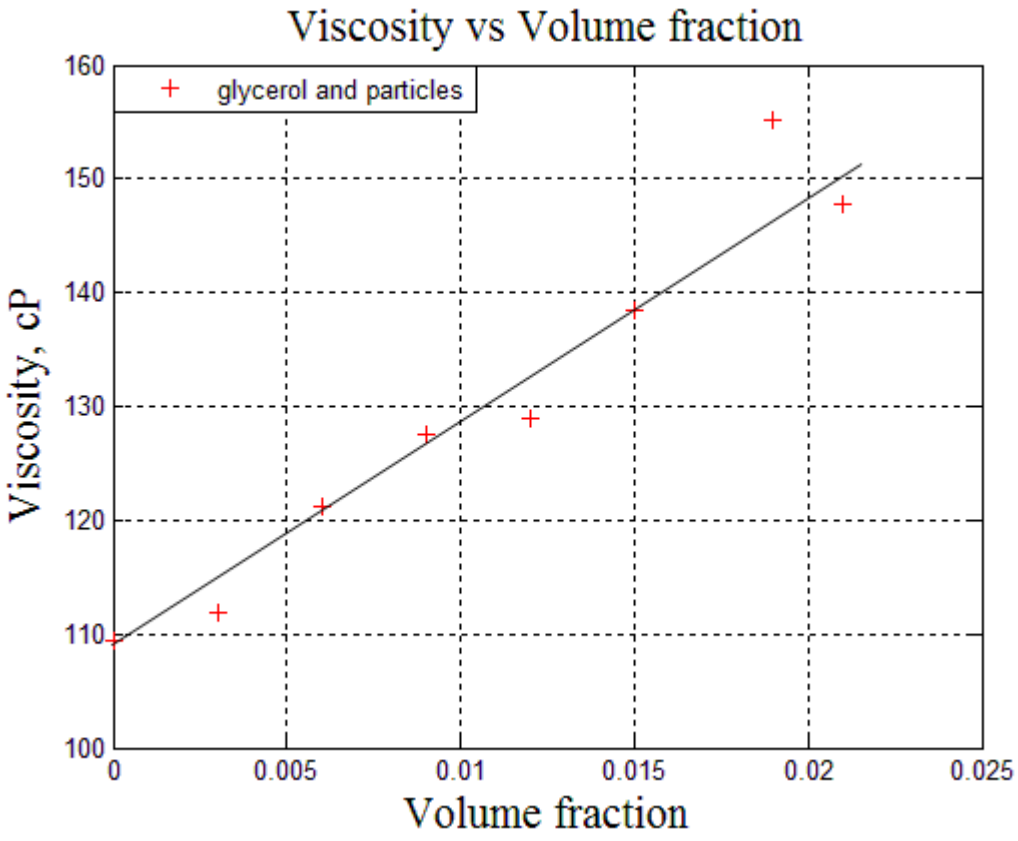

Figure 4.9 *Experimental data of glycerol and glass beads dispersed system, showing viscosity as a function of glass beads volume fraction. The experimental data is represented with the trend line*

According to Einstein model (**2.34**) the slope should be 2.5. Table 4.7 shows calculations of viscosity using Einstein model. The volume fraction of particles is calculated using Eq. (**2.15**).

Table 4.7 *Calculated volume of particles, volume fraction and viscosity of glycerol and glass beads dispersed system*

Mass of particles, g	0.3	0.6	0.9	1.2	1.5	1.8	2.1
Volume of particles, cm^3	0.44	0.88	1.32	1.76	2.20	2.64	3.08
Volume fraction, %	0.292	0.583	0.872	1.159	1.444	1.823	2.011
Viscosity of suspension, cP	110.28	111.08	111.87	112.65	113.43	114.47	114.98

Experimental data and calculation results are represented in Figure 4.10. Since Einstein model was obtained for special conditions and it neglects effects of interaction between particles, forces which present in the flow, the higher viscosity obtained in the experiments.

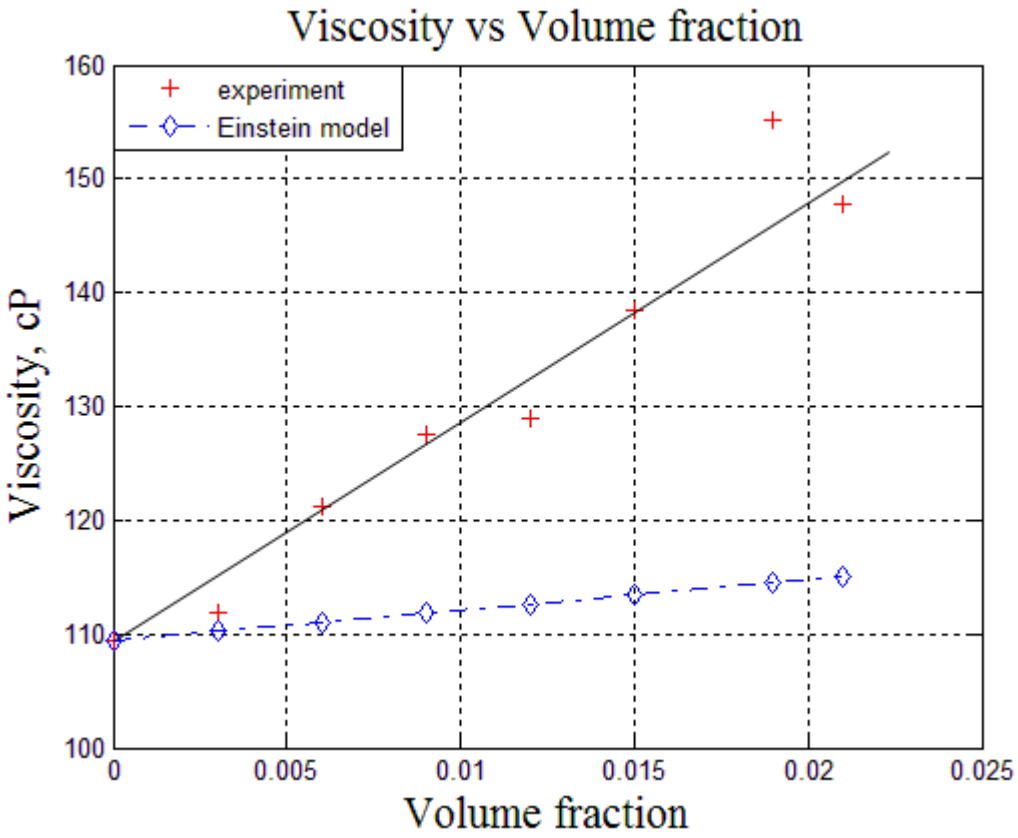

Figure 4.10 *Viscosity data of glycerol and glass beads dispersed system as a function of glass beads volume fraction. Experimental data are represented by the pluses with the trend line and calculated data corresponded to Einstein model are shown by the dash-and-dot line*

Predict the viscosity of dispersed system using different viscosity models. Calculated data are represented in Table 4.8. It can be seen from Table 4.8 and Figure 4.11 that determined viscosities similar to viscosity calculated by Einstein model. The viscosity defined by empirical formula suggested by Chong is close to the viscosity obtained in the experiments and Frankel and Acirvos model can be used for dispersed system with high volume fraction (close to φ_m) and for dilute dispersed system it is not suited.

Table 4.8 *Viscosity calculations of glycerol and glass beads dispersed system, using different viscosity correlations*

φ	Frankel-Acirvos	Batchelor	Kitano	Mooney	Krieger-Dougherty	Chong
0.0029	23.12	110.29	110.35	110.29	110.35	116.09
0.0058	30.59	111.10	111.23	111.10	111.22	122.91
0.0087	36.28	111.92	112.11	111.92	112.10	129.93
0.0116	41.10	112.74	112.99	112.75	112.99	137.17
0.0144	45.38	113.58	113.88	113.59	113.88	144.61
0.0182	50.40	114.69	115.08	114.72	115.07	154.88
0.0201	52.94	115.26	115.68	115.29	115.67	166.15

The viscosities in Table 4.7 and Table 4.8 were calculated for volume fraction of entire dispersed system volume. But during experiments volume fraction in the gap can change. For example, lift force affects on particles immediately below the gap making them move into the gap. Also in rotating system centrifugal force, Coriolis force and Euler force operate on particle. Consider possible particle distribution in the gap.

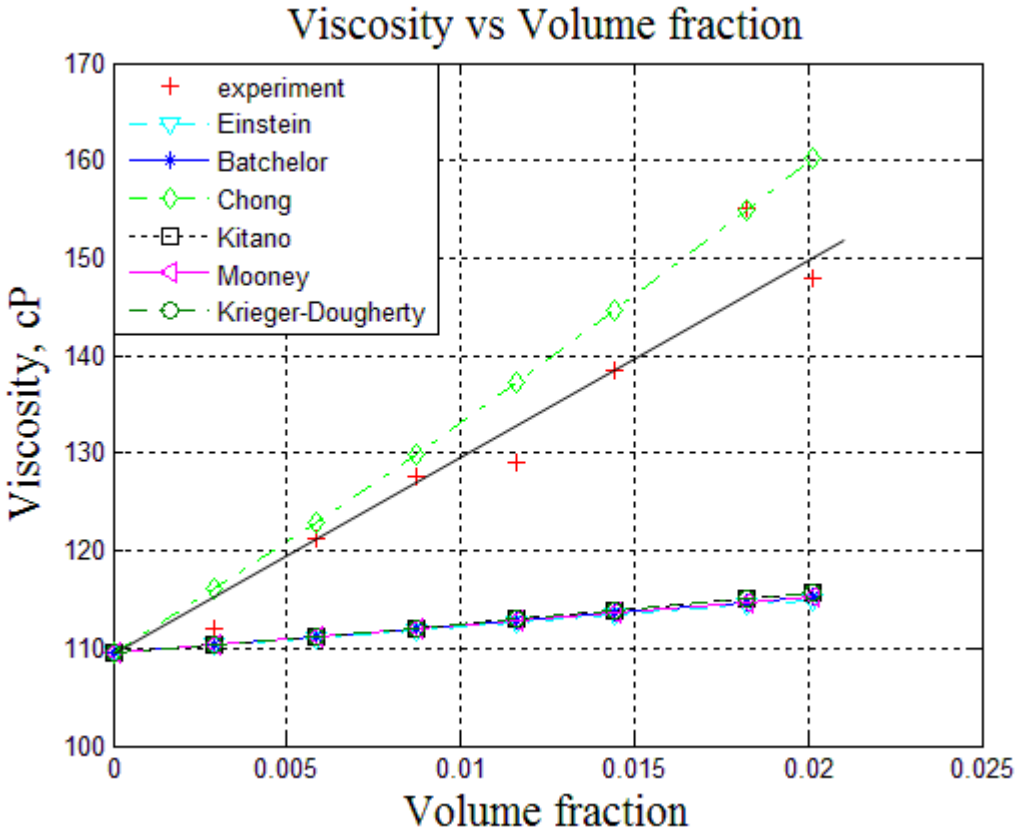

Figure 4.11 *Viscosity data of glycerol and glass beads dispersed system as a function of glass beads volume fraction. Experimental data are represented by the pluses with the trend line and calculated data are shown by the lines corresponded to different viscosity correlations*

Since some of the particles have lighter density than density of continuous phase they have tendency to float. Due to forces mentioned previously more particles gather in the gap. When certain amount of particles comes into the gap from outer chamber volume fraction of particles in the gap changes and it causes changes in shear stress and viscosity. Calculate initial amount of particles in the gap and estimate how the volume fraction changes when the particle amount increases in the gap. This situation is schematically shown in Figure 4.12

Volume of the suspension, $V_{susp.}$, in the gap is equal to the volume of gap, V_{gap}, and determined as

$$V_{susp.} = V_s + V_p = 5334.82 mm^3,$$

where V_p is volume of particles, cm^3,

V_s is volume of suspending medium, cm^3.

The initial volume fraction is $\varphi = 0.0029$. Using previous equation volume of particles is found as

$$V_{susp.} = \frac{V_p}{\phi} + V_p = V_p \cdot \left(\frac{1}{\phi} + 1\right), \tag{4.3}$$

$$V_p = \frac{V_{susp.}}{\left(\frac{1}{\phi}+1\right)} = \frac{5334.82}{\left(\frac{1}{0.0029}+1\right)} = 15.43 mm^3 .$$

Determine initial mass of particles in the gap as

$$m_p = \rho_p \cdot V_p = 0.6823 \cdot 0.01543 = 0.0105 g .$$

Consider situation when a beaker outside rotor contains 150 ml of glycerol and 0.3 g of glass beads in suspension. Assume that mass of particles in the gap increased twice during rotation and became $m_p = 0.021 g$. This situation is represented in Figure 4.12.

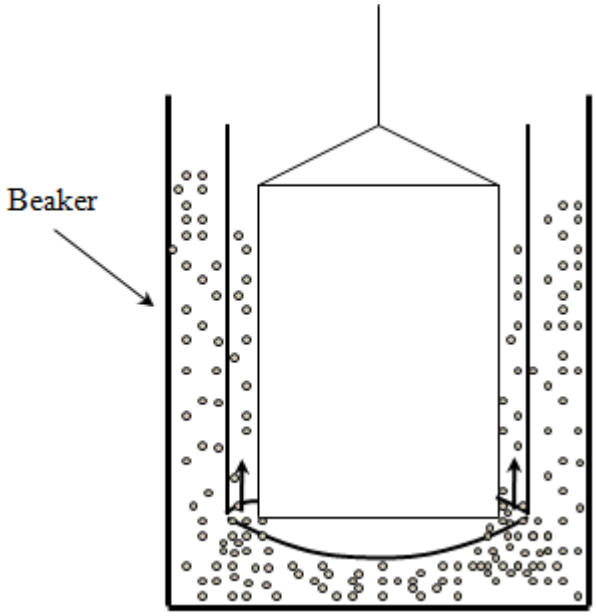

Figure 4.12 *Particle distribution in the annulus. Volume fraction of particles increases in the gap, if more particles come into the annulus from the beaker*

Calculate the volume of particles, V_p , volume fraction, φ , and viscosity of suspension, η , in the gap using formulas:

$$V_p = \frac{m_p}{\rho_p} = \frac{0.021}{0.6823} = 0.0308 cm^3 \ , \ \varphi = \frac{0.0308}{5.33} = 0.0058 .$$

Consequently, the volume fraction of particles increased twice with the twice increasing particle amount in the gap. Repeat calculation of the viscosity using different models with changed volume fraction and tabulate the results. The calculated data are represented in Table 4.9 and plotted in Figure 4.13.

Table 4.9 *Viscosity calculations of glycerol and glass beads dispersed system with twice increased volume fraction* φ

φ	Einstein	Batchelor	Chong	Kitano	Mooney	Krieger-Dougherty
0	109.48	109.48	109.48	109.48	109.48	109.48
0.0058	111.08	111.10	122.95	111.23	111.10	111.23
0.0117	112.67	112.76	137.34	113.01	112.77	113.01

Table 4.9 continued

φ	Einstein	Batchelor	Chong	Kitano	Mooney	Krieger-Dougherty
0.0174	114.25	114.46	152.69	114.83	114.48	114.82
0.0232	115.82	116.19	169.02	116.67	116.23	116.67
0.0289	117.39	117.95	186.36	118.56	118.03	118.55
0.0365	119.46	120.36	211.10	121.12	120.49	121.11
0.0402	120.49	121.58	224.18	122.42	121.76	122.41

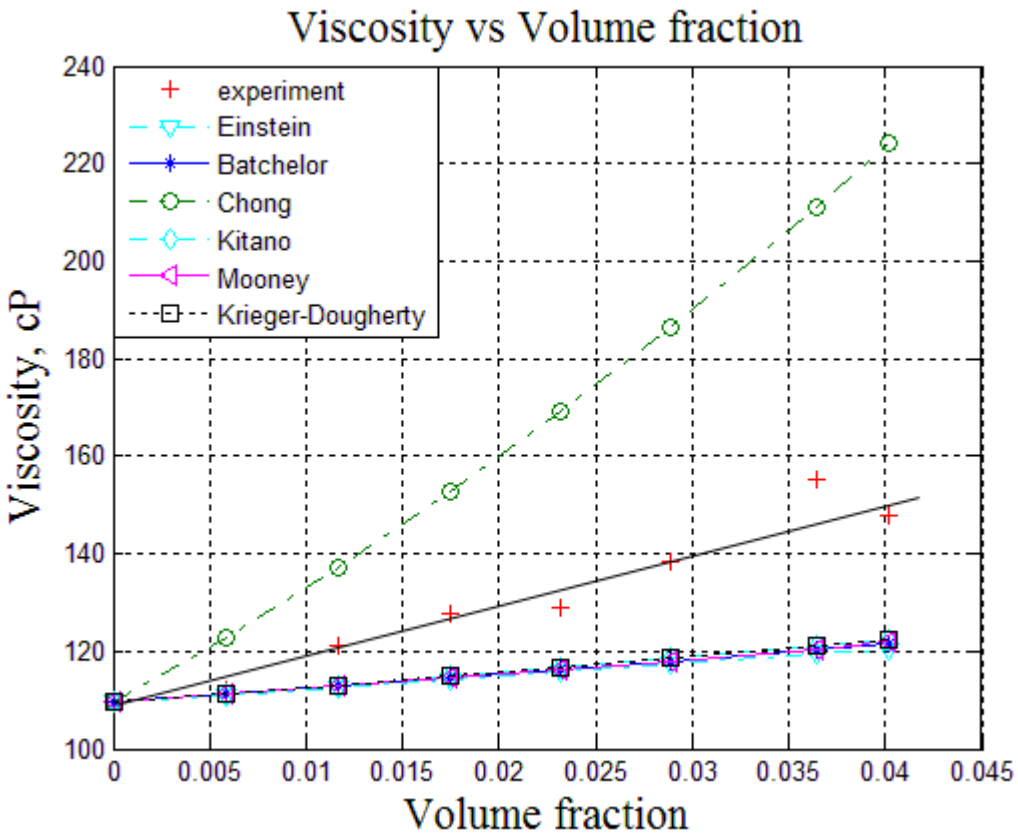

Figure 4.13 *Viscosity data of glycerol and glass beads dispersed system as a function of glass beads volume fraction. Experimental data are represented by the pluses with the trend line and calculated data are shown by the lines corresponded to different viscosity correlations. Calculated data were obtained for volume fraction increased twice*

From Table 4.9 and Figure 4.13 it is possible to see that Chong empirical formula does not fit to the proposed analysis so it will be excluded from further calculations.

Using iteration the optimal results of viscosity models were obtained when volume fraction was increased six times from initial volume fraction. This data are shown in Table 4.10 and Figure 4.14.

It can be seen from Table 4.10 and Figure 4.14 that one of the experimental points belongs to Einstein model, the line obtained by Batchelor's formula paths through one of the experimental points, and two experimental points are lying on the Krieger-Dougherty viscosity curve.

Table 4.10 *Viscosity calculations of glycerol and glass beads dispersed system with 6 times increased volume fraction φ*

φ	Einstein	Batchelor	Kitano	Mooney	Krieger-Dougherty
0	109.48	109.48	109.48	109.48	109.48
0.0175	114.28	114.49	114.86	114.51	114.85
0.0350	119.05	119.88	120.61	120.00	120.60
0.0523	123.80	125.65	126.77	126.02	126.75
0.0695	128.51	131.79	133.37	132.64	133.34
0.0867	133.20	138.30	140.45	139.93	140.42
0.1094	139.41	147.53	150.74	150.89	150.69
0.1206	142.50	152.38	156.28	156.97	156.23

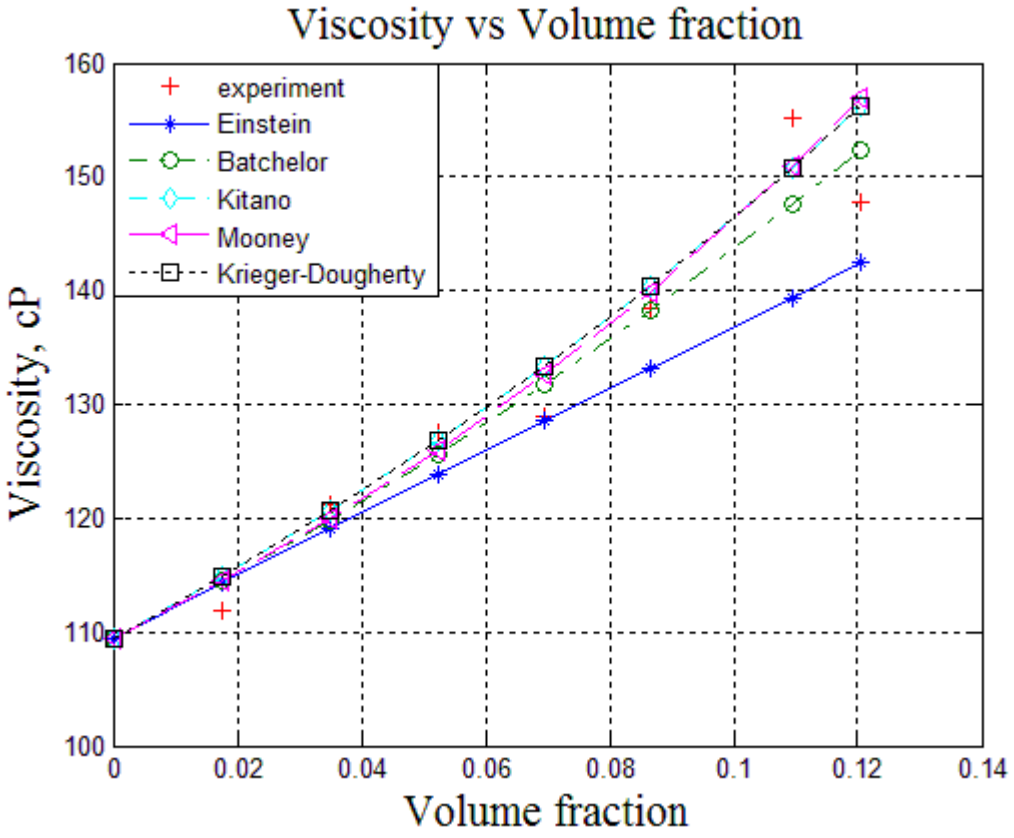

Figure 4.14 *Viscosity data of glycerol and glass beads dispersed system as a function of glass beads volume fraction. Experimental data are represented by the pluses with the trend line and calculated data are shown by the lines corresponded to different viscosity correlations. Calculated data were obtained for volume fraction increased 6 times*

4.4 Salt water and spherical glass beads system

The experimental shear stresses and viscosities data are represented in Table C. 17 – Table C. 24 (Appendix C – Measured Data of Multiphase Systems). The data obtained at 1021 s^{-1} shear rate are represented in Table 4.11.

Table 4.11 *Viscosity and shear stress of salt water and glass beads dispersed system for different volume fraction of glass beads*

Volume fraction, %	0	0.3	0.6	0.9	1.2	1.5	1.8	2.1
Shear stress, Pa	1.44	1.66	1.80	2.42	2.46	3.02	3.06	3.8
Viscosity, cP	1.42	1.6	1.8	2.4	2.42	2.92	2.98	3.72

From Table 4.11 and Figure 4.15 it can be seen that viscosity of the dispersed system increases with volume fraction non-linearly. By plotting a trend line it is possible to observe a range in measurements. The slope of the trend line is determined by Eq. (**4.2**).

$$k = \frac{1}{\eta_o} \cdot \frac{\partial \eta}{\partial \phi} = \frac{1}{1.42} \cdot \frac{3.25 - 1.42}{0.02} = 64.44 .$$

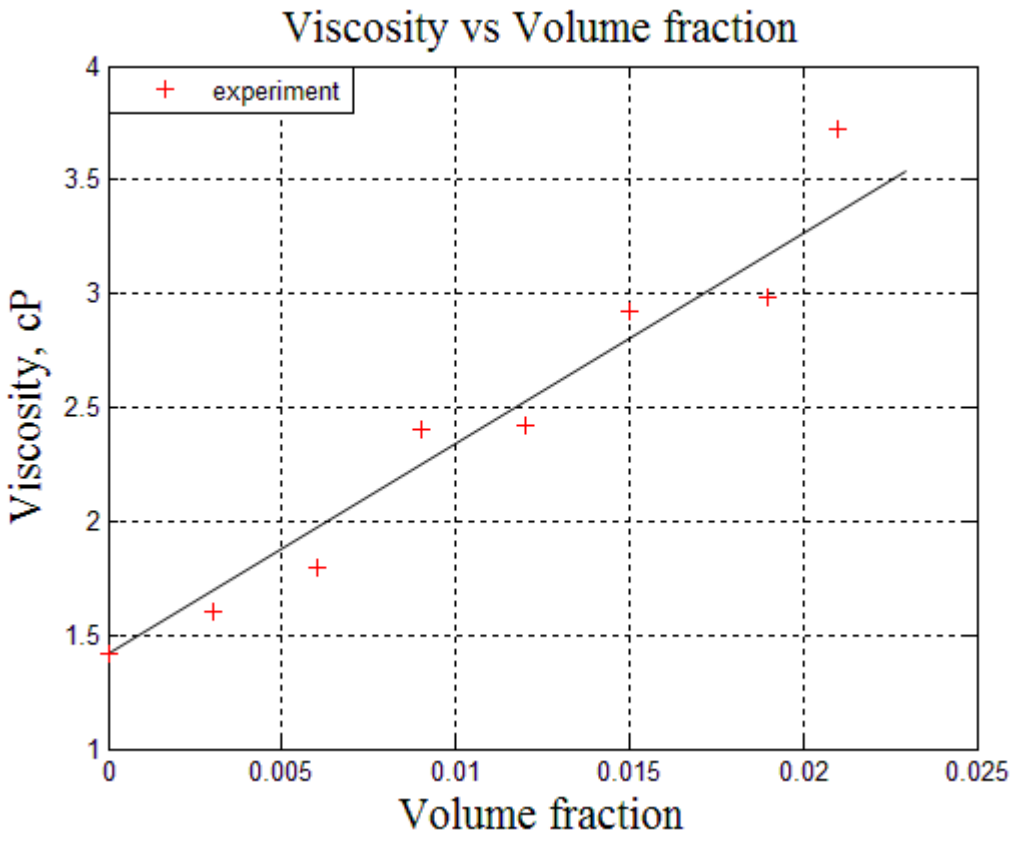

Figure 4.15 *Experimental data of salt water and glass beads dispersed system, showing viscosity as a function of glass beads volume fraction. The experimental data is represented with the trend line*

For this dispersed system the slope is much higher than it should be according to Einstein model. Observe the difference between experimental results and Einstein model in Table 4.12 and Figure 4.16. The volume fraction of particles is calculated by using (**2.15**).

Table 4.12 *Calculated volume of particles, volume fraction and viscosity of salt water and glass beads dispersed system*

Mass of particles, g	0.3	0.6	0.9	1.2	1.5	1.8	2.1
Volume of particles, cm^3	0.44	0.88	1.32	1.76	2.20	2.64	3.08

Volume fraction, %	0.292	0.583	0.872	1.159	1.444	1.823	2.011
Viscosity of suspension, cP	1.43	1.44	1.45	1.46	1.47	1.48	1.49

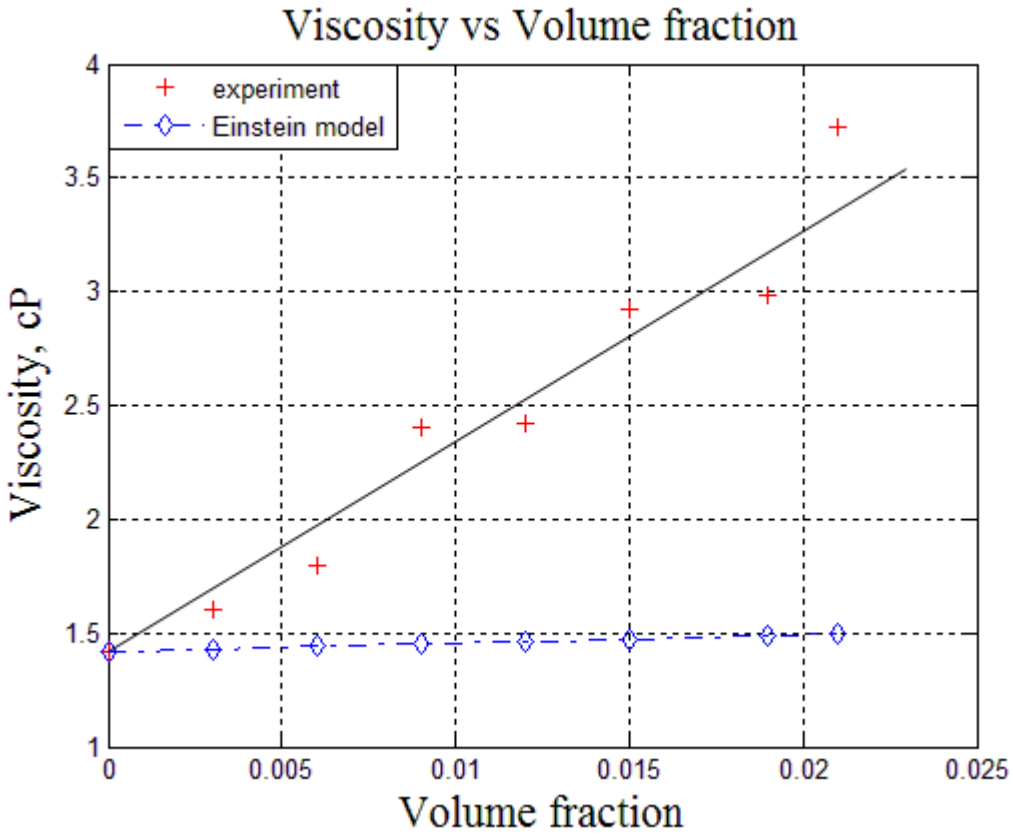

Figure 4.16 *Viscosity data of salt water and glass beads dispersed system as a function of glass beads volume fraction. Experimental data are represented by the pluses with the trend line and calculated data corresponded to Einstein model are shown by the dash-and-dot line*

Repeat analysis which was made for the previous dispersed system to predict the viscosity of salt water and glass beads system. Calculated data are represented in Table 4.13 and Figure 4.17. It can be seen from Table 4.13 and Figure 4.17 that determined viscosity defined by empirical formula suggested by Chong is close to the viscosity obtained in the experiments. Figure 4.18 and Table 4.14 represent the data calculated for twice increased volume fraction. It is possible to see from fig and table that Chong model covers two experimental points. To find out the volume fraction at which rest of the models fit the experimental results use iteration. This data are shown in Table 4.15 and Figure 4.19 for volume fraction which increased 15 times from initial volume fraction.

Table 4.13 *Viscosity calculations of salt water and glass beads dispersed system using different viscosity correlations*

φ	Batchelor	Kitano	Mooney	Krieger-Dougherty	Chong
0.0029	1.42	1.42	1.42	1.42	1.42
0.0058	1.43	1.43	1.43	1.43	1.51
0.0087	1.44	1.44	1.44	1.44	1.59
0.0116	1.45	1.45	1.45	1.45	1.69
0.0144	1.46	1.47	1.46	1.47	1.78
0.0182	1.47	1.48	1.47	1.48	1.88
0.0201	1.49	1.49	1.49	1.49	2.01

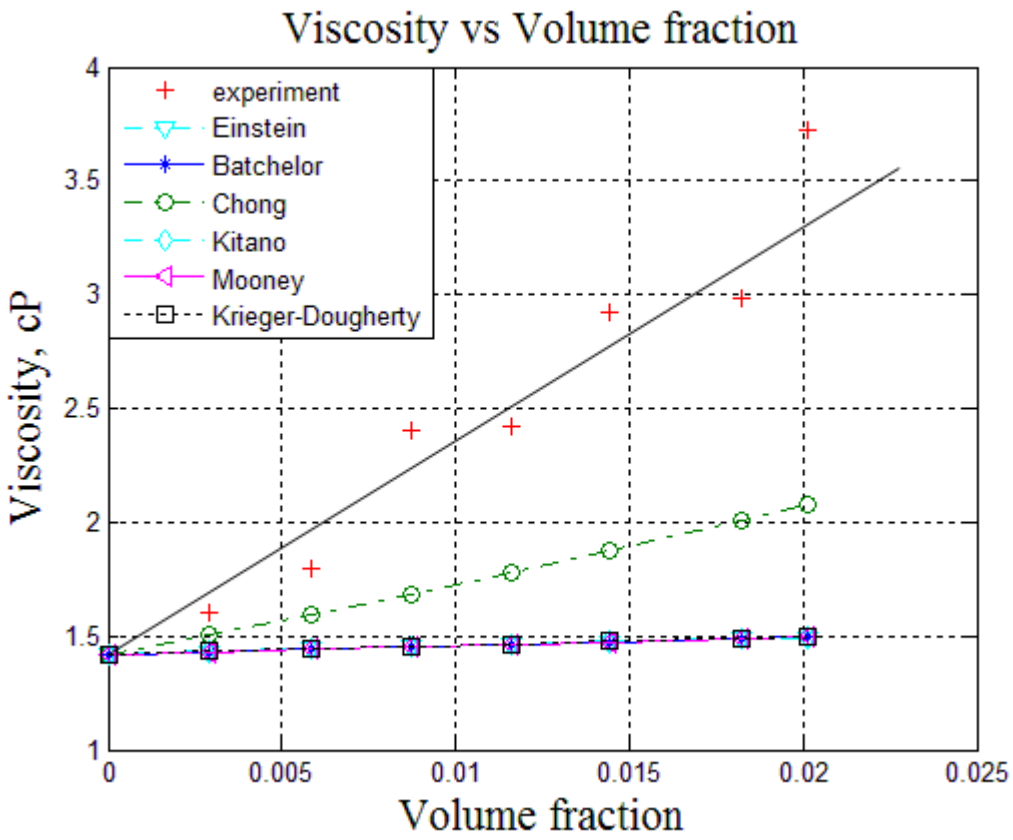

Figure 4.17 *Viscosity data of salt water and glass beads dispersed system as a function of glass beads volume fraction. Experimental data are represented by the pluses with the trend line and calculated data are shown by the lines corresponded to different viscosity correlations*

Table 4.14 *Viscosity calculations of salt water and glass beads dispersed system with twice increased volume fraction φ*

φ	Einstein	Batchelor	Kitano	Mooney	Krieger-Dougherty	Chong
0	1.42	1.42	1.42	1.42	1.42	1.42
0.0058	1.44	1.44	1.44	1.44	1.44	1.59
0.0117	1.46	1.46	1.47	1.46	1.47	1.78
0.0174	1.48	1.48	1.49	1.48	1.49	1.98
0.0232	1.50	1.51	1.51	1.51	1.51	2.19
0.0289	1.52	1.53	1.54	1.53	1.54	2.42
0.0365	1.55	1.56	1.57	1.56	1.57	2.74
0.0402	1.56	1.58	1.59	1.58	1.59	2.91

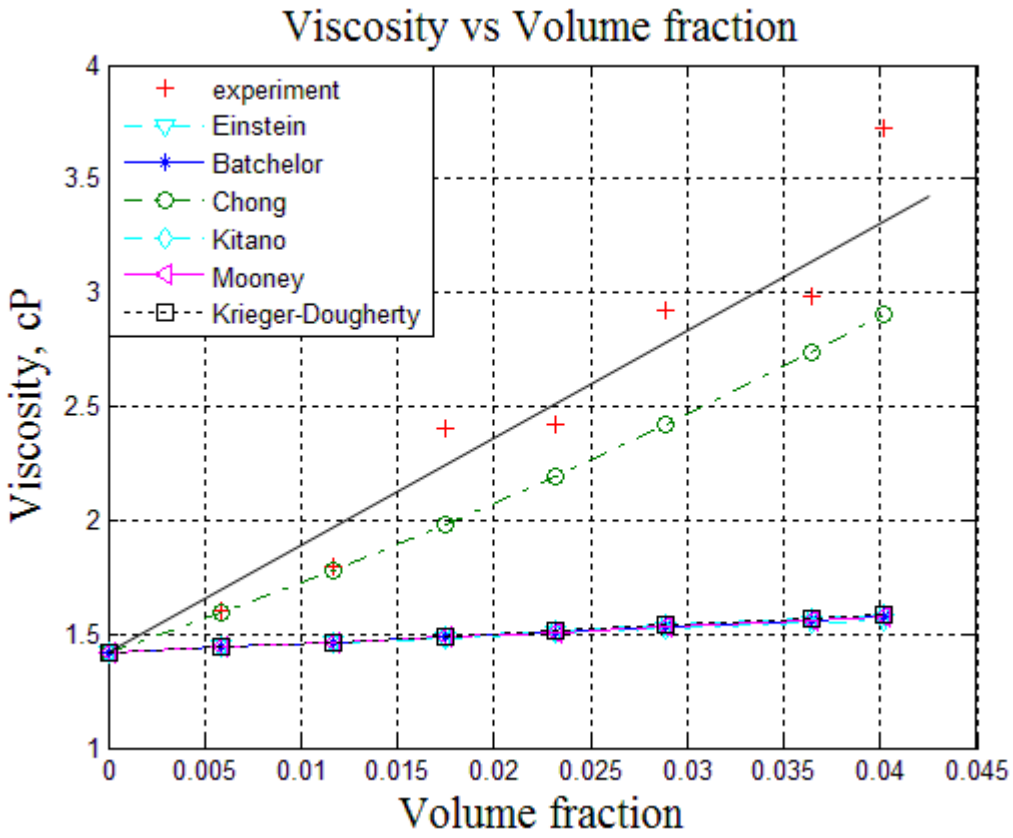

Figure 4.18 *Viscosity data of salt water and glass beads dispersed system as a function of glass beads volume fraction. Experimental data are represented by the pluses with the trend line and calculated data are shown by the lines corresponded to different viscosity correlations. Calculated data were obtained for volume fraction increased twice*

Table 4.15 *Viscosity calculations of salt water and glass beads dispersed system with 15 times increased volume fraction φ*

φ	Einstein	Batchelor	Kitano	Mooney	Krieger-Dougherty
0.00	1.42	1.42	1.42	1.42	1.42
0.04	1.58	1.59	1.60	1.60	1.60
0.09	1.73	1.80	1.83	1.82	1.83
0.13	1.88	2.03	2.09	2.11	2.09
0.17	2.04	2.30	2.43	2.51	2.42
0.22	2.19	2.60	2.84	3.05	2.84
0.27	2.39	3.05	3.57	4.20	3.57
0.30	2.49	3.29	4.05	5.07	4.04

It can be seen from Table 4.15 and Figure 4.19 that one of the experimental points belongs to Einstein model, the lines obtained by Batchelor's formula and Money path through two of the experimental points, and three experimental points are lying on the Krieger-Dougherty and Kitano viscosity curves.

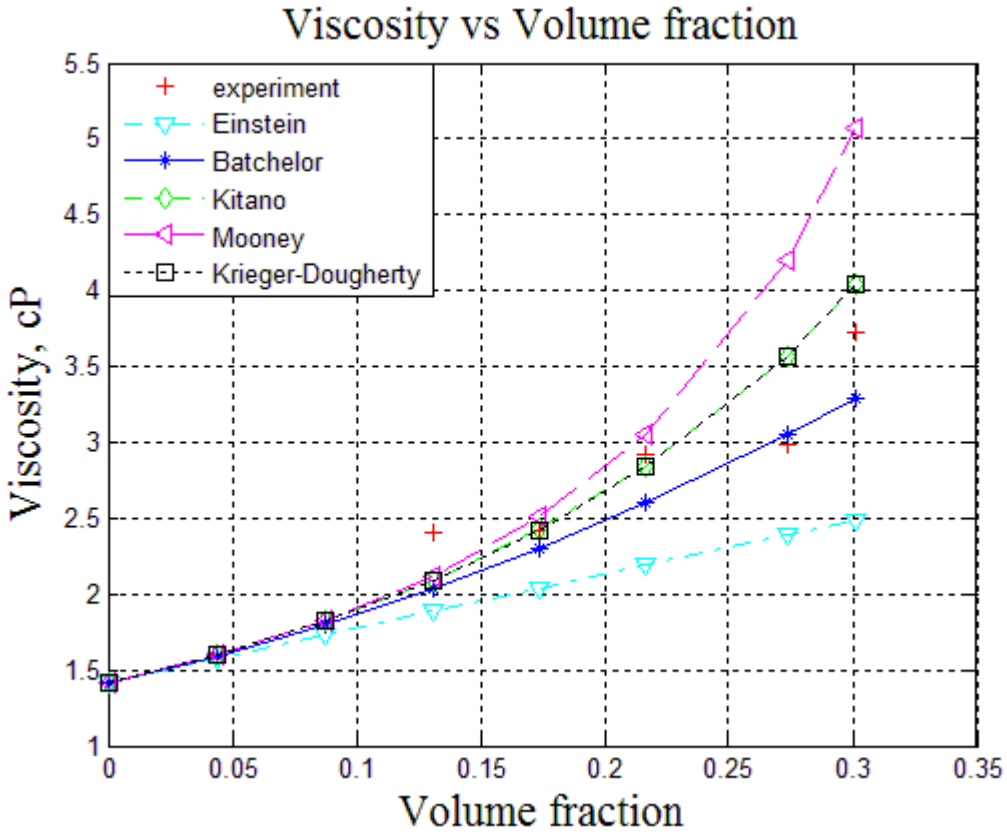

Figure 4.19 *Viscosity data of salt water and glass beads dispersed system as a function of glass beads volume fraction. Experimental data are represented by the pluses with the trend line and calculated data are shown by the lines corresponded to different viscosity correlations. Calculated data were obtained for volume fraction increased 15 times*

The volume fraction increase can be explained by density difference of the particles and continuous phase. Consider situation schematically represented in Figure 4.20

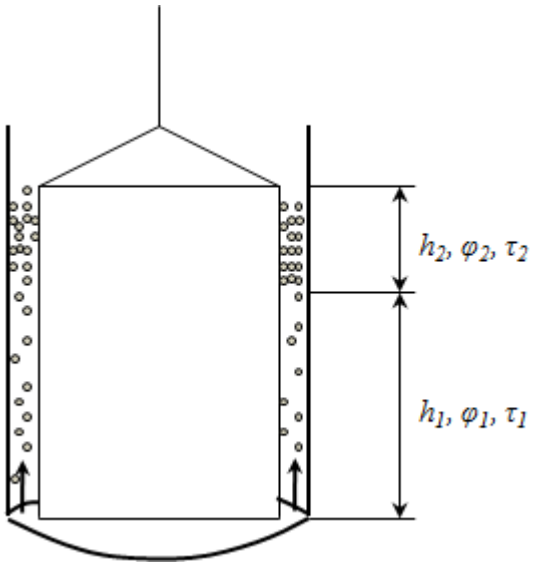

Figure 4.20 *Particle distribution in the annulus. Volume fraction of particles increases in the gap, if more particles come into the annulus from the beaker, and lighter particles gather on the upper part of the annulus*

According to particle distribution, Table 3.3 and Figure 3.9, there is a range in particle size and consequently, the density of individual particle is different from the effective density of glass

beads. Lighter particles due to lift force, centrifugal force, Coriolis force and Euler force drag into the gap and go up gathering on upper part of the gap.

Since viscosity of continuous phase is low the drag force which is acting on a moving particle is low and particles move up (float) faster. The amount of particles on top of the gap becomes higher than at the lower part (non-homogeneous distribution) and consequently, volume fraction at upper part increases. This situation can be compared with “water - Marcol 82” system. The range in experimental data and non-linearity can be explained by particle distribution in the gap.

5 CONCLUSION AND RECOMMENDATION

Dynamics of four multiphase systems have been investigated in the thesis. Properties of each system were carefully measured during investigation.

Water and oil Marcol 82 system: experimental results showed that tiny amount of oil was present in water phase in the rotating annulus. Essentially, stratified flow was obtained in the gap.

Diluted red ethanol and oil Bayol 35 system: during experiments oil and water mixing was observed in the rotating annulus.

Glycerol and spherical glass beads system: the results obtained in the experiments exceed the results calculated using viscosity models for the corresponding volume fraction. Iteration indicated the 6 times increase in volume fraction of the system in the rotating annulus.

Salt water and spherical glass beads system: analyzed data showed that experimental viscosity is greater than viscosity obtained in calculations for corresponding volume fraction. According to iteration the volume fraction during experiments increased 15 times in the annulus.

To investigate the dynamics of these dispersed systems in detail high speed/high resolution camera is required. It allows determining the velocity of particles, trajectory and interaction between particles (structures appearing), particle distribution in the gap. Also it is necessary to have isolated (integrity) annulus to prevent volume fraction changes.

BIBLIOGRAFY

1. **Bibik, E.** *Rheology of disperse systems.* Leningrad : Leningrad University, 1981.
2. **Barnes, Howard A.** *A HANDBOOK OF ELEMENTARY RHEOLOGY.* Wales : University of Wales, 2000.
3. **Hiemenz, Paul C.** *Principles of Colloid and Surface Chemistry, 2nd Edition, Volume 4.* New York : MARCEL DEKKER, INC, 1986.
4. **Dabir S. Viswanath, Tushar K. Ghosh, Dasika H. L. Prasad, Nidamarty V. K.Dutt, Kalipatnapu Y. Rani.** *Viscosity of liquids: theory, estimation, experiment, and data.* Dordrecht, The Netherlands : Springer, 2007.
5. *Preparation characteristics of oil-in-water emulsions using differently charged surfactants in straight-through microchannel emulsification.* **Isao Kobayashi, Mitsutoshi Nakajima, Sukekuni Mukataka.** 2003.
6. **Barnes H.A., Hutton J.F., Walters K.** *An Introduction to Rheology.* Amsterdam : Elsevier Science Publishers B.V./Physical Sciences and Engineering Division, The Netherlands, 1993.
7. **Hunter, Robert J.** *Introduction to Modern Colloid Science.* New York : Oxford University Press, 1992.
8. *Viscosity of "live" water-in-crude-oil emulsions: experimental work and validation of correlations.* **Einar Eng Johnsena, Hans Petter Rønningsen.** 2003.
9. *New development of Einstein's viscose law for powder suspension systems.* **LIANG Shu-quan, XIE Xiao-sheng, XIE Gui-liang, HANG Bai-yun.** 2002.
10. **Chhabra, R.** *Bubbles, Drops, and Particles in Non-Newtonian Fluids.* Kanpur : Indian Institute of Technology, 2006.
11. **Clayton T. Crowe, Martin Sommerfeld, Yutaka Tsuji.** *Multiphase flows with droplets and particles.* USA : CRC Press LLC, 1998.
12. **Equipment, OFI Testing.** *Model 900 Viscometer, Instruction Manual.* Houston : OFI Testing Equipment, 2009.
13. —. *Model 900, Installation and Operation Instructions for Orcada Ver. 5.0.* Houston : s.n.
14. *Universal Software US 200, Volume 3 - Analysis, Operating Instructions.* Stuttgart, Germany : Physica Messtechnik GmbH, 2001.
15. **Dipl. Ing. Houm, AS.** *Anton Paar, DMA 4500/5000, Density/Specific Gravity/Concentration Meter, Instruction Handbook.* Oslo : Grefsen.
16. **Rabenjafimanantsoa A. H., Svein Myhren.** *Laboratory exercise in reservoir engineering.* Stavanger : University of Stavanger, 2010.
17. *AccuPyc II 1340 Preinstalation Instructions and Checklist.* Dec. 06.
18. **AS, ESSO NORGE.** *BAYOL 35, Prod.nr; N-63-L5891, "Helse-, Miljø- og Sikkerhetsdatablad".* Oslo : s.n., 19.sep.2002.
19. *Esso Imperial Oil, Product Data Sheet, White Oil, Marcol, Primol, Bayol.* s.l. : Downloaded from http://www.imperialoil.ca/Canada-English/Files/Products_Lubes/IOCAENWPOESWhiteoil.pdf, 30.03.2010.
20. **Mobile, Exxon.** *Safety data sheet, HSSE for Marcol82.* Antwerpen : ExxonMobile Lubricants & Specialties Europe, Petroleum & Chemical, 2008.
21. **Walpole, RE, Myers, RH, Myers, SL, and Ye, K.** *Probability and Statistics for Engineers and Scientists, 8th Edition.* Englewood Cliffs, New Jersey : Prentice Hall, 2006.

22. **Industries, CYRO.** *Physical properties of acrylite.ff, acrylic sheet.* Parsippany, New Jersey : CYRO Industries, 2001.

Appendix A - Particle Size Distribution

Sample 1. The size range from 41 µm to 50 µm

Particle sample with particle size range from 41 µm to 50 µm is represented on Figure A. 1. Picture was obtained with scanning electron microscope (SEM).

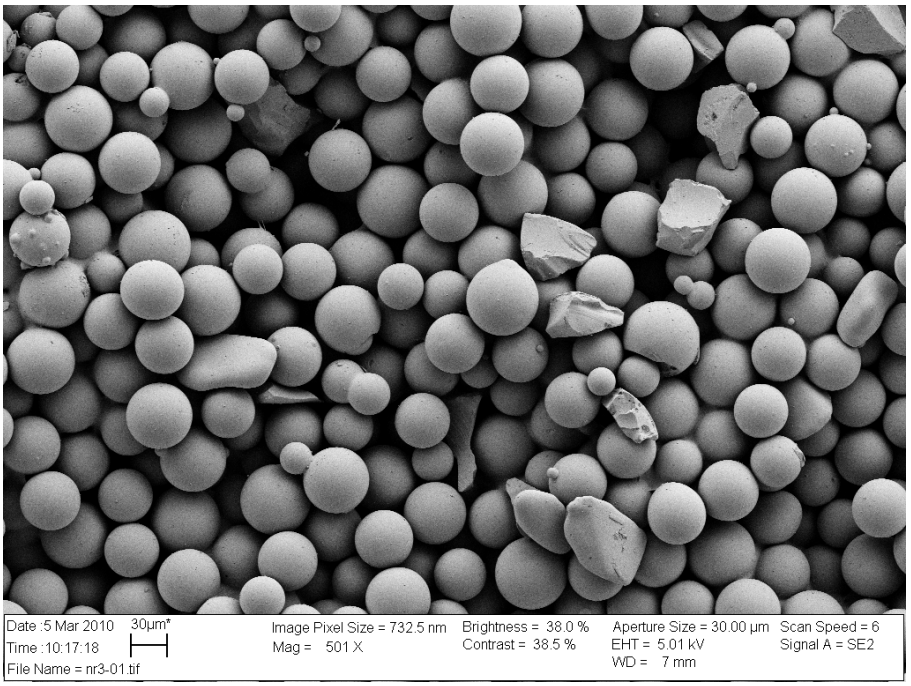

Figure A. 1 *Particle sample with particle size range from 41 µm to 50 µm*

Table A. 1 *Particle size distribution sample 1:* $\sum n_i = 71 = N$, $\sum f_i = 1.00$, $f_i = \frac{n_i}{\sum n_i}$

Class range, µm	Mid-point of class range, d_i, µm	Number of particles, n_i	Fraction in this class, f_i	Total number with $d<d_i$	Cumulative per cent
Size range 41 – 50 µm					
41 – 43	42	24	0.338	24	33.8
44 – 46	45	22	0.310	46	31.0
47 – 50	48.5	25	0.352	71	35.2

The mean and standard deviation (Walpole, 2006)

$$\bar{d} = 0.338 \cdot 42 + 0.310 \cdot 45 + 0.352 \cdot 48.5 = 45.218\,\mu\text{m}.$$

$$\sigma = \left(0.338 \cdot (42 - 45.218)^2 + 0.310 \cdot (45 - 45.218)^2 + 0.352 \cdot (48.5 - 45.218)^2\right)^{\frac{1}{2}} = 2.703\,\mu\text{m}.$$

The resulting data is plotted as a histogram in Figure A. 2

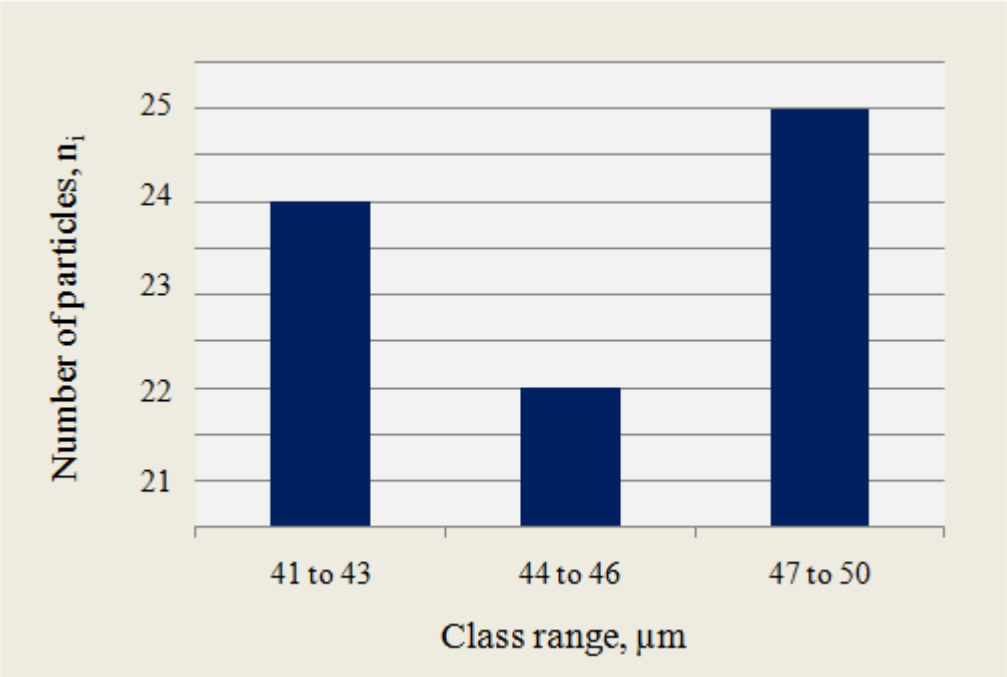

Figure A. 2 *Particle size distribution of sample 1*

Sample 2. The size range from 21 µm to 40 µm

Particle sample with particle size range from 21 µm to 40 µm is represented on Figure A. 3.

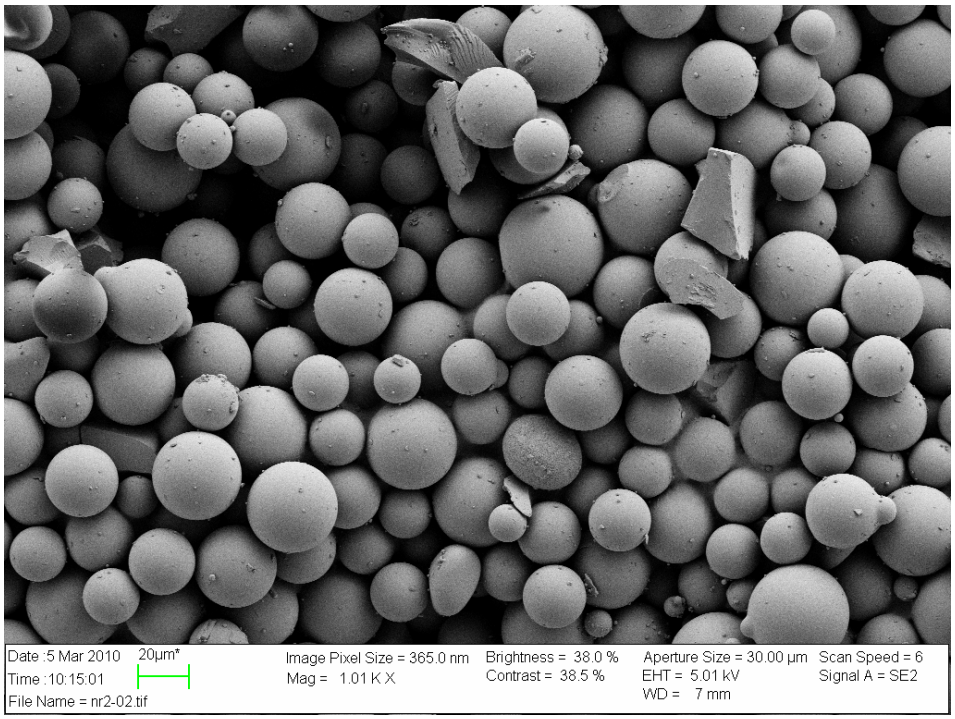

Figure A. 3 *Particle sample with particle size range from 21 µm to 40 µm*

Table A. 2 *Particle size distribution sample 2:* $\sum n_i = 60 = N$, $\sum f_i = 1.00$, $f_i = \frac{n_i}{\sum n_i}$

Class range, µm	Mid-point of class range, d_i, µm	Number of particles, n_i	Fraction in this class, f_i	Total number with $d<d_i$	Cumulative per cent
Size range 21 – 40 µm					
21 – 23	22	10	0.167	10	16.7
24 – 27	25.5	19	0.317	29	31.7
28 – 32	30	9	0.150	38	15.0
33 – 36	34.5	13	0.216	51	21.6
37 – 40	38.5	9	0.150	60	15.0

The resulting data is plotted as a histogram and it is represented in Figure A. 4.

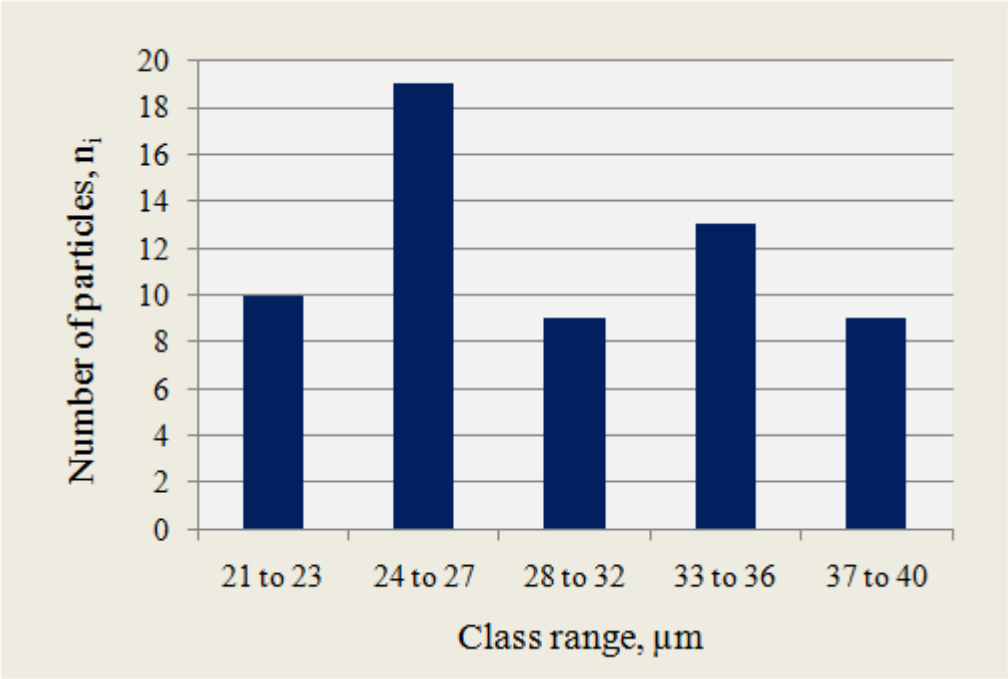

Figure A. 4 *Particle size distribution of sample 2*

The mean and standard deviation of the distribution are

$\bar{d} = 29.485$ µm.

$\sigma = 5.662$ µm.

Sample 3. The size range from 1 µm to 20 µm

Particle sample with particle size range from 21 µm to 40 µm is shown on Figure A. 5.

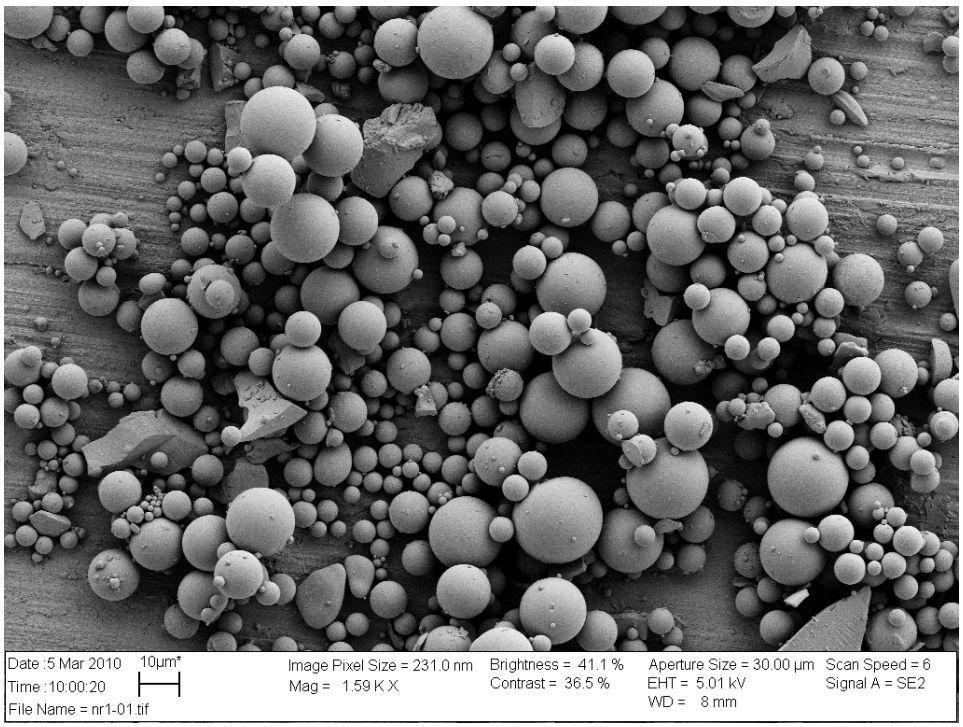

Figure A. 5 *Particle sample with particle size range from 1 µm to 20 µm*

Table A. 3 *Particle size distribution sample 3:* $\sum n_i = 100 = N$, $\sum f_i = 1.00$, $f_i = \frac{n_i}{\sum n_i}$

Class range, µm	Mid-point of class range, d_i, µm	Number of particles, n_i	Fraction in this class, f_i	Total number with $d<d_i$	Cumulative per cent
Size range 1 – 20 µm					
1 – 4	2.5	17	0.170	17	17.0
5 – 8	6.5	38	0.380	55	38.0
9 – 12	10.5	21	0.210	76	21.0
13 – 16	14.5	12	0.120	88	12.0
17 – 20	18.5	12	0.120	100	12.0

The particle size distribution of the sample 3 is plotted as a histogram and it is represented on Figure A. 6.

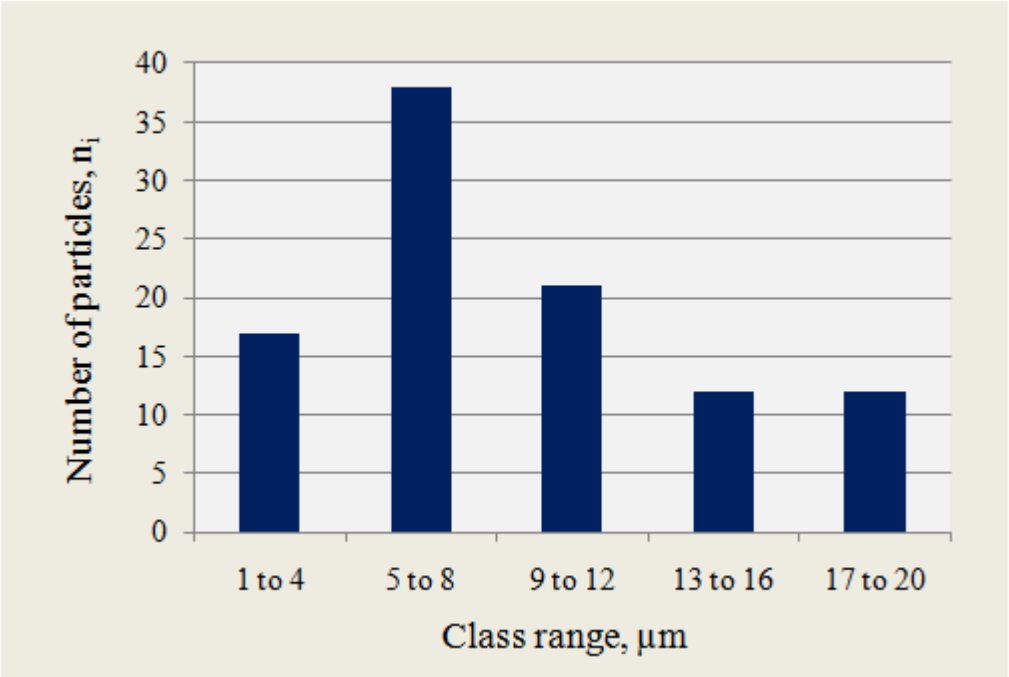

Figure A. 6 *Particle size distribution of sample 3*

The mean and standard deviation of the distribution are

$\bar{d} = 9.060\,\mu\text{m}.$

$\sigma = 4.948\,\mu\text{m}.$

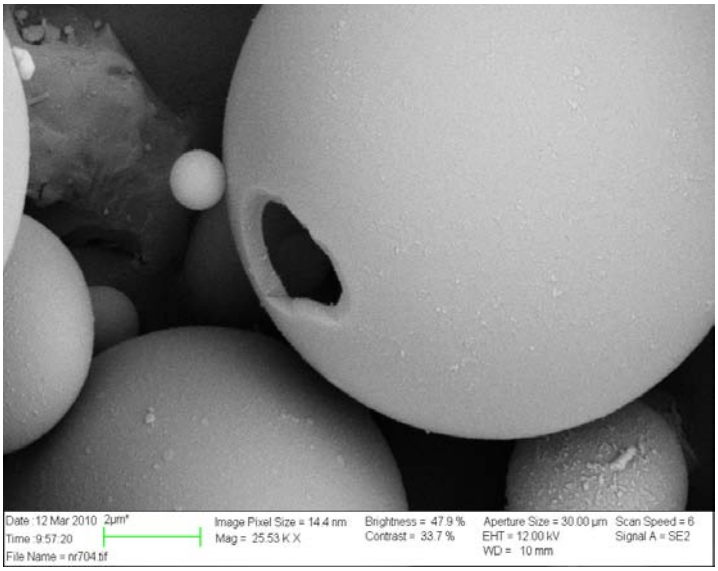

Figure A. 7 *Hollow particle in the sample*

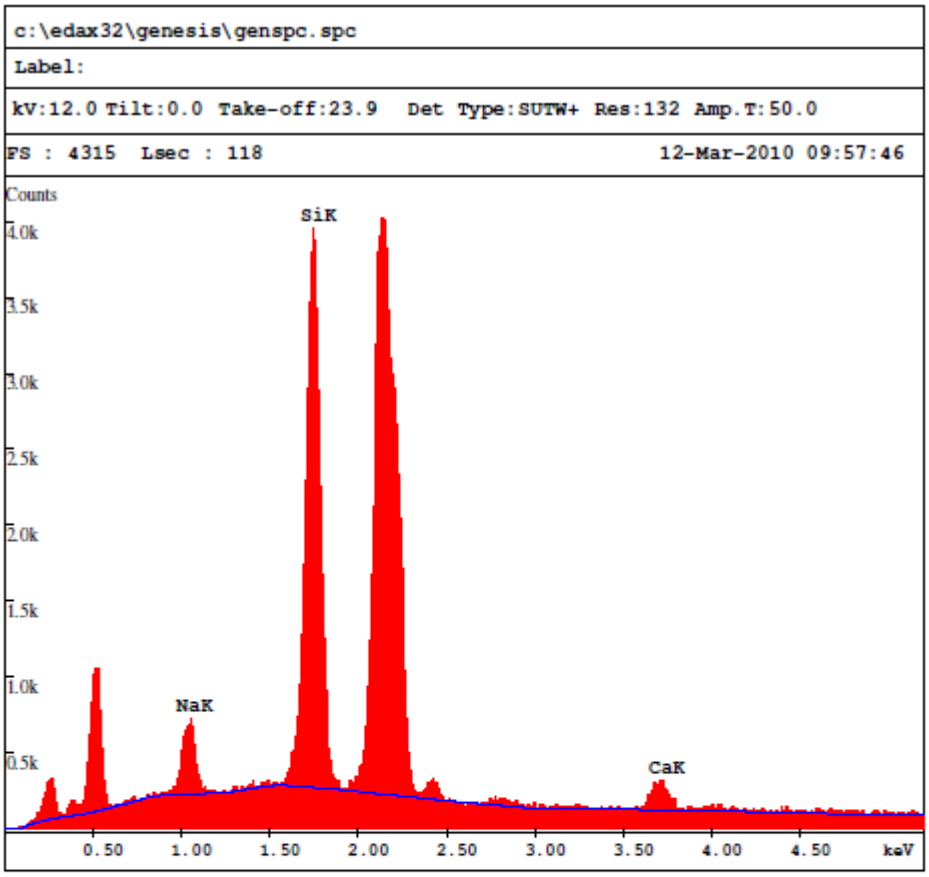

EDAX ZAF Quantification (Standardless)
Element Normalized
SEC Table : User c:\edax32\eds\genuser.sec

Element	Wt %	At %	K-Ratio	Z	A	F
NaK	10.02	12.39	0.0736	0.9871	0.7384	1.0077
SiK	78.46	79.44	0.7271	1.0059	0.9205	1.0008
CaK	11.51	8.17	0.1017	0.9677	0.9130	1.0000
Total	100.00	100.00				

Element	Net Inte.	Bkgd Inte.	Inte. Error	P/B
NaK	28.12	15.42	2.51	1.82
SiK	227.92	20.69	0.66	11.02
CaK	14.74	12.33	3.92	1.20

Figure A. 8 *Chemical compositin of particles*

Appendix B – Properties of Glycerol and Water Mixture

Properties of glycerol and water mixture are represented in Table B. 1, Figure B. 1 Figure B. 2.

Table B. 1 *Density, specific gravity, surface tension*

Composition G – Glycerol, W - Water	Density, g/cm^3 at 20° C	Specific gravity at 20° C	Surface tension, air – glycerol, mN/m at 20° C
100% - W	0.998	1	69.5
25% - G, 75% - W	1.055	1.057	67
40% - G, 60% - W	1.093	1.095	65.1
50% - G, 50% - W	1.118	1.120	64.2
60% - G, 40% - W	1.143	1.145	63
75% - G, 25% - W	1.176	1.178	62.5
80% - G, 20% - W	1.185	1.187	62.2
85% - G, 15% - W	1.197	1.199	61.8
90% - G, 10% - W	1.205	1.207	61.5
95% - G, 5% - W	1.214	1.216	61.2
100% - G	1.223	1.225	61

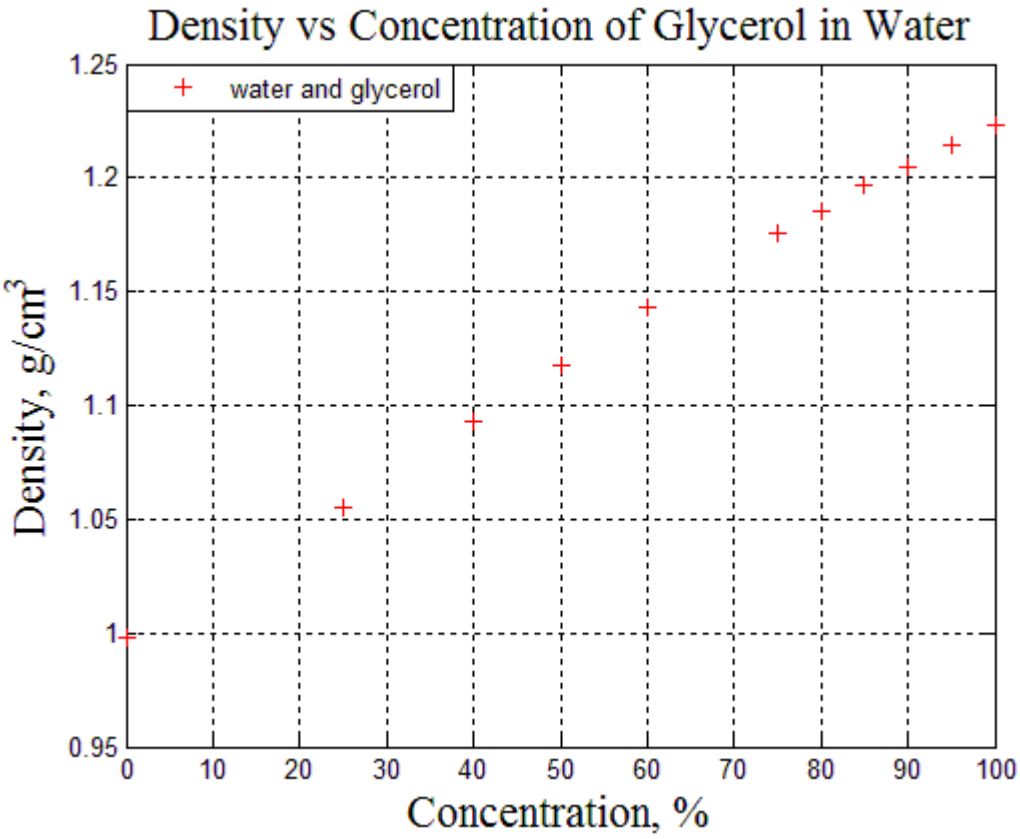

Figure B. 1 *Density of glycerol water mixture*

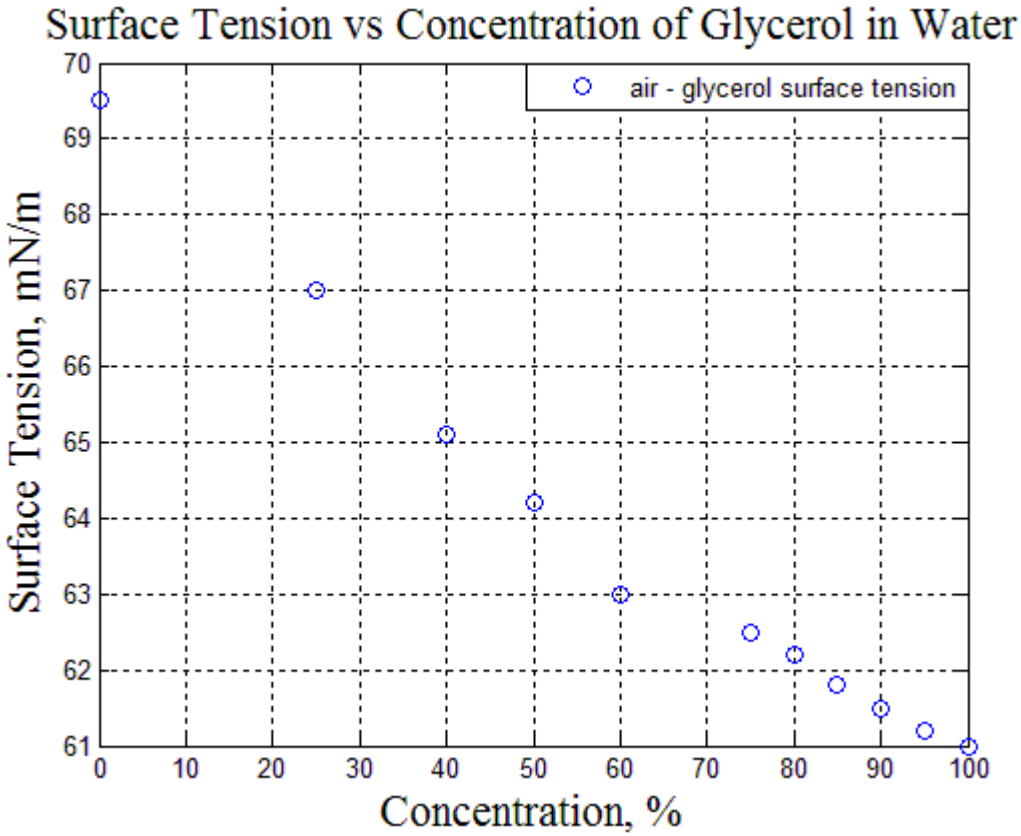

Figure B. 2 *Surface tension of glycerol water mixture*

Appendix C – Measured Data of Multiphase Systems

Table C. 1 *Water and oil Marcol 82 measured data*

Water				Water and 28% of Marcol 82 in the gap			Water and 56% of Marcol 82 in the gap			Water and 84% of Marcol 82 in the gap			Marcol 82		
Shear Rate [1/s]	Shear Stress [Pa]	Viscosity [cP]	Viscosity [Pa·s]	Shear Stress [Pa]	Viscosity [cP]	Viscosity [Pa·s]	Shear Stress [Pa]	Viscosity [cP]	Viscosity [Pa·s]	Shear Stress [Pa]	Viscosity [cP]	Viscosity [Pa·s]	Shear Stress [Pa]	Viscosity [cP]	Viscosity [Pa·s]
1.5	0	0	0	0	0	0	0	0	0	0	0	0	0.1	100	0.1
1.5	0	0	0	0	0	0	0	0	0	0	0	0	0.1	100	0.1
1.5	0	0	0	0	0	0	0	0	0	0	0	0	0.1	100	0.1
1.5	0	0	0	0	0	0	0	0	0	0	0	0	0.1	100	0.1
1.5	0	0	0	0	0	0	0	0	0	0	0	0	0.1	100	0.1
3.1	0	0	0	0	0	0	0	0	0	0.1	33.3	0.0333	0.1	44.4	0.0444
3.1	0	0	0	0	0	0	0	0	0	0.1	33.3	0.0333	0.1	46.1	0.0461
3.1	0	0	0	0	0	0	0	0	0	0.1	33.3	0.0333	0.1	46.1	0.0461
3.1	0	0	0	0	0	0	0	0	0	0.1	33.3	0.0333	0.1	46.4	0.0464
3.1	0	0	0	0	0	0	0	0	0	0.1	33.3	0.0333	0.1	45.8	0.0458
5.1	0	0	0	0	0	0	0.1	20	0.02	0.1	20	0.02	0.2	40	0.04
5.1	0	0	0	0	0	0	0.1	20	0.02	0.1	20	0.02	0.2	40	0.04
5.1	0	0	0	0	0	0	0.1	20	0.02	0.1	20	0.02	0.2	40	0.04
5.1	0	0	0	0	0	0	0.1	20	0.02	0.1	20	0.02	0.2	40	0.04
5.1	0	0	0	0	0	0	0.1	20	0.02	0.1	20	0.02	0.2	40	0.04
10.2	0	0	0	0	0	0	0.1	10	0.01	0.2	20	0.02	0.3	31	0.031
10.2	0	0	0	0	0	0	0.1	10	0.01	0.2	20	0.02	0.3	31.8	0.0318
10.2	0	0	0	0	0	0	0.1	10	0.01	0.2	20	0.02	0.3	32.2	0.0322
10.2	0	0	0	0	0	0	0.1	10	0.01	0.2	20	0.02	0.3	32.3	0.0323
10.2	0	0	0	0	0	0	0.1	10	0.01	0.2	20	0.02	0.3	32.8	0.0328
51.1	0	0	0	0.5	8.8	0.0088	1.2	23.5	0.0235	1.5	29.4	0.0294	1.6	31.4	0.0314
51.1	0	0	0	0.5	9.8	0.0098	1.2	23.5	0.0235	1.5	29.4	0.0294	1.6	31.4	0.0314
51.1	0	0	0	0.5	9.8	0.0098	1.2	23.5	0.0235	1.5	29.4	0.0294	1.6	31.4	0.0314
51.1	0	0	0	0.5	9.8	0.0098	1.2	23.5	0.0235	1.5	29.4	0.0294	1.6	31.4	0.0314
51.1	0	0	0	0.5	9.8	0.0098	1.2	23.5	0.0235	1.5	29.4	0.0294	1.6	31.4	0.0314
102.0	0	0	0	1.2	11.8	0.0118	2	19.6	0.0196	2.8	27.5	0.0275	2.8	27.5	0.0275
102.0	0	0	0	1.2	11.8	0.0118	2	19.6	0.0196	2.8	27.5	0.0275	2.8	27.5	0.0275
102.0	0	0	0	1.2	11.8	0.0118	2	19.6	0.0196	2.8	27.5	0.0275	2.8	27.5	0.0275
102.0	0	0	0	1.2	11.8	0.0118	2	19.6	0.0196	2.8	27.5	0.0275	2.8	27.5	0.0275
102.0	0	0	0	1.2	11.8	0.0118	2	19.6	0.0196	2.8	27.5	0.0275	2.8	27.5	0.0275
153.0	0	0	0	1.8	10.6	0.0106	3.3	19.4	0.0194	4.5	26.3	0.0263	4.9	28.8	0.0288
153.0	0	0	0	1.8	10.6	0.0106	3.3	19.4	0.0194	4.5	26.5	0.0265	4.9	28.8	0.0288
153.0	0	0	0	1.8	10.6	0.0106	3.3	19.4	0.0194	4.5	26.5	0.0265	4.9	28.8	0.0288
153.0	0	0	0	1.8	10.6	0.0106	3.3	19.4	0.0194	4.5	26.5	0.0265	4.9	28.8	0.0288
153.0	0	0	0	1.8	10.6	0.0106	3.3	19.4	0.0194	4.5	26.5	0.0265	4.9	28.8	0.0288
340.0	0.2	0.6	0.0006	3.4	10	0.01	6.6	19.5	0.0195	9.1	26.7	0.0267	9.5	27.9	0.0279
340.0	0.2	0.6	0.0006	3.4	10	0.01	6.7	19.7	0.0197	9.1	26.8	0.0268	9.5	27.9	0.0279

Table C. 1 continued

Shear Rate [1/s]	Shear Stress [Pa]	Viscosity [cP]	Viscosity [Pa·s]	Shear Stress [Pa]	Viscosity [cP]	Viscosity [Pa·s]	Shear Stress [Pa]	Viscosity [cP]	Viscosity [Pa·s]	Shear Stress [Pa]	Viscosity [cP]	Viscosity [Pa·s]	Shear Stress [Pa]	Viscosity [cP]	Viscosity [Pa·s]
340.0	0.2	0.6	0.0006	3.4	10	0.01	6.7	19.7	0.0197	9.1	26.8	0.0268	9.5	27.9	0.0279
340.0	0.2	0.6	0.0006	3.4	10	0.01	6.7	19.7	0.0197	9.1	26.8	0.0268	9.5	27.9	0.0279
340.0	0.2	0.6	0.0006	3.4	10	0.01	6.7	19.7	0.0197	9.1	26.8	0.0268	9.5	27.9	0.0279
511.0	0.4	0.8	0.0008	5	9.8	0.0098	9.7	19	0.019	13.7	26.9	0.0269	14.1	27.6	0.0276
511.0	0.4	0.8	0.0008	5	9.8	0.0098	9.8	19.1	0.0191	13.8	27	0.027	14.1	27.6	0.0276
511.0	0.4	0.8	0.0008	5	9.8	0.0098	9.8	19.1	0.0191	13.7	26.9	0.0269	14.1	27.6	0.0276
511.0	0.4	0.8	0.0008	5	9.8	0.0098	9.7	19	0.019	13.7	26.9	0.0269	14.1	27.6	0.0276
511.0	0.4	0.8	0.0008	5	9.8	0.0098	9.7	19.1	0.0191	13.7	26.9	0.0269	14.1	27.6	0.0276
1021.0	1	0.9	0.0009	9.9	9.7	0.0097	19.4	19	0.019	27.1	26.5	0.0265	27.9	27.4	0.0274
1021.0	1	1	0.001	9.9	9.7	0.0097	19.4	19	0.019	26.5	26	0.026	27.9	27.3	0.0273
1021.0	1	1	0.001	9.9	9.7	0.0097	19.4	19	0.019	26.3	25.8	0.0258	27.9	27.3	0.0273
1021.0	1	1	0.001	9.9	9.7	0.0097	19.4	19	0.019	26.2	25.7	0.0257	27.8	27.2	0.0272
1021.0	1	1	0.001	9.9	9.7	0.0097	19.4	19	0.019	26.2	25.7	0.0257	27.8	27.2	0.0272

Table C. 2 *Diluted red ethanol measured data - 3 repetitions*

Shear Rate [1/s]	Shear Stress [Pa]	Viscosity [cP]	Viscosity [Pa·s]	Shear Stress [Pa]	Viscosity [cP]	Viscosity [Pa·s]	Shear Stress [Pa]	Viscosity [cP]	Viscosity [Pa·s]
1.5	0	0	0	0	0	0	0	0	0
1.5	0	0	0	0	0	0	0	0	0
1.5	0	0	0	0	0	0	0	0	0
1.5	0	0	0	0	0	0	0	0	0
1.5	0	0	0	0	0	0	0	0	0
3.1	0	0	0	0	0	0	0	0	0
3.1	0	0	0	0	0	0	0	0	0
3.1	0	0	0	0	0	0	0	0	0
3.1	0	0	0	0	0	0	0	0	0
3.1	0	0	0	0	0	0	0	0	0
5.1	0	0	0	0	0	0	0	0	0
5.1	0	0	0	0	0	0	0	0	0
5.1	0	0	0	0	0	0	0	0	0
5.1	0	0	0	0	0	0	0	0	0
5.1	0	0	0	0	0	0	0	0	0
10.2	0	0	0	0	0	0	0	0	0
10.2	0	0	0	0	0	0	0	0	0
10.2	0	0	0	0	0	0	0	0	0
10.2	0	0	0	0	0	0	0	0	0
10.2	0	0	0	0	0	0	0	0	0
51.1	0.1	2	0.002	0.1	2	0.002	0.1	2	0.002
51.1	0.1	2	0.002	0.1	2	0.002	0.1	2	0.002
51.1	0.1	2	0.002	0.1	2	0.002	0.1	2	0.002
51.1	0.1	2	0.002	0.1	2	0.002	0.1	2	0.002
51.1	0.1	2	0.002	0.1	2	0.002	0.1	2	0.002
102.0	0.1	1	0.001	0.1	1	0.001	0.1	1	0.001
102.0	0.1	1	0.001	0.1	1	0.001	0.1	1	0.001
102.0	0.1	1	0.001	0.1	1	0.001	0.1	1	0.001
102.0	0.1	1	0.001	0.1	1	0.001	0.1	1	0.001
102.0	0.1	1	0.001	0.1	1	0.001	0.1	1	0.001
153.0	0.2	1.2	0.0012	0.2	1.2	0.0012	0.2	1.2	0.0012
153.0	0.2	1.2	0.0012	0.2	1.2	0.0012	0.2	1.2	0.0012
153.0	0.2	1.2	0.0012	0.2	1.2	0.0012	0.2	1.2	0.0012
153.0	0.2	1.2	0.0012	0.2	1.2	0.0012	0.2	1.4	0.0014
153.0	0.2	1.2	0.0012	0.3	1.8	0.0018	0.3	1.8	0.0018
340.0	0.8	2.4	0.0024	0.8	2.4	0.0024	0.7	2	0.002
340.0	0.8	2.4	0.0024	0.8	2.4	0.0024	0.8	2.4	0.0024
340.0	0.8	2.4	0.0024	0.8	2.4	0.0024	0.8	2.4	0.0024
340.0	0.8	2.4	0.0024	0.8	2.4	0.0024	0.8	2.4	0.0024
340.0	0.8	2.4	0.0024	0.8	2.4	0.0024	0.8	2.4	0.0024
511.0	1	2	0.002	1.1	2.2	0.0022	1.1	2.2	0.0022

Table C. 2 continued

Shear Rate [1/s]	Shear Stress [Pa]	Viscosity [cP]	Viscosity [Pa·s]	Shear Stress [Pa]	Viscosity [cP]	Viscosity [Pa·s]	Shear Stress [Pa]	Viscosity [cP]	Viscosity [Pa·s]
511.0	1	2	0.002	1.1	2.2	0.0022	1.1	2.2	0.0022
511.0	1	2	0.002	1.1	2.2	0.0022	1.1	2.2	0.0022
511.0	1	2	0.002	1.1	2.2	0.0022	1.1	2.2	0.0022
511.0	1	2	0.002	1.1	2.2	0.0022	1.1	2.2	0.0022
1021.0	1.9	1.9	0.0019	1.9	1.9	0.0019	2	2	0.002
1021.0	1.9	1.9	0.0019	2	2	0.002	2	2	0.002
1021.0	1.9	1.9	0.0019	2	2	0.002	2	2	0.002
1021.0	1.9	1.9	0.0019	2	2	0.002	2	2	0.002
1021.0	1.9	1.9	0.0019	2	2	0.002	2	2	0.002

Table C. 3 *Diluted red ethanol and oil Bayol 35, volume fraction 0.1874 measured data - 3 repetitions*

Shear Rate [1/s]	Shear Stress [Pa]	Viscosity [cP]	Viscosity [Pa·s]	Shear Stress [Pa]	Viscosity [cP]	Viscosity [Pa·s]	Shear Stress [Pa]	Viscosity [cP]	Viscosity [Pa·s]
1.5	0	0	0	0	0	0	0	0	0
1.5	0	0	0	0	0	0	0	0	0
1.5	0	0	0	0	0	0	0	0	0
1.5	0	0	0	0	0	0	0	0	0
1.5	0	0	0	0	0	0	0	0	0
3.1	0	0	0	0	0	0	0	0	0
3.1	0	0	0	0	0	0	0	0	0
3.1	0	0	0	0	0	0	0	0	0
3.1	0	0	0	0	0	0	0	0	0
3.1	0	0	0	0	0	0	0	0	0
5.1	0	0	0	0	0	0	0	0	0
5.1	0	0	0	0	0	0	0	0	0
5.1	0	0	0	0	0	0	0	0	0
5.1	0	0	0	0	0	0	0	0	0
5.1	0	0	0	0	0	0	0	0	0
10.2	0	0	0	0	0	0	0	0	0
10.2	0	0	0	0	0	0	0	0	0
10.2	0	0	0	0	0	0	0	0	0
10.2	0	0	0	0	0	0	0	0	0
10.2	0	0	0	0	0	0	0	0	0
51.1	0.1	2	0.002	0.1	2	0.002	0.1	2	0.002
51.1	0.1	2	0.002	0.1	2	0.002	0.1	2	0.002
51.1	0.1	2	0.002	0.1	2	0.002	0.1	2	0.002
51.1	0.1	2	0.002	0.1	2	0.002	0.1	2	0.002
51.1	0.1	2	0.002	0.1	2	0.002	0.1	2	0.002
102.0	0.1	1	0.001	0.1	1	0.001	0.1	1	0.001
102.0	0.1	1	0.001	0.1	1	0.001	0.1	1	0.001

Table C. 3 continued

Shear Rate [1/s]	Shear Stress [Pa]	Viscosity [cP]	Viscosity [Pa·s]	Shear Stress [Pa]	Viscosity [cP]	Viscosity [Pa·s]	Shear Stress [Pa]	Viscosity [cP]	Viscosity [Pa·s]
102.0	0.1	1	0.001	0.1	1	0.001	0.1	1	0.001
102.0	0.1	1	0.001	0.1	1	0.001	0.1	1	0.001
102.0	0.1	1	0.001	0.1	1	0.001	0.1	1	0.001
153.0	0.2	1.2	0.0012	0.2	1.2	0.0012	0.2	1.2	0.0012
153.0	0.2	1.2	0.0012	0.2	1.2	0.0012	0.2	1.2	0.0012
153.0	0.2	1.2	0.0012	0.2	1.2	0.0012	0.2	1.2	0.0012
153.0	0.2	1.2	0.0012	0.2	1.2	0.0012	0.2	1.2	0.0012
153.0	0.2	1.2	0.0012	0.2	1.2	0.0012	0.2	1.2	0.0013
340.0	0.4	1.3	0.0013	0.5	1.5	0.0015	0.5	1.5	0.0015
340.0	0.5	1.5	0.0015	0.5	1.5	0.0015	0.5	1.5	0.0015
340.0	0.5	1.5	0.0015	0.5	1.5	0.0015	0.5	1.5	0.0015
340.0	0.5	1.5	0.0015	0.5	1.5	0.0015	0.5	1.5	0.0015
340.0	0.5	1.5	0.0015	0.5	1.5	0.0015	0.5	1.5	0.0015
511.0	1.8	3.5	0.0035	1.8	3.5	0.0035	1.8	3.5	0.0035
511.0	1.8	3.5	0.0035	1.8	3.5	0.0035	1.8	3.5	0.0035
511.0	1.8	3.5	0.0035	1.8	3.5	0.0035	1.8	3.5	0.0035
511.0	1.8	3.5	0.0035	1.8	3.5	0.0035	1.8	3.5	0.0035
511.0	1.8	3.5	0.0035	1.8	3.5	0.0035	1.8	3.5	0.0035
1021.0	2.2	2.3	0.0023	2.2	2.4	0.0024	2.2	2.4	0.0024
1021.0	2.2	2.2	0.0022	2.2	2.2	0.0022	2.2	2.2	0.0022
1021.0	2.2	2.2	0.0022	2.2	2.2	0.0022	2.2	2.2	0.0022
1021.0	2.2	2.2	0.0022	2.2	2.2	0.0022	2.2	2.2	0.0022
1021.0	2.2	2.2	0.0022	2.2	2.2	0.0022	2.2	2.2	0.0022

Table C. 4 *Diluted red ethanol and oil Bayol 35, volume fraction 0.3749 measured data - 3 repetitions*

Shear Rate [1/s]	Shear Stress [Pa]	Viscosity [cP]	Viscosity [Pa·s]	Shear Stress [Pa]	Viscosity [cP]	Viscosity [Pa·s]	Shear Stress [Pa]	Viscosity [cP]	Viscosity [Pa·s]
1.5	0.1	100	0.1	0	0	0	0	0	0
1.5	0.1	100	0.1	0	0	0	0	0	0
1.5	0.1	100	0.1	0	0	0	0	0	0
1.5	0.1	100	0.1	0	0	0	0	0	0
1.5	0.1	100	0.1	0	0	0	0	0	0
3.1	0.1	33.3	0.0333	0	0	0	0	0	0
3.1	0.1	33.3	0.0333	0	0	0	0	0	0
3.1	0.1	33.3	0.0333	0	0	0	0	0	0
3.1	0.1	33.3	0.0333	0	0	0	0	0	0
3.1	0.1	33.3	0.0333	0	0	0	0	0	0
5.1	0.1	20	0.02	0	0	0	0	0	0
5.1	0.1	20	0.02	0	0	0	0	0	0
5.1	0.1	20	0.02	0	0	0	0	0	0

Table C. 4 continued

Shear Rate [1/s]	Shear Stress [Pa]	Viscosity [cP]	Viscosity [Pa·s]	Shear Stress [Pa]	Viscosity [cP]	Viscosity [Pa·s]	Shear Stress [Pa]	Viscosity [cP]	Viscosity [Pa·s]
5.1	0.1	20	0.02	0	0	0	0	0	0
5.1	0.1	20	0.02	0	0	0	0	0	0
10.2	0.1	10	0.01	0	0	0	0	0	0
10.2	0.1	10	0.01	0	0	0	0	0	0
10.2	0.1	10	0.01	0	0	0	0	0	0
10.2	0.1	10	0.01	0	0	0	0	0	0
10.2	0.1	10	0.01	0	0	0	0	0	0
51.1	0.1	2	0.002	0.1	2	0.002	0.1	2	0.002
51.1	0.1	2	0.002	0.1	2	0.002	0.1	2	0.002
51.1	0.1	2	0.002	0.1	2	0.002	0.1	2	0.002
51.1	0.1	2	0.002	0.1	2	0.002	0.1	2	0.002
51.1	0.1	2	0.002	0.1	2	0.002	0.1	2	0.002
102.0	0.2	2	0.002	0.1	1	0.001	0.1	1	0.001
102.0	0.2	2	0.002	0.1	1	0.001	0.1	1	0.001
102.0	0.2	2	0.002	0.1	1	0.001	0.1	1	0.001
102.0	0.2	2	0.002	0.1	1	0.001	0.1	1	0.001
102.0	0.2	2	0.002	0.1	1	0.001	0.1	1	0.001
153.0	0.2	1.2	0.0012	0.2	1.2	0.0012	0.2	1.2	0.0012
153.0	0.2	1.2	0.0012	0.2	1.2	0.0012	0.2	1.2	0.0012
153.0	0.2	1.2	0.0012	0.2	1.2	0.0012	0.2	1.2	0.0012
153.0	0.2	1.2	0.0012	0.2	1.2	0.0012	0.2	1.2	0.0012
153.0	0.2	1.2	0.0012	0.2	1.2	0.0012	0.2	1.2	0.0012
340.0	0.4	1.2	0.0012	0.4	1.2	0.0012	0.4	1.2	0.0012
340.0	0.4	1.2	0.0012	0.5	1.5	0.0015	0.5	1.5	0.0015
340.0	0.4	1.2	0.0012	0.5	1.5	0.0015	0.5	1.5	0.0015
340.0	0.4	1.2	0.0012	0.5	1.5	0.0015	0.5	1.5	0.0015
340.0	0.4	1.2	0.0012	0.5	1.5	0.0015	0.5	1.5	0.0015
511.0	1.8	3.5	0.0035	1.8	3.5	0.0035	1.8	3.5	0.0035
511.0	1.8	3.5	0.0035	1.8	3.5	0.0035	1.8	3.5	0.0035
511.0	1.8	3.5	0.0035	1.8	3.5	0.0035	1.8	3.5	0.0035
511.0	1.8	3.5	0.0035	1.8	3.5	0.0035	1.8	3.5	0.0035
511.0	1.8	3.5	0.0035	1.8	3.5	0.0035	1.8	3.5	0.0035
1021.0	2.2	2.4	0.0024	2.2	2.4	0.0024	2.2	2.4	0.0024
1021.0	2.2	2.2	0.0022	2.2	2.2	0.0022	2.2	2.2	0.0022
1021.0	2.2	2.2	0.0022	2.2	2.2	0.0022	2.2	2.2	0.0022
1021.0	2.2	2.2	0.0022	2.2	2.2	0.0022	2.2	2.2	0.0022
1021.0	2.2	2.2	0.0022	2.2	2.2	0.0022	2.2	2.2	0.0022

Table C. 5 *Diluted red ethanol and oil Bayol 35, volume fraction 0.5623 measured data - 3 repetitions*

Shear Rate [1/s]	Shear Stress [Pa]	Viscosity [cP]	Viscosity [Pa·s]	Shear Stress [Pa]	Viscosity [cP]	Viscosity [Pa·s]	Shear Stress [Pa]	Viscosity [cP]	Viscosity [Pa·s]
1.5	0.1	100	0.1	0	0	0	0	0	0
1.5	0.1	100	0.1	0	0	0	0	0	0
1.5	0.1	100	0.1	0	0	0	0	0	0
1.5	0.1	100	0.1	0	0	0	0	0	0
1.5	0.1	100	0.1	0	0	0	0	0	0
3.1	0.1	33.3	0.0333	0	0	0	0	0	0
3.1	0.1	33.3	0.0333	0	0	0	0	0	0
3.1	0.1	33.3	0.0333	0	0	0	0	0	0
3.1	0.1	33.3	0.0333	0	0	0	0	0	0
3.1	0.1	33.3	0.0333	0	0	0	0	0	0
5.1	0.1	20	0.02	0	0	0	0	0	0
5.1	0.1	20	0.02	0	0	0	0	0	0
5.1	0.1	20	0.02	0	0	0	0	0	0
5.1	0.1	20	0.02	0	0	0	0	0	0
5.1	0.1	20	0.02	0	0	0	0	0	0
10.2	0.1	10	0.01	0	0	0	0	0	0
10.2	0.1	10	0.01	0	0	0	0	0	0
10.2	0.1	10	0.01	0	0	0	0	0	0
10.2	0.1	10	0.01	0	0	0	0	0	0
10.2	0.1	10	0.01	0	0	0	0	0	0
51.1	0.1	2	0.002	0.1	2	0.002	0.1	2	0.002
51.1	0.1	2	0.002	0.1	2	0.002	0.1	2	0.002
51.1	0.1	2	0.002	0.1	2	0.002	0.1	2	0.002
51.1	0.1	2	0.002	0.1	2	0.002	0.1	2	0.002
51.1	0.1	2	0.002	0.1	2	0.002	0.1	2	0.002
102.0	0.2	2	0.002	0.1	1	0.001	0.1	1	0.001
102.0	0.2	2	0.002	0.1	1	0.001	0.1	1	0.001
102.0	0.2	2	0.002	0.1	1	0.001	0.1	1	0.001
102.0	0.2	2	0.002	0.1	1	0.001	0.1	1	0.001
102.0	0.2	2	0.002	0.1	1	0.001	0.1	1	0.001
153.0	0.2	1.2	0.0012	0.2	1.2	0.0012	0.2	1.2	0.0012
153.0	0.2	1.2	0.0012	0.2	1.2	0.0012	0.2	1.2	0.0012
153.0	0.2	1.2	0.0012	0.2	1.2	0.0012	0.2	1.2	0.0012
153.0	0.2	1.2	0.0012	0.2	1.2	0.0012	0.2	1.2	0.0012
153.0	0.2	1.2	0.0012	0.2	1.2	0.0012	0.2	1.2	0.0012
340.0	0.4	1.2	0.0012	0.4	1.2	0.0012	0.4	1.2	0.0012
340.0	0.4	1.2	0.0012	0.4	1.2	0.0012	0.4	1.2	0.0012
340.0	0.4	1.2	0.0012	0.4	1.2	0.0012	0.4	1.2	0.0012
340.0	0.4	1.2	0.0012	0.4	1.2	0.0012	0.4	1.2	0.0012
340.0	0.4	1.2	0.0012	0.4	1.2	0.0012	0.4	1.2	0.0012
511.0	1.8	3.5	0.0035	1.8	3.5	0.0035	1.8	3.5	0.0035

Table C. 5 continued

Shear Rate [1/s]	Shear Stress [Pa]	Viscosity [cP]	Viscosity [Pa·s]	Shear Stress [Pa]	Viscosity [cP]	Viscosity [Pa·s]	Shear Stress [Pa]	Viscosity [cP]	Viscosity [Pa·s]
511.0	1.8	3.5	0.0035	1.8	3.5	0.0035	1.8	3.5	0.0035
511.0	1.8	3.5	0.0035	1.8	3.5	0.0035	1.8	3.5	0.0035
511.0	1.8	3.5	0.0035	1.8	3.5	0.0035	1.8	3.5	0.0035
511.0	1.8	3.5	0.0035	1.8	3.5	0.0035	1.8	3.5	0.0035
1021.0	2.2	2.3	0.0023	2.2	2.3	0.0023	2.2	2.3	0.0023
1021.0	2.2	2.2	0.0022	2.2	2.2	0.0022	2.2	2.2	0.0022
1021.0	2.2	2.2	0.0022	2.2	2.2	0.0022	2.2	2.2	0.0022
1021.0	2.2	2.2	0.0022	2.2	2.2	0.0022	2.2	2.2	0.0022
1021.0	2.2	2.2	0.0022	2.2	2.2	0.0022	2.2	2.2	0.0022

Table C. 6 *Diluted red ethanol and oil Bayol 35, volume fraction 0.7498 measured data - 3 repetitions*

Shear Rate [1/s]	Shear Stress [Pa]	Viscosity [cP]	Viscosity [Pa·s]	Shear Stress [Pa]	Viscosity [cP]	Viscosity [Pa·s]	Shear Stress [Pa]	Viscosity [cP]	Viscosity [Pa·s]
1.5	0.1	100	0.1	0	0	0	0	0	0
1.5	0.1	100	0.1	0	0	0	0	0	0
1.5	0.1	100	0.1	0	0	0	0	0	0
1.5	0.1	100	0.1	0	0	0	0	0	0
1.5	0.1	100	0.1	0	0	0	0	0	0
3.1	0.1	33.3	0.0333	0	0	0	0	0	0
3.1	0.1	33.3	0.0333	0	0	0	0	0	0
3.1	0.1	33.3	0.0333	0	0	0	0	0	0
3.1	0.1	33.3	0.0333	0	0	0	0	0	0
3.1	0.1	33.3	0.0333	0	0	0	0	0	0
5.1	0.1	20	0.02	0	0	0	0	0	0
5.1	0.1	20	0.02	0	0	0	0	0	0
5.1	0.1	20	0.02	0	0	0	0	0	0
5.1	0.1	20	0.02	0	0	0	0	0	0
5.1	0.1	20	0.02	0	0	0	0	0	0
10.2	0.1	10	0.01	0	0	0	0	0	0
10.2	0.1	10	0.01	0	0	0	0	0	0
10.2	0.1	10	0.01	0	0	0	0	0	0
10.2	0.1	10	0.01	0	0	0	0	0	0
10.2	0.1	10	0.01	0	0	0	0	0	0
51.1	0.1	2	0.002	0.1	2	0.002	0.1	2	0.002
51.1	0.1	2	0.002	0.1	2	0.002	0.1	2	0.002
51.1	0.1	2	0.002	0.1	2	0.002	0.1	2	0.002
51.1	0.1	2	0.002	0.1	2	0.002	0.1	2	0.002
51.1	0.1	2	0.002	0.1	2	0.002	0.1	2	0.002
102.0	0.1	1	0.001	0.1	1	0.001	0.1	1	0.001
102.0	0.1	1	0.001	0.1	1	0.001	0.1	1	0.001

Table C. 6 continued

Shear Rate [1/s]	Shear Stress [Pa]	Viscosity [cP]	Viscosity [Pa·s]	Shear Stress [Pa]	Viscosity [cP]	Viscosity [Pa·s]	Shear Stress [Pa]	Viscosity [cP]	Viscosity [Pa·s]
102.0	0.1	1	0.001	0.1	1	0.001	0.1	1	0.001
102.0	0.1	1	0.001	0.1	1	0.001	0.1	1	0.001
102.0	0.1	1	0.001	0.1	1	0.001	0.1	1	0.001
153.0	0.2	1.2	0.0012	0.2	1.2	0.0012	0.2	1.2	0.0012
153.0	0.2	1.2	0.0012	0.2	1.2	0.0012	0.2	1.2	0.0012
153.0	0.2	1.2	0.0012	0.2	1.2	0.0012	0.2	1.2	0.0012
153.0	0.2	1.2	0.0012	0.2	1.2	0.0012	0.2	1.2	0.0012
153.0	0.2	1.2	0.0012	0.2	1.2	0.0012	0.2	1.2	0.0012
340.0	0.4	1.2	0.0012	0.4	1.2	0.0012	0.4	1.2	0.0012
340.0	0.4	1.2	0.0012	0.4	1.2	0.0012	0.4	1.2	0.0012
340.0	0.4	1.2	0.0012	0.4	1.2	0.0012	0.4	1.2	0.0012
340.0	0.4	1.2	0.0012	0.4	1.2	0.0012	0.4	1.2	0.0012
340.0	0.4	1.2	0.0012	0.4	1.2	0.0012	0.4	1.2	0.0012
511.0	0.8	1.5	0.0015	0.7	1.4	0.0014	0.7	1.4	0.0014
511.0	1.2	2.4	0.0024	0.7	1.4	0.0014	0.7	1.4	0.0014
511.0	1.8	3.5	0.0035	0.7	1.4	0.0014	0.7	1.4	0.0014
511.0	1.8	3.5	0.0035	0.7	1.4	0.0014	0.7	1.4	0.0014
511.0	1.8	3.5	0.0035	0.8	1.5	0.0015	0.8	1.5	0.0015
1021.0	2.2	2.3	0.0023	2.2	2.1	0.0021	2.2	2.1	0.0021
1021.0	2.2	2.2	0.0022	2.2	2.2	0.0022	2.2	2.2	0.0022
1021.0	2.2	2.2	0.0022	2.2	2.2	0.0022	2.2	2.2	0.0022
1021.0	2.2	2.2	0.0022	2.2	2.2	0.0022	2.2	2.2	0.0022
1021.0	2.2	2.2	0.0022	2.2	2.2	0.0022	2.2	2.2	0.0022

Table C. 7 *Diluted red ethanol and oil Bayol 35, volume fraction 0.9372 measured data - 3 repetitions*

Shear Rate [1/s]	Shear Stress [Pa]	Viscosity [cP]	Viscosity [Pa·s]	Shear Stress [Pa]	Viscosity [cP]	Viscosity [Pa·s]	Shear Stress [Pa]	Viscosity [cP]	Viscosity [Pa·s]
1.5	0	0	0	0	0	0	0	0	0
1.5	0	0	0	0	0	0	0	0	0
1.5	0	0	0	0	0	0	0	0	0
1.5	0	0	0	0	0	0	0	0	0
1.5	0	0	0	0	0	0	0	0	0
3.1	0	0	0	0	0	0	0	0	0
3.1	0	0	0	0	0	0	0	0	0
3.1	0	0	0	0	0	0	0	0	0
3.1	0	0	0	0	0	0	0	0	0
3.1	0	0	0	0	0	0	0	0	0
5.1	0	0	0	0	0	0	0	0	0
5.1	0	0	0	0	0	0	0	0	0
5.1	0	0	0	0	0	0	0	0	0

Table C. 7 continued

Shear Rate [1/s]	Shear Stress [Pa]	Viscosity [cP]	Viscosity [Pa·s]	Shear Stress [Pa]	Viscosity [cP]	Viscosity [Pa·s]	Shear Stress [Pa]	Viscosity [cP]	Viscosity [Pa·s]
5.1	0	0	0	0	0	0	0	0	0
5.1	0	0	0	0	0	0	0	0	0
10.2	0	0	0	0	4.8	0.0048	0	4.8	0.0048
10.2	0	0	0	0.1	10	0.01	0.1	10	0.01
10.2	0	0	0	0.1	10	0.01	0.1	10	0.01
10.2	0	0	0	0.1	10	0.01	0.1	10	0.01
10.2	0	0	0	0.1	10	0.01	0.1	10	0.01
51.1	0.1	2	0.002	0.1	2	0.002	0.1	2	0.002
51.1	0.1	2	0.002	0.1	2	0.002	0.1	2	0.002
51.1	0.1	2	0.002	0.1	2	0.002	0.1	2	0.002
51.1	0.1	2	0.002	0.1	2	0.002	0.1	2	0.002
51.1	0.1	2	0.002	0.1	2	0.002	0.1	2	0.002
102.0	0.1	1	0.001	0.1	1	0.001	0.1	1	0.001
102.0	0.1	1	0.001	0.1	1	0.001	0.1	1	0.001
102.0	0.1	1	0.001	0.1	1	0.001	0.1	1	0.001
102.0	0.1	1	0.001	0.1	1	0.001	0.1	1	0.001
102.0	0.1	1	0.001	0.1	1	0.001	0.1	1	0.001
153.0	0.2	1.2	0.0012	0.2	1.2	0.0012	0.2	1.2	0.0012
153.0	0.2	1.2	0.0012	0.2	1.2	0.0012	0.2	1.2	0.0012
153.0	0.2	1.2	0.0012	0.2	1.2	0.0012	0.2	1.2	0.0012
153.0	0.2	1.2	0.0012	0.2	1.2	0.0012	0.2	1.2	0.0012
153.0	0.2	1.2	0.0012	0.2	1.2	0.0012	0.2	1.2	0.0012
340.0	0.4	1.2	0.0012	0.4	1.2	0.0012	0.4	1.2	0.0012
340.0	0.4	1.2	0.0012	0.4	1.2	0.0012	0.4	1.2	0.0012
340.0	0.4	1.2	0.0012	0.4	1.2	0.0012	0.4	1.2	0.0012
340.0	0.4	1.2	0.0012	0.4	1.2	0.0012	0.4	1.2	0.0012
340.0	0.4	1.2	0.0012	0.4	1.2	0.0012	0.4	1.2	0.0012
511.0	0.8	1.6	0.0016	0.8	1.5	0.0015	0.8	1.5	0.0015
511.0	1.8	3.5	0.0035	1.8	3.5	0.0035	1.8	3.5	0.0035
511.0	1.8	3.5	0.0035	1.8	3.5	0.0035	1.8	3.5	0.0035
511.0	1.8	3.5	0.0035	1.8	3.5	0.0035	1.8	3.5	0.0035
511.0	1.8	3.5	0.0035	1.8	3.5	0.0035	1.8	3.5	0.0035
1021.0	2.2	2.3	0.0023	2.2	2.3	0.0023	2.2	2.3	0.0023
1021.0	2.2	2.2	0.0022	2.2	2.2	0.0022	2.2	2.2	0.0022
1021.0	2.2	2.2	0.0022	2.2	2.2	0.0022	2.2	2.2	0.0022
1021.0	2.2	2.2	0.0022	2.2	2.2	0.0022	2.2	2.2	0.0022
1021.0	2.2	2.2	0.0022	2.2	2.2	0.0022	2.2	2.2	0.0022

Table C. 8 *Oil Bayol 35 measured data - 3 repetitions*

Shear Rate [1/s]	Shear Stress [Pa]	Viscosity [cP]	Viscosity [Pa·s]	Shear Stress [Pa]	Viscosity [cP]	Viscosity [Pa·s]	Shear Stress [Pa]	Viscosity [cP]	Viscosity [Pa·s]
1.5	0.3	300	0.3	0.3	300	0.3	0.3	300	0.3
1.5	0.3	300	0.3	0.3	300	0.3	0.3	300	0.3
1.5	0.3	300	0.3	0.3	300	0.3	0.3	300	0.3
1.5	0.3	300	0.3	0.3	300	0.3	0.3	300	0.3
1.5	0.3	300	0.3	0.3	300	0.3	0.3	300	0.3
3.1	0.3	100	0.1	0.3	100	0.1	0.3	100	0.1
3.1	0.3	100	0.1	0.3	100	0.1	0.3	100	0.1
3.1	0.3	100	0.1	0.3	100	0.1	0.3	100	0.1
3.1	0.3	100	0.1	0.3	100	0.1	0.3	100	0.1
3.1	0.3	100	0.1	0.3	100	0.1	0.3	100	0.1
5.1	0.3	60	0.06	0.3	60	0.06	0.3	60	0.06
5.1	0.3	60	0.06	0.3	60	0.06	0.3	60	0.06
5.1	0.3	60	0.06	0.3	60	0.06	0.3	60	0.06
5.1	0.3	60	0.06	0.3	60	0.06	0.3	60	0.06
5.1	0.3	60	0.06	0.3	60	0.06	0.3	60	0.06
10.2	0.3	30	0.03	0.3	30	0.03	0.3	30	0.03
10.2	0.3	30	0.03	0.3	30	0.03	0.3	30	0.03
10.2	0.3	30	0.03	0.3	30	0.03	0.3	30	0.03
10.2	0.3	30	0.03	0.3	30	0.03	0.3	30	0.03
10.2	0.3	30	0.03	0.3	30	0.03	0.3	30	0.03
51.1	0.4	7.8	0.0078	0.4	7.8	0.0078	0.4	7.8	0.0078
51.1	0.4	7.8	0.0078	0.4	7.8	0.0078	0.4	7.8	0.0078
51.1	0.4	7.8	0.0078	0.4	7.8	0.0078	0.4	7.8	0.0078
51.1	0.4	7.8	0.0078	0.4	7.8	0.0078	0.4	7.8	0.0078
51.1	0.4	7.8	0.0078	0.4	7.8	0.0078	0.4	7.8	0.0078
102.0	0.5	4.9	0.0049	0.5	4.9	0.0049	0.5	4.9	0.0049
102.0	0.5	4.9	0.0049	0.5	4.9	0.0049	0.5	4.9	0.0049
102.0	0.5	4.9	0.0049	0.5	4.9	0.0049	0.5	4.9	0.0049
102.0	0.5	4.9	0.0049	0.5	4.9	0.0049	0.5	4.9	0.0049
102.0	0.5	4.9	0.0049	0.5	4.9	0.0049	0.5	4.9	0.0049
153.0	0.6	3.5	0.0035	0.6	3.5	0.0035	0.6	3.5	0.0035
153.0	0.6	3.5	0.0035	0.6	3.5	0.0035	0.6	3.5	0.0035
153.0	0.6	3.5	0.0035	0.6	3.5	0.0035	0.6	3.5	0.0035
153.0	0.6	3.5	0.0035	0.6	3.5	0.0035	0.6	3.5	0.0035
153.0	0.6	3.5	0.0035	0.6	3.5	0.0035	0.6	3.5	0.0035
340.0	0.9	2.6	0.0026	0.9	2.6	0.0026	0.9	2.6	0.0026
340.0	0.9	2.6	0.0026	0.9	2.6	0.0026	0.9	2.6	0.0026
340.0	0.9	2.6	0.0026	0.9	2.6	0.0026	0.9	2.6	0.0026
340.0	0.9	2.6	0.0026	0.9	2.6	0.0026	0.9	2.6	0.0026
340.0	0.9	2.6	0.0026	0.9	2.6	0.0026	0.9	2.6	0.0026
511.0	1.2	2.4	0.0024	1.2	2.4	0.0024	1.2	2.4	0.0024

Table C. 8 continued

Shear Rate [1/s]	Shear Stress [Pa]	Viscosity [cP]	Viscosity [Pa·s]	Shear Stress [Pa]	Viscosity [cP]	Viscosity [Pa·s]	Shear Stress [Pa]	Viscosity [cP]	Viscosity [Pa·s]
511.0	1.2	2.4	0.0024	1.2	2.4	0.0024	1.2	2.4	0.0024
511.0	1.2	2.4	0.0024	1.2	2.4	0.0024	1.2	2.4	0.0024
511.0	1.2	2.4	0.0024	1.2	2.4	0.0024	1.2	2.4	0.0024
511.0	1.2	2.4	0.0024	1.2	2.4	0.0024	1.2	2.4	0.0024
1021.0	2.2	2.2	0.0022	2.2	2.2	0.0022	2.2	2.2	0.0022
1021.0	2.2	2.2	0.0022	2.2	2.2	0.0022	2.2	2.2	0.0022
1021.0	2.2	2.2	0.0022	2.2	2.2	0.0022	2.2	2.2	0.0022
1021.0	2.2	2.2	0.0022	2.2	2.2	0.0022	2.2	2.2	0.0022
1021.0	2.2	2.2	0.0022	2.2	2.2	0.0022	2.2	2.2	0.0022

Table C. 9 *Glycerol measured data - 5 repetitions*

Shear Rate [1/s]	Shear Stress [Pa]	Viscosity [cP]	Viscosity [Pa·s]	Shear Stress [Pa]	Viscosity [cP]	Viscosity [Pa·s]	Shear Stress [Pa]	Viscosity [cP]	Viscosity [Pa·s]	Shear Stress [Pa]	Viscosity [cP]	Viscosity [Pa·s]	Shear Stress [Pa]	Viscosity [cP]	Viscosity [Pa·s]
1.5	0.1	100	0.1	0.1	100	0.1	0	0	0	0.1	100	0.1	0.1	100	0.1
1.5	0.1	100	0.1	0.1	100	0.1	0	0	0	0.1	100	0.1	0.1	100	0.1
1.5	0.1	100	0.1	0.1	100	0.1	0	0	0	0.1	100	0.1	0.1	100	0.1
1.5	0.1	100	0.1	0.1	100	0.1	0	0	0	0.1	100	0.1	0.1	100	0.1
1.5	0.1	100	0.1	0.1	100	0.1	0	0	0	0.1	100	0.1	0.1	100	0.1
3.1	0.2	66.7	0.0667	0.3	98.3	0.0983	0.2	66.7	0.0667	0.2	66.7	0.0667	0.2	66.7	0.0667
3.1	0.2	66.7	0.0667	0.3	100	0.1	0.2	66.7	0.0667	0.2	66.7	0.0667	0.2	66.7	0.0667
3.1	0.2	66.7	0.0667	0.3	100	0.1	0.2	66.7	0.0667	0.2	66.7	0.0667	0.2	66.7	0.0667
3.1	0.2	66.7	0.0667	0.3	100	0.1	0.2	66.7	0.0667	0.2	66.7	0.0667	0.2	66.7	0.0667
3.1	0.2	66.7	0.0667	0.3	100	0.1	0.2	66.7	0.0667	0.2	66.7	0.0667	0.2	66.7	0.0667
5.1	0.4	80	0.08	0.5	100	0.1	0.4	80	0.08	0.4	80	0.08	0.4	80	0.08
5.1	0.4	80	0.08	0.5	100	0.1	0.4	80	0.08	0.4	80	0.08	0.4	80	0.08
5.1	0.4	80	0.08	0.5	100	0.1	0.4	80	0.08	0.4	80	0.08	0.4	80	0.08
5.1	0.4	80	0.08	0.5	100	0.1	0.4	80	0.08	0.4	80	0.08	0.4	80	0.08
5.1	0.4	80	0.08	0.5	100	0.1	0.4	80	0.08	0.4	80	0.08	0.4	80	0.08
10.2	1	100	0.1	1.1	110	0.11	1.1	110	0.11	1	101	0.101	1.1	110	0.11
10.2	1	100	0.1	1.1	110	0.11	1.1	110	0.11	1	100	0.1	1.1	110	0.11
10.2	1	100	0.1	1.1	110	0.11	1.1	110	0.11	1	100	0.1	1.1	110	0.11
10.2	1	100	0.1	1.1	110	0.11	1.1	110	0.11	1	100	0.1	1.1	110	0.11
10.2	1	100	0.1	1.1	110	0.11	1.1	110	0.11	1	100.5	0.1005	1.1	110	0.11
51.1	6	117.6	0.1176	5.9	115.7	0.1157	5.8	113.7	0.1137	5.8	113.7	0.1137	5.7	111.8	0.1118
51.1	6	117.6	0.1176	5.9	115.7	0.1157	5.8	113.7	0.1137	5.8	113.7	0.1137	5.7	111.8	0.1118
51.1	6	117.6	0.1176	5.9	115.7	0.1157	5.8	113.7	0.1137	5.8	113.7	0.1137	5.7	111.8	0.1118
51.1	6	117.6	0.1176	5.9	115.7	0.1157	5.8	113.7	0.1137	5.8	113.7	0.1137	5.7	111.8	0.1118
51.1	6	117.6	0.1176	5.9	115.7	0.1157	5.8	113.7	0.1137	5.8	113.7	0.1137	5.7	111.8	0.1118
102.0	12.2	119.7	0.1197	11.8	115.7	0.1157	11.7	115	0.115	11.6	113.7	0.1137	11.5	112.7	0.1127
102.0	12.2	119.7	0.1197	11.8	115.7	0.1157	11.8	115.5	0.1155	11.6	114	0.114	11.5	112.7	0.1127
102.0	12.2	119.6	0.1196	11.8	115.7	0.1157	11.8	115.3	0.1153	11.7	114.2	0.1142	11.5	112.7	0.1127
102.0	12.2	119.6	0.1196	11.8	115.7	0.1157	11.8	115.6	0.1156	11.7	114.4	0.1144	11.5	112.7	0.1127
102.0	12.2	119.7	0.1197	11.8	115.7	0.1157	11.8	115.5	0.1155	11.7	114.6	0.1146	11.5	112.7	0.1127
153.0	18.5	120.7	0.1207	17.8	116.4	0.1164	17.8	116.4	0.1164	17.7	115.7	0.1157	17.6	114.9	0.1149
153.0	18.5	120.7	0.1207	17.8	116.6	0.1166	17.9	116.7	0.1167	17.7	115.7	0.1157	17.6	115	0.115
153.0	18.5	120.7	0.1207	17.9	116.9	0.1169	17.9	116.8	0.1168	17.7	115.7	0.1157	17.6	115	0.115
153.0	18.5	120.7	0.1207	17.9	116.9	0.1169	17.9	116.9	0.1169	17.7	115.7	0.1157	17.6	115	0.115
153.0	18.5	120.7	0.1207	17.9	117	0.117	17.9	116.8	0.1168	17.7	115.7	0.1157	17.6	115	0.115
340.0	41	105.5	0.1055	39.8	117	0.117	39.5	116.2	0.1162	39.1	114.9	0.1149	38.8	114.1	0.1141
340.0	41	120.6	0.1206	39.8	117.1	0.1171	39.6	116.5	0.1165	39.1	114.9	0.1149	38.8	114.2	0.1142
340.0	41	120.6	0.1206	39.8	117.1	0.1171	39.5	116.3	0.1163	39	114.7	0.1147	38.8	114.1	0.1141
340.0	41	120.6	0.1206	39.8	117.1	0.1171	39.6	116.5	0.1165	39	114.7	0.1147	38.8	114.1	0.1141
340.0	41	120.6	0.1206	39.7	116.8	0.1168	39.6	116.3	0.1163	39	114.7	0.1147	38.8	114.1	0.1141

Table C. 9 continued

Shear Rate [1/s]	Shear Stress [Pa]	Viscosity [cP]	Viscosity [Pa·s]	Shear Stress [Pa]	Viscosity [cP]	Viscosity [Pa·s]	Shear Stress [Pa]	Viscosity [cP]	Viscosity [Pa·s]	Shear Stress [Pa]	Viscosity [cP]	Viscosity [Pa·s]	Shear Stress [Pa]	Viscosity [cP]	Viscosity [Pa·s]
511.0	61.2	89.9	0.0899	59.2	116.1	0.1161	58.8	115.3	0.1153	58.6	114.8	0.1148	58	113.7	0.1137
511.0	61.1	119.8	0.1198	59.2	116	0.116	58.7	115.2	0.1152	58.3	114.3	0.1143	58	113.7	0.1137
511.0	61	119.6	0.1196	59.1	115.9	0.1159	58.7	115.1	0.1151	58.2	114.1	0.1141	57.9	113.5	0.1135
511.0	61	119.6	0.1196	59	115.7	0.1157	58.6	114.9	0.1149	58.1	114	0.114	57.8	113.3	0.1133
511.0	60.9	119.4	0.1194	59	115.7	0.1157	58.6	114.9	0.1149	58.1	113.9	0.1139	57.8	113.3	0.1133
1021.0	111.6	53.1	0.0531	115.4	113	0.113	114.6	112.2	0.1122	113.9	111.5	0.1115	113.5	111.1	0.1111
1021.0	119.2	116.8	0.1168	114.2	111.9	0.1119	113.7	111.3	0.1113	112.9	110.6	0.1106	112.4	110	0.11
1021.0	118.8	116.4	0.1164	113.7	111.3	0.1113	113.1	110.7	0.1107	112.1	109.8	0.1098	111.5	109.2	0.1092
1021.0	118.3	115.9	0.1159	113.4	111.1	0.1111	112.6	110.3	0.1103	111.5	109.2	0.1092	111	108.7	0.1087
1021.0	118.1	115.7	0.1157	113.1	110.8	0.1108	112.1	109.8	0.1098	111.2	108.9	0.1089	110.7	108.4	0.1084

Table C. 10 *Glycerol and particles, volume fraction 0.0029 measured data - 5 repetitions*

Shear Rate [1/s]	Shear Stress [Pa]	Viscosity [cP]	Viscosity [Pa·s]	Shear Stress [Pa]	Viscosity [cP]	Viscosity [Pa·s]	Shear Stress [Pa]	Viscosity [cP]	Viscosity [Pa·s]	Shear Stress [Pa]	Viscosity [cP]	Viscosity [Pa·s]	Shear Stress [Pa]	Viscosity [cP]	Viscosity [Pa·s]
1.5	0.1	100	0.1	0.1	100	0.1	0.1	100	0.1	0	0	0	0	0	0
1.5	0.1	100	0.1	0.1	100	0.1	0.1	100	0.1	0	0	0	0	0	0
1.5	0.1	100	0.1	0.1	100	0.1	0.1	100	0.1	0	0	0	0	0	0
1.5	0.1	100	0.1	0.1	100	0.1	0.1	100	0.1	0	0	0	0	0	0
1.5	0.1	100	0.1	0.1	100	0.1	0.1	100	0.1	0	0	0	0	0	0
3.1	0.3	100	0.1	0.3	100	0.1	0.3	86.7	0.0867	0.2	66.7	0.0667	0.2	66.7	0.0667
3.1	0.3	100	0.1	0.3	100	0.1	0.3	94.2	0.0942	0.2	66.7	0.0667	0.2	66.7	0.0667
3.1	0.3	100	0.1	0.3	100	0.1	0.3	94.7	0.0947	0.2	66.7	0.0667	0.2	66.7	0.0667
3.1	0.3	100	0.1	0.3	100	0.1	0.3	97.2	0.0972	0.2	66.7	0.0667	0.2	66.7	0.0667
3.1	0.3	100	0.1	0.3	100	0.1	0.3	100	0.1	0.2	66.7	0.0667	0.2	66.7	0.0667
5.1	0.6	113.5	0.1135	0.6	120	0.12	0.4	80	0.08	0.3	62.5	0.0625	0.3	60	0.06
5.1	0.6	115	0.115	0.6	120	0.12	0.4	80	0.08	0.3	62.5	0.0625	0.3	60	0.06
5.1	0.6	118.3	0.1183	0.6	120	0.12	0.4	80	0.08	0.3	60.3	0.0603	0.3	60	0.06
5.1	0.6	118.3	0.1183	0.6	120	0.12	0.4	80	0.08	0.3	62	0.062	0.3	60	0.06
5.1	0.6	120	0.12	0.6	120	0.12	0.4	80	0.08	0.3	60	0.06	0.3	60	0.06
10.2	1.2	120	0.12	1.1	114.2	0.1142	1.2	120	0.12	1.2	120	0.12	1.2	120	0.12
10.2	1.2	120	0.12	1.1	111.9	0.1119	1.2	120	0.12	1.2	120	0.12	1.2	120	0.12
10.2	1.2	120	0.12	1.1	111.2	0.1112	1.2	120	0.12	1.2	120	0.12	1.2	120	0.12
10.2	1.2	120	0.12	1.1	110	0.11	1.2	120	0.12	1.2	120	0.12	1.2	120	0.12
10.2	1.2	120	0.12	1.1	110	0.11	1.2	120	0.12	1.2	120	0.12	1.2	120	0.12
51.1	5.8	113.7	0.1137	5.7	111.8	0.1118	5.6	109.8	0.1098	5.6	110.8	0.1108	5.7	111.8	0.1118
51.1	5.8	113.7	0.1137	5.7	111.8	0.1118	5.6	109.8	0.1098	5.7	111.5	0.1115	5.7	111.8	0.1118
51.1	5.8	113.7	0.1137	5.7	111.8	0.1118	5.6	109.8	0.1098	5.7	111.8	0.1118	5.7	111.8	0.1118
51.1	5.8	113.7	0.1137	5.7	111.8	0.1118	5.6	109.8	0.1098	5.7	111.7	0.1117	5.7	111.8	0.1118

Table C. 10 continued

Shear Rate [1/s]	Shear Stress [Pa]	Viscosity [cP]	Viscosity [Pa·s]	Shear Stress [Pa]	Viscosity [cP]	Viscosity [Pa·s]	Shear Stress [Pa]	Viscosity [cP]	Viscosity [Pa·s]	Shear Stress [Pa]	Viscosity [cP]	Viscosity [Pa·s]	Shear Stress [Pa]	Viscosity [cP]	Viscosity [Pa·s]
102.0	11.9	116.7	0.1167	11.7	114.7	0.1147	11.7	114.7	0.1147	11.7	114.7	0.1147	11.6	113.7	0.1137
102.0	11.9	116.7	0.1167	11.7	114.7	0.1147	11.7	114.7	0.1147	11.7	114.7	0.1147	11.6	113.7	0.1137
102.0	11.9	116.7	0.1167	11.7	114.7	0.1147	11.7	114.7	0.1147	11.7	114.7	0.1147	11.6	113.7	0.1137
102.0	11.9	116.7	0.1167	11.7	114.7	0.1147	11.7	114.7	0.1147	11.7	114.7	0.1147	11.6	113.7	0.1137
102.0	11.9	116.7	0.1167	11.7	114.7	0.1147	11.7	114.7	0.1147	11.7	114.7	0.1147	11.6	113.7	0.1137
153.0	17.8	116.3	0.1163	17.7	115.5	0.1155	17.5	114.4	0.1144	17.4	113.8	0.1138	17.4	113.7	0.1137
153.0	17.8	116.3	0.1163	17.6	115	0.115	17.5	114.4	0.1144	17.4	113.9	0.1139	17.4	113.7	0.1137
153.0	17.8	116.3	0.1163	17.6	115	0.115	17.5	114.4	0.1144	17.4	113.9	0.1139	17.4	113.7	0.1137
153.0	17.8	116.3	0.1163	17.6	115	0.115	17.5	114.4	0.1144	17.4	114	0.114	17.4	113.7	0.1137
153.0	17.8	116.3	0.1163	17.6	115	0.115	17.5	114.4	0.1144	17.5	114.2	0.1142	17.4	113.7	0.1137
340.0	39.8	117.1	0.1171	39.5	116.2	0.1162	39.3	115.6	0.1156	39.1	115	0.115	38.8	114.2	0.1142
340.0	39.8	117.1	0.1171	39.4	116	0.116	39.3	115.6	0.1156	39	114.7	0.1147	38.8	114.1	0.1141
340.0	39.7	116.9	0.1169	39.4	115.9	0.1159	39.3	115.6	0.1156	39	114.7	0.1147	38.8	114.1	0.1141
340.0	39.7	116.8	0.1168	39.4	115.9	0.1159	39.3	115.5	0.1155	39	114.7	0.1147	38.8	114.1	0.1141
340.0	39.8	116.9	0.1169	39.4	115.9	0.1159	39.2	115.4	0.1154	39	114.7	0.1147	38.8	114.1	0.1141
511.0	59.4	116.6	0.1166	58.7	115.1	0.1151	58.4	114.5	0.1145	58.1	113.9	0.1139	57.9	113.5	0.1135
511.0	59.3	116.3	0.1163	58.6	115	0.115	58.3	114.3	0.1143	58.1	113.8	0.1138	57.8	113.3	0.1133
511.0	59.2	116.1	0.1161	58.6	114.9	0.1149	58.3	114.3	0.1143	58	113.7	0.1137	57.7	113.1	0.1131
511.0	59.1	115.9	0.1159	58.6	114.9	0.1149	58.3	114.3	0.1143	58	113.7	0.1137	57.7	113.1	0.1131
511.0	59.1	115.9	0.1159	58.5	114.7	0.1147	58.2	114.1	0.1141	57.9	113.5	0.1135	57.7	113.1	0.1131
1021.0	115.9	113.5	0.1135	115.1	112.8	0.1128	114.3	111.9	0.1119	113.8	111.4	0.1114	113.4	111.1	0.1111
1021.0	114.8	112.4	0.1124	113.9	111.5	0.1115	113.4	111.1	0.1111	113	110.7	0.1107	112.4	110.1	0.1101
1021.0	113.9	111.6	0.1116	113.4	111.1	0.1111	113.1	110.7	0.1107	112.2	109.9	0.1099	111.8	109.5	0.1095
1021.0	113.5	111.2	0.1112	113.1	110.8	0.1108	112.5	110.2	0.1102	111.9	109.6	0.1096	111.4	109.1	0.1091
1021.0	113.3	110.9	0.1109	112.9	110.5	0.1105	112	109.7	0.1097	111.6	109.3	0.1093	111.2	108.9	0.1089

Table C. 11 *Glycerol and particles, volume fraction 0.0058 measuring data - 5 repetitions*

Shear Rate [1/s]	Shear Stress [Pa]	Viscosity [cP]	Viscosity [Pa·s]	Shear Stress [Pa]	Viscosity [cP]	Viscosity [Pa·s]	Shear Stress [Pa]	Viscosity [cP]	Viscosity [Pa·s]	Shear Stress [Pa]	Viscosity [cP]	Viscosity [Pa·s]	Shear Stress [Pa]	Viscosity [cP]	Viscosity [Pa·s]
1.5	0.1	100	0.1	0.1	100	0.1	0.1	100	0.1	0.1	100	0.1	0.1	100	0.1
1.5	0.1	100	0.1	0.1	100	0.1	0.1	100	0.1	0.1	100	0.1	0.1	100	0.1
1.5	0.1	100	0.1	0.1	100	0.1	0.1	100	0.1	0.1	100	0.1	0.1	100	0.1
1.5	0.1	100	0.1	0.1	100	0.1	0.1	100	0.1	0.1	100	0.1	0.1	100	0.1
1.5	0.1	100	0.1	0.1	100	0.1	0.1	100	0.1	0.1	100	0.1	0.1	100	0.1
3.1	0.2	66.7	0.0667	0.3	100	0.1	0.3	100	0.1	0.3	100	0.1	0.3	100	0.1
3.1	0.2	66.7	0.0667	0.3	100	0.1	0.3	100	0.1	0.3	100	0.1	0.3	100	0.1
3.1	0.2	66.7	0.0667	0.3	100	0.1	0.3	100	0.1	0.3	100	0.1	0.3	100	0.1
3.1	0.2	66.7	0.0667	0.3	100	0.1	0.3	100	0.1	0.3	100	0.1	0.3	100	0.1

Table C. 11 continued

Shear Rate [1/s]	Shear Stress [Pa]	Viscosity [cP]	Viscosity [Pa·s]	Shear Stress [Pa]	Viscosity [cP]	Viscosity [Pa·s]	Shear Stress [Pa]	Viscosity [cP]	Viscosity [Pa·s]	Shear Stress [Pa]	Viscosity [cP]	Viscosity [Pa·s]	Shear Stress [Pa]	Viscosity [cP]	Viscosity [Pa·s]
3.1	0.2	66.7	0.0667	0.3	100	0.1	0.3	100	0.1	0.3	100	0.1	0.3	100	0.1
5.1	0.4	80	0.08	0.4	80.5	0.0805	0.4	80	0.08	0.4	80	0.08	0.5	92.5	0.0925
5.1	0.4	80	0.08	0.4	85	0.085	0.4	80	0.08	0.4	80	0.08	0.5	96.2	0.0962
5.1	0.4	80	0.08	0.4	85.2	0.0852	0.4	80	0.08	0.4	80.1	0.0801	0.5	98.2	0.0982
5.1	0.4	80	0.08	0.4	89.8	0.0898	0.4	80	0.08	0.4	80	0.08	0.5	95.2	0.0952
5.1	0.4	80	0.08	0.4	87.5	0.0875	0.4	80	0.08	0.4	80.1	0.0801	0.5	96.5	0.0965
10.2	0.9	90	0.09	1	100	0.1	1	100	0.1	0.9	90	0.09	0.9	90	0.09
10.2	0.9	90	0.09	1	100	0.1	1	100	0.1	0.9	90	0.09	0.9	90	0.09
10.2	0.9	90	0.09	1	100	0.1	1	100	0.1	0.9	90	0.09	0.9	90	0.09
10.2	0.9	90	0.09	1	100	0.1	1	100	0.1	0.9	90	0.09	0.9	90	0.09
10.2	0.9	90	0.09	1	100	0.1	1	100	0.1	0.9	90.7	0.0907	0.9	90	0.09
51.1	6	117.6	0.1176	6.3	123.5	0.1235	6.3	123.5	0.1235	6.3	122.6	0.1226	6.2	121.6	0.1216
51.1	6	117.8	0.1178	6.3	123.5	0.1235	6.3	123.5	0.1235	6.3	123	0.123	6.2	121.6	0.1216
51.1	6	118.2	0.1182	6.3	123.6	0.1236	6.3	123.5	0.1235	6.3	123.4	0.1234	6.2	121.6	0.1216
51.1	6	118.4	0.1184	6.3	123.8	0.1238	6.3	123.5	0.1235	6.3	123.5	0.1235	6.2	121.6	0.1216
51.1	6.1	118.7	0.1187	6.3	124	0.124	6.3	123.5	0.1235	6.3	123.5	0.1235	6.2	121.6	0.1216
102.0	12.2	119.6	0.1196	12.9	126.5	0.1265	12.7	124.8	0.1248	12.6	123.5	0.1235	12.5	122.5	0.1225
102.0	12.2	119.6	0.1196	12.9	126.5	0.1265	12.7	125	0.125	12.6	123.5	0.1235	12.5	122.5	0.1225
102.0	12.2	119.6	0.1196	12.9	126.5	0.1265	12.8	125.2	0.1252	12.6	123.5	0.1235	12.5	122.5	0.1225
102.0	12.2	119.6	0.1196	12.9	126.5	0.1265	12.8	125.4	0.1254	12.6	123.5	0.1235	12.5	122.5	0.1225
102.0	12.2	119.6	0.1196	12.9	126.5	0.1265	12.8	125.4	0.1254	12.6	123.5	0.1235	12.5	122.5	0.1225
153.0	18.6	121.6	0.1216	19.4	126.9	0.1269	19.2	125.8	0.1258	19.1	124.8	0.1248	18.9	123.5	0.1235
153.0	18.6	121.6	0.1216	19.4	127	0.127	19.2	125.5	0.1255	19.1	124.8	0.1248	18.9	123.5	0.1235
153.0	18.6	121.6	0.1216	19.5	127.2	0.1272	19.2	125.6	0.1256	19.1	124.8	0.1248	18.9	123.5	0.1235
153.0	18.6	121.6	0.1216	19.5	127.4	0.1274	19.2	125.7	0.1257	19.1	124.8	0.1248	18.9	123.5	0.1235
153.0	18.6	121.8	0.1218	19.5	127.4	0.1274	19.2	125.7	0.1257	19.1	124.8	0.1248	18.9	123.5	0.1235
340.0	41.4	121.7	0.1217	43.6	128.2	0.1282	43.3	127.4	0.1274	43	126.3	0.1263	42.3	124.4	0.1244
340.0	41.3	121.5	0.1215	43.6	128.2	0.1282	43.2	127.1	0.1271	42.9	126.2	0.1262	42.2	124.2	0.1242
340.0	41.3	121.5	0.1215	43.5	128	0.128	43.2	127.1	0.1271	42.9	126.2	0.1262	42.2	124.1	0.1241
340.0	41.3	121.5	0.1215	43.5	128	0.128	43.2	127.1	0.1271	42.9	126.2	0.1262	42.2	124.1	0.1241
340.0	41.3	121.5	0.1215	43.5	127.9	0.1279	43.2	127.1	0.1271	42.9	126.2	0.1262	42.2	124.1	0.1241
511.0	62.4	122.4	0.1224	65.2	127.8	0.1278	64.4	126.3	0.1263	63.8	125	0.125	63.4	124.2	0.1242
511.0	62.2	122	0.122	64.9	127.2	0.1272	64.2	125.9	0.1259	63.6	124.7	0.1247	63.2	123.9	0.1239
511.0	62.2	122	0.122	64.8	127.1	0.1271	64.1	125.7	0.1257	63.6	124.7	0.1247	63.2	123.8	0.1238
511.0	62.1	121.8	0.1218	64.7	126.9	0.1269	64	125.5	0.1255	63.5	124.5	0.1245	63.1	123.7	0.1237
511.0	62.1	121.8	0.1218	64.7	126.9	0.1269	64	125.5	0.1255	63.5	124.5	0.1245	63.1	123.7	0.1237
1021.0	121.6	119.1	0.1191	126.8	124.1	0.1241	125.5	123	0.123	124.5	122	0.122	123.4	120.9	0.1209
1021.0	120.1	117.6	0.1176	125.3	122.7	0.1227	124.2	121.6	0.1216	123.2	120.7	0.1207	122.2	119.7	0.1197
1021.0	119.5	117.1	0.1171	124.5	122	0.122	123.5	120.9	0.1209	122.6	120	0.12	121.4	118.9	0.1189
1021.0	119.2	116.7	0.1167	124.1	121.6	0.1216	123.1	120.5	0.1205	122.1	119.6	0.1196	121.1	118.6	0.1186
1021.0	118.8	116.3	0.1163	123.7	121.2	0.1212	122.7	120.2	0.1202	121.8	119.2	0.1192	120.6	118.1	0.1181

Table C. 12 *Glycerol and particles, volume fraction 0.0087 measuring data - 3 repetitions*

Shear Rate [1/s]	Shear Stress [Pa]	Viscosity [cP]	Viscosity [Pa·s]	Shear Stress [Pa]	Viscosity [cP]	Viscosity [Pa·s]	Shear Stress [Pa]	Viscosity [cP]	Viscosity [Pa·s]
1.5	0.3	300	0.3	0.3	300	0.3	0.4	400	0.4
1.5	0.3	300	0.3	0.3	300	0.3	0.4	400	0.4
1.5	0.3	300	0.3	0.3	300	0.3	0.4	400	0.4
1.5	0.3	300	0.3	0.3	300	0.3	0.4	400	0.4
1.5	0.3	300	0.3	0.3	300	0.3	0.4	400	0.4
3.1	0.5	166.7	0.1667	0.5	166.7	0.1667	0.5	166.7	0.1667
3.1	0.5	166.7	0.1667	0.5	166.7	0.1667	0.5	166.7	0.1667
3.1	0.5	166.7	0.1667	0.5	166.7	0.1667	0.5	166.7	0.1667
3.1	0.5	166.7	0.1667	0.5	166.7	0.1667	0.5	166.7	0.1667
3.1	0.5	166.7	0.1667	0.5	166.7	0.1667	0.5	166.7	0.1667
5.1	0.7	140	0.14	0.7	140	0.14	0.7	136	0.136
5.1	0.7	140	0.14	0.7	140	0.14	0.7	140	0.14
5.1	0.7	140	0.14	0.7	140	0.14	0.7	140	0.14
5.1	0.7	140	0.14	0.7	140	0.14	0.7	140	0.14
5.1	0.7	140	0.14	0.7	140	0.14	0.7	140	0.14
10.2	1.3	130	0.13	1.2	120	0.12	1.2	123.5	0.1235
10.2	1.3	130	0.13	1.2	120	0.12	1.2	122.5	0.1225
10.2	1.3	130	0.13	1.2	120	0.12	1.2	121	0.121
10.2	1.3	130	0.13	1.2	120	0.12	1.2	123.8	0.1238
10.2	1.3	130	0.13	1.2	120	0.12	1.2	123.8	0.1238
51.1	7	137.3	0.1373	6.9	135.3	0.1353	6.9	135.3	0.1353
51.1	7	137.3	0.1373	6.9	135.3	0.1353	6.9	135.3	0.1353
51.1	7	137.3	0.1373	6.9	135.3	0.1353	6.9	135.3	0.1353
51.1	7	137.3	0.1373	6.9	135.3	0.1353	6.9	135.3	0.1353
51.1	7	137.3	0.1373	6.9	135.3	0.1353	6.9	135.3	0.1353
102.0	13.9	136.8	0.1368	13.8	135.3	0.1353	13.7	134.3	0.1343
102.0	14	136.8	0.1368	13.8	135.3	0.1353	13.7	134.3	0.1343
102.0	14	137.2	0.1372	13.8	135.3	0.1353	13.7	134.3	0.1343
102.0	14	137.3	0.1373	13.8	135.3	0.1353	13.7	134.5	0.1345
102.0	14	137.3	0.1373	13.8	135.4	0.1354	13.7	134.8	0.1348
153.0	23.5	138.2	0.1382	23.2	136.5	0.1365	23	135.3	0.1353
153.0	23.5	138.2	0.1382	23.2	136.5	0.1365	23	135.3	0.1353
153.0	23.6	138.5	0.1385	23.2	136.6	0.1366	23	135.3	0.1353
153.0	23.5	138.2	0.1382	23.2	136.7	0.1367	23	135.3	0.1353
153.0	23.5	138.4	0.1384	23.2	136.6	0.1366	23	135.3	0.1353
340.0	46.7	137.4	0.1374	46.2	135.9	0.1359	45.9	134.9	0.1349
340.0	46.7	137.4	0.1374	46.1	135.6	0.1356	45.8	134.7	0.1347
340.0	46.6	137.1	0.1371	46.1	135.6	0.1356	45.8	134.7	0.1347
340.0	46.6	137.1	0.1371	46.1	135.6	0.1356	45.8	134.7	0.1347
340.0	46.6	137.1	0.1371	46	135.3	0.1353	45.8	134.7	0.1347
511.0	69.6	136.5	0.1365	69.1	135.4	0.1354	68.8	134.9	0.1349
511.0	69.4	136.1	0.1361	68.9	135.1	0.1351	68.6	134.5	0.1345

Table C. 12 continued									
Shear Rate [1/s]	Shear Stress [Pa]	Viscosity [cP]	Viscosity [Pa·s]	Shear Stress [Pa]	Viscosity [cP]	Viscosity [Pa·s]	Shear Stress [Pa]	Viscosity [cP]	Viscosity [Pa·s]
511.0	69.3	135.9	0.1359	68.8	134.9	0.1349	68.5	134.3	0.1343
511.0	69.2	135.7	0.1357	68.8	134.8	0.1348	68.4	134.1	0.1341
511.0	69.2	135.7	0.1357	68.7	134.7	0.1347	68.3	133.9	0.1339
1021.0	134.4	131.6	0.1316	133.1	130.4	0.1304	132.5	129.8	0.1298
1021.0	132.5	129.8	0.1298	131.3	128.6	0.1286	130.9	128.2	0.1282
1021.0	131.6	128.9	0.1289	130.6	127.9	0.1279	129.8	127.1	0.1271
1021.0	130.9	128.2	0.1282	130	127.3	0.1273	129.2	126.6	0.1266
1021.0	130.5	127.9	0.1279	129.4	126.8	0.1268	128.8	126.1	0.1261

Table C. 13 *Glycerol and particles, volume fraction 0.0116 measuring data - 3 repetitions*

Shear Rate [1/s]	Shear Stress [Pa]	Viscosity [cP]	Viscosity [Pa·s]	Shear Stress [Pa]	Viscosity [cP]	Viscosity [Pa·s]	Shear Stress [Pa]	Viscosity [cP]	Viscosity [Pa·s]
1.5	0.3	300	0.3	0.3	300	0.3	0.4	400	0.4
1.5	0.3	300	0.3	0.3	300	0.3	0.4	400	0.4
1.5	0.3	300	0.3	0.3	300	0.3	0.4	400	0.4
1.5	0.3	300	0.3	0.3	300	0.3	0.4	400	0.4
1.5	0.3	300	0.3	0.3	300	0.3	0.4	400	0.4
3.1	0.5	166.7	0.1667	0.5	166.7	0.1667	0.5	166.7	0.1667
3.1	0.5	166.7	0.1667	0.5	166.7	0.1667	0.5	166.7	0.1667
3.1	0.5	166.7	0.1667	0.5	166.7	0.1667	0.5	166.7	0.1667
3.1	0.5	166.7	0.1667	0.5	166.7	0.1667	0.5	166.7	0.1667
3.1	0.5	166.7	0.1667	0.5	166.7	0.1667	0.5	166.7	0.1667
5.1	0.7	140	0.14	0.7	140	0.14	0.7	136	0.136
5.1	0.7	140	0.14	0.7	140	0.14	0.7	140	0.14
5.1	0.7	140	0.14	0.7	140	0.14	0.7	140	0.14
5.1	0.7	140	0.14	0.7	140	0.14	0.7	140	0.14
5.1	0.7	140	0.14	0.7	140	0.14	0.7	140	0.14
10.2	1.3	130	0.13	1.2	120	0.12	1.2	123.5	0.1235
10.2	1.3	130	0.13	1.2	120	0.12	1.2	122.5	0.1225
10.2	1.3	130	0.13	1.2	120	0.12	1.2	121	0.121
10.2	1.3	130	0.13	1.2	120	0.12	1.2	123.8	0.1238
10.2	1.3	130	0.13	1.2	120	0.12	1.2	123.8	0.1238
51.1	7	137.3	0.1373	6.9	135.3	0.1353	6.9	135.3	0.1353
51.1	7	137.3	0.1373	6.9	135.3	0.1353	6.9	135.3	0.1353
51.1	7	137.3	0.1373	6.9	135.3	0.1353	6.9	135.3	0.1353
51.1	7	137.3	0.1373	6.9	135.3	0.1353	6.9	135.3	0.1353
51.1	7	137.3	0.1373	6.9	135.3	0.1353	6.9	135.3	0.1353
102.0	13.9	136.8	0.1368	13.8	135.3	0.1353	13.7	134.3	0.1343
102.0	14	136.8	0.1368	13.8	135.3	0.1353	13.7	134.3	0.1343
102.0	14	137.2	0.1372	13.8	135.3	0.1353	13.7	134.3	0.1343
102.0	14	137.3	0.1373	13.8	135.3	0.1353	13.7	134.5	0.1345

Table C. 13 continued

Shear Rate [1/s]	Shear Stress [Pa]	Viscosity [cP]	Viscosity [Pa·s]	Shear Stress [Pa]	Viscosity [cP]	Viscosity [Pa·s]	Shear Stress [Pa]	Viscosity [cP]	Viscosity [Pa·s]
102.0	14	137.3	0.1373	13.8	135.4	0.1354	13.7	134.8	0.1348
153.0	23.5	138.2	0.1382	23.2	136.5	0.1365	23	135.3	0.1353
153.0	23.5	138.2	0.1382	23.2	136.5	0.1365	23	135.3	0.1353
153.0	23.6	138.5	0.1385	23.2	136.6	0.1366	23	135.3	0.1353
153.0	23.5	138.2	0.1382	23.2	136.7	0.1367	23	135.3	0.1353
153.0	23.5	138.4	0.1384	23.2	136.6	0.1366	23	135.3	0.1353
340.0	46.7	137.4	0.1374	46.2	135.9	0.1359	45.9	134.9	0.1349
340.0	46.7	137.4	0.1374	46.1	135.6	0.1356	45.8	134.7	0.1347
340.0	46.6	137.1	0.1371	46.1	135.6	0.1356	45.8	134.7	0.1347
340.0	46.6	137.1	0.1371	46.1	135.6	0.1356	45.8	134.7	0.1347
340.0	46.6	137.1	0.1371	46	135.3	0.1353	45.8	134.7	0.1347
511.0	69.6	136.5	0.1365	69.1	135.4	0.1354	68.8	134.9	0.1349
511.0	69.4	136.1	0.1361	68.9	135.1	0.1351	68.6	134.5	0.1345
511.0	69.3	135.9	0.1359	68.8	134.9	0.1349	68.5	134.3	0.1343
511.0	69.2	135.7	0.1357	68.8	134.8	0.1348	68.4	134.1	0.1341
511.0	69.2	135.7	0.1357	68.7	134.7	0.1347	68.3	133.9	0.1339
1021.0	134.4	131.6	0.1316	133.1	130.4	0.1304	132.5	129.8	0.1298
1021.0	132.5	129.8	0.1298	131.3	128.6	0.1286	130.9	128.2	0.1282
1021.0	131.6	128.9	0.1289	130.6	127.9	0.1279	129.8	127.1	0.1271
1021.0	130.9	128.2	0.1282	130	127.3	0.1273	129.2	126.6	0.1266
1021.0	130.5	127.9	0.1279	129.4	126.8	0.1268	128.8	126.1	0.1261

Table C. 14 *Glycerol and particles, volume fraction 0.0144 measuring data - 3 repetitions*

Shear Rate [1/s]	Shear Stress [Pa]	Viscosity [cP]	Viscosity [Pa·s]	Shear Stress [Pa]	Viscosity [cP]	Viscosity [Pa·s]	Shear Stress [Pa]	Viscosity [cP]	Viscosity [Pa·s]
1.5	0.2	194.6	0.1946	0.2	200	0.2	0.2	200	0.2
1.5	0.2	194.6	0.1946	0.2	200	0.2	0.2	200	0.2
1.5	0.2	161.7	0.1617	0.2	200	0.2	0.2	200	0.2
1.5	0.1	133.7	0.1337	0.2	200	0.2	0.2	200	0.2
1.5	0.1	135	0.135	0.2	200	0.2	0.2	200	0.2
3.1	0.3	100	0.1	0.3	100	0.1	0.4	133.3	0.1333
3.1	0.3	100	0.1	0.3	100	0.1	0.4	133.3	0.1333
3.1	0.3	100	0.1	0.3	100	0.1	0.4	133.3	0.1333
3.1	0.3	100	0.1	0.3	100	0.1	0.4	133.3	0.1333
3.1	0.3	100	0.1	0.3	100	0.1	0.4	133.3	0.1333
5.1	0.6	120	0.12	0.6	120	0.12	0.6	120	0.12
5.1	0.6	120	0.12	0.6	120	0.12	0.6	120	0.12
5.1	0.6	120	0.12	0.6	120	0.12	0.6	120	0.12
5.1	0.6	120	0.12	0.6	120	0.12	0.6	120	0.12
5.1	0.6	120	0.12	0.6	120	0.12	0.6	120	0.12
10.2	1.5	150	0.15	1.4	140	0.14	1.4	140	0.14

Table C. 14 continued

Shear Rate [1/s]	Shear Stress [Pa]	Viscosity [cP]	Viscosity [Pa·s]	Shear Stress [Pa]	Viscosity [cP]	Viscosity [Pa·s]	Shear Stress [Pa]	Viscosity [cP]	Viscosity [Pa·s]
10.2	1.5	150	0.15	1.4	140	0.14	1.4	140	0.14
10.2	1.5	150	0.15	1.4	140	0.14	1.4	140	0.14
10.2	1.5	150	0.15	1.4	140	0.14	1.4	140	0.14
10.2	1.5	150	0.15	1.4	140	0.14	1.4	140	0.14
51.1	7.5	147.1	0.1471	7.4	145.9	0.1459	7.5	147.2	0.1472
51.1	7.5	147.1	0.1471	7.5	146.8	0.1468	7.5	147.2	0.1472
51.1	7.5	147.1	0.1471	7.5	146.9	0.1469	7.5	147.4	0.1474
51.1	7.5	147.1	0.1471	7.5	147.1	0.1471	7.5	147.5	0.1475
51.1	7.5	147.1	0.1471	7.5	147.1	0.1471	7.5	147.8	0.1478
102.0	15.1	148	0.148	15	146.9	0.1469	15.2	149	0.149
102.0	15.1	148.1	0.1481	15	147.1	0.1471	15.2	149	0.149
102.0	15.1	148.1	0.1481	15	147.1	0.1471	15.2	149	0.149
102.0	15.1	148.3	0.1483	15	147.1	0.1471	15.2	149	0.149
102.0	15.1	148.4	0.1484	15	147.1	0.1471	15.2	149	0.149
153.0	25.1	147.6	0.1476	24.8	145.9	0.1459	25.2	148.2	0.1482
153.0	25.1	147.6	0.1476	24.8	145.9	0.1459	25.2	148.2	0.1482
153.0	25.1	147.6	0.1476	24.8	145.9	0.1459	25.2	148.2	0.1482
153.0	25.1	147.6	0.1476	24.8	145.9	0.1459	25.2	148.3	0.1483
153.0	25.1	147.6	0.1476	24.8	145.9	0.1459	25.3	148.7	0.1487
340.0	50.6	148.8	0.1488	50.1	147.2	0.1472	50.8	149.4	0.1494
340.0	50.6	148.8	0.1488	50	147.1	0.1471	50.8	149.4	0.1494
340.0	50.5	148.5	0.1485	50	147.1	0.1471	50.7	149.1	0.1491
340.0	50.5	148.5	0.1485	50	147.1	0.1471	50.7	149.1	0.1491
340.0	50.4	148.2	0.1482	50	147.1	0.1471	50.7	149.1	0.1491
511.0	75.1	147.3	0.1473	74.6	146.3	0.1463	75.5	148.1	0.1481
511.0	75	147.1	0.1471	74.5	146	0.146	75.4	147.8	0.1478
511.0	74.9	146.9	0.1469	74.4	145.8	0.1458	75.4	147.8	0.1478
511.0	74.9	146.9	0.1469	74.3	145.7	0.1457	75.3	147.6	0.1476
511.0	74.8	146.7	0.1467	74.3	145.7	0.1457	75.3	147.6	0.1476
1021.0	144	141	0.141	143.4	140.4	0.1404	145.2	142.2	0.1422
1021.0	142	139.1	0.1391	141.8	138.8	0.1388	143.9	141	0.141
1021.0	141.3	138.4	0.1384	141.1	138.2	0.1382	142.8	139.8	0.1398
1021.0	139.9	137	0.137	139.8	136.9	0.1369	142	139.1	0.1391
1021.0	139.4	136.6	0.1366	139.5	136.6	0.1366	141.7	138.8	0.1388

Table C. 15 *Glycerol and particles, volume fraction 0.0182 measuring data - 3 repetitions*

Shear Rate [1/s]	Shear Stress [Pa]	Viscosity [cP]	Viscosity [Pa·s]	Shear Stress [Pa]	Viscosity [cP]	Viscosity [Pa·s]	Shear Stress [Pa]	Viscosity [cP]	Viscosity [Pa·s]
1.5	0.2	200	0.2	0.2	200	0.2	0.2	200	0.2
1.5	0.2	200	0.2	0.2	200	0.2	0.2	200	0.2
1.5	0.2	200	0.2	0.2	200	0.2	0.2	200	0.2
1.5	0.2	200	0.2	0.2	200	0.2	0.2	200	0.2
1.5	0.2	200	0.2	0.2	200	0.2	0.2	200	0.2
3.1	0.4	133.3	0.1333	0.5	166.7	0.1667	0.5	166.7	0.1667
3.1	0.4	133.3	0.1333	0.5	166.7	0.1667	0.5	166.7	0.1667
3.1	0.4	133.3	0.1333	0.5	166.7	0.1667	0.5	166.7	0.1667
3.1	0.4	133.3	0.1333	0.5	166.7	0.1667	0.5	166.7	0.1667
3.1	0.4	133.3	0.1333	0.5	166.7	0.1667	0.5	166.7	0.1667
5.1	0.6	120	0.12	0.7	140	0.14	0.7	140	0.14
5.1	0.6	120	0.12	0.7	140	0.14	0.7	140	0.14
5.1	0.6	120.5	0.1205	0.7	140	0.14	0.7	140	0.14
5.1	0.6	121	0.121	0.7	140	0.14	0.7	140	0.14
5.1	0.6	121.5	0.1215	0.7	140	0.14	0.7	140	0.14
10.2	1.3	134.8	0.1348	1.7	170	0.17	1.8	180	0.18
10.2	1.4	136.6	0.1366	1.7	170.7	0.1707	1.8	180	0.18
10.2	1.4	139.2	0.1392	1.7	170	0.17	1.8	180	0.18
10.2	1.4	140	0.14	1.7	170	0.17	1.8	180	0.18
10.2	1.4	140	0.14	1.7	170	0.17	1.8	180	0.18
51.1	8.3	162.7	0.1627	8.3	162.7	0.1627	8.3	162.7	0.1627
51.1	8.3	162.7	0.1627	8.3	162.7	0.1627	8.3	162.7	0.1627
51.1	8.3	162.7	0.1627	8.3	163	0.163	8.3	162.7	0.1627
51.1	8.3	162.7	0.1627	8.3	163	0.163	8.3	162.7	0.1627
51.1	8.3	162.7	0.1627	8.3	163.2	0.1632	8.3	162.7	0.1627
102.0	16.4	160.8	0.1608	16.5	161.8	0.1618	16.4	160.8	0.1608
102.0	16.5	161.7	0.1617	16.5	162	0.162	16.4	160.8	0.1608
102.0	16.5	161.8	0.1618	16.6	162.4	0.1624	16.4	160.8	0.1608
102.0	16.5	161.8	0.1618	16.6	162.6	0.1626	16.4	161	0.161
102.0	16.5	161.8	0.1618	16.6	162.7	0.1627	16.4	161	0.161
153.0	27.9	164.1	0.1641	27.8	163.5	0.1635	27.5	161.8	0.1618
153.0	28	164.7	0.1647	27.8	163.7	0.1637	27.5	161.8	0.1618
153.0	28	164.7	0.1647	27.9	163.8	0.1638	27.5	161.8	0.1618
153.0	28	164.7	0.1647	27.9	164	0.164	27.5	161.8	0.1618
153.0	28	164.7	0.1647	27.9	164.1	0.1641	27.5	161.8	0.1618
340.0	55.8	164.1	0.1641	55.6	163.5	0.1635	55.1	162.1	0.1621
340.0	55.8	164.1	0.1641	55.6	163.5	0.1635	55	161.8	0.1618
340.0	55.7	163.8	0.1638	55.6	163.4	0.1634	54.9	161.6	0.1616
340.0	55.7	163.8	0.1638	55.5	163.2	0.1632	54.9	161.5	0.1615
340.0	55.7	163.8	0.1638	55.5	163.2	0.1632	54.9	161.4	0.1614
511.0	82.8	162.3	0.1623	82.6	161.9	0.1619	81.9	160.5	0.1605

Table C. 15 continued

Shear Rate [1/s]	Shear Stress [Pa]	Viscosity [cP]	Viscosity [Pa·s]	Shear Stress [Pa]	Viscosity [cP]	Viscosity [Pa·s]	Shear Stress [Pa]	Viscosity [cP]	Viscosity [Pa·s]
511.0	82.5	161.8	0.1618	82.2	161.1	0.1611	81.6	160.1	0.1601
511.0	82.3	161.3	0.1613	82.1	160.9	0.1609	81.6	159.9	0.1599
511.0	82.1	161	0.161	82	160.7	0.1607	81.5	159.7	0.1597
511.0	82	160.8	0.1608	81.9	160.6	0.1606	81.4	159.6	0.1596
1021.0	161.3	158.1	0.1581	161.1	158	0.158	160.1	157.1	0.1571
1021.0	159.4	156.1	0.1561	159.1	155.8	0.1558	158.2	154.9	0.1549
1021.0	158.2	154.9	0.1549	158	154.7	0.1547	157	153.8	0.1538
1021.0	157.4	154.1	0.1541	157.2	153.9	0.1539	156.3	153.1	0.1531
1021.0	156.7	153.4	0.1534	156.6	153.4	0.1534	155.8	152.6	0.1526

Table C. 16 *Glycerol and particles, volume fraction 0.0201 measuring data - 3 repetitions*

Shear Rate [1/s]	Shear Stress [Pa]	Viscosity [cP]	Viscosity [Pa·s]	Shear Stress [Pa]	Viscosity [cP]	Viscosity [Pa·s]	Shear Stress [Pa]	Viscosity [cP]	Viscosity [Pa·s]
1.5	0.3	300	0.3	0.3	300	0.3	0.2	200	0.2
1.5	0.3	300	0.3	0.3	300	0.3	0.2	200	0.2
1.5	0.3	300	0.3	0.3	300	0.3	0.2	200	0.2
1.5	0.3	300	0.3	0.3	300	0.3	0.2	200	0.2
1.5	0.3	300	0.3	0.3	300	0.3	0.2	200	0.2
3.1	0.6	200.1	0.2001	0.7	233.3	0.2333	0.6	215.3	0.2153
3.1	0.6	203.5	0.2035	0.7	233.3	0.2333	0.7	226.1	0.2261
3.1	0.6	203.6	0.2036	0.7	233.3	0.2333	0.7	226.9	0.2269
3.1	0.6	205	0.205	0.7	233.3	0.2333	0.7	230.3	0.2303
3.1	0.6	202.2	0.2022	0.7	233.3	0.2333	0.7	228.9	0.2289
5.1	0.9	180	0.18	0.9	180	0.18	1	200	0.2
5.1	0.9	180	0.18	0.9	180	0.18	1	200	0.2
5.1	0.9	180	0.18	0.9	180	0.18	1	200	0.2
5.1	0.9	180	0.18	0.9	180	0.18	1	200	0.2
5.1	0.9	180	0.18	0.9	180	0.18	1	200	0.2
10.2	1.5	150	0.15	1.6	160	0.16	1.6	156	0.156
10.2	1.5	150	0.15	1.6	160	0.16	1.6	157	0.157
10.2	1.5	150	0.15	1.6	160	0.16	1.6	158	0.158
10.2	1.5	150	0.15	1.6	160	0.16	1.6	157.6	0.1576
10.2	1.5	150	0.15	1.6	160	0.16	1.6	159.2	0.1592
51.1	7.8	152.9	0.1529	7.8	152.9	0.1529	7.8	152.9	0.1529
51.1	7.8	152.9	0.1529	7.8	152.9	0.1529	7.8	152.9	0.1529
51.1	7.8	152.9	0.1529	7.8	152.9	0.1529	7.8	152.9	0.1529
51.1	7.8	152.9	0.1529	7.8	152.9	0.1529	7.8	152.9	0.1529
51.1	7.8	152.9	0.1529	7.8	153.1	0.1531	7.8	152.9	0.1529
102.0	16.1	157.8	0.1578	15.9	155.9	0.1559	15.9	155.9	0.1559

Table C. 16 continued

Shear Rate [1/s]	Shear Stress [Pa]	Viscosity [cP]	Viscosity [Pa·s]	Shear Stress [Pa]	Viscosity [cP]	Viscosity [Pa·s]	Shear Stress [Pa]	Viscosity [cP]	Viscosity [Pa·s]
102.0	16.1	157.8	0.1578	16	156.4	0.1564	15.9	155.9	0.1559
102.0	16.1	157.8	0.1578	16	156.6	0.1566	15.9	155.9	0.1559
102.0	16.1	157.8	0.1578	16	156.9	0.1569	15.9	156	0.156
102.0	16.1	157.8	0.1578	16	156.9	0.1569	15.9	156.2	0.1562
153.0	26.5	155.9	0.1559	26.4	155.3	0.1553	26.4	155.3	0.1553
153.0	26.5	155.9	0.1559	26.4	155.3	0.1553	26.4	155.3	0.1553
153.0	26.5	155.9	0.1559	26.4	155.3	0.1553	26.4	155.3	0.1553
153.0	26.5	155.9	0.1559	26.4	155.3	0.1553	26.5	155.9	0.1559
153.0	26.5	155.9	0.1559	26.4	155.3	0.1553	26.5	155.9	0.1559
340.0	52.8	155.3	0.1553	52.7	155	0.155	52.8	155.3	0.1553
340.0	52.8	155.3	0.1553	52.7	155	0.155	52.8	155.3	0.1553
340.0	52.8	155.3	0.1553	52.7	155	0.155	52.8	155.3	0.1553
340.0	52.8	155.3	0.1553	52.7	155	0.155	52.8	155.2	0.1552
340.0	52.8	155.2	0.1552	52.7	155	0.155	52.7	155	0.155
511.0	78.7	154.4	0.1544	78.3	153.5	0.1535	78.5	153.9	0.1539
511.0	78.5	153.9	0.1539	78.1	153.1	0.1531	78.3	153.5	0.1535
511.0	78.4	153.7	0.1537	77.8	152.6	0.1526	78.2	153.3	0.1533
511.0	78.3	153.5	0.1535	77.8	152.5	0.1525	78.1	153.1	0.1531
511.0	78.2	153.3	0.1533	77.7	152.4	0.1524	78	152.9	0.1529
1021.0	153	150.3	0.1503	152.8	149.9	0.1499	153.3	150.3	0.1503
1021.0	151.4	148.3	0.1483	151.1	148	0.148	151.4	148.3	0.1483
1021.0	150.4	147.3	0.1473	150.3	147.2	0.1472	150.6	147.5	0.1475
1021.0	149.9	146.9	0.1469	149.6	146.5	0.1465	150	146.9	0.1469
1021.0	149.5	146.4	0.1464	149.1	146.1	0.1461	149.5	146.4	0.1464

Table C. 17 *Salt water measured data - 5 repetitions*

Shear Rate [1/s]	Shear Stress [Pa]	Viscosity [cP]	Viscosity [Pa·s]	Shear Stress [Pa]	Viscosity [cP]	Viscosity [Pa·s]	Shear Stress [Pa]	Viscosity [cP]	Viscosity [Pa·s]	Shear Stress [Pa]	Viscosity [cP]	Viscosity [Pa·s]	Shear Stress [Pa]	Viscosity [cP]	Viscosity [Pa·s]
1.5	0	0	0	0	0	0	0	0	0	0	0	0	0	0	0
1.5	0	0	0	0	0	0	0	0	0	0	0	0	0	0	0
1.5	0	0	0	0	0	0	0	0	0	0	0	0	0	0	0
1.5	0	0	0	0	0	0	0	0	0	0	0	0	0	0	0
1.5	0	0	0	0	0	0	0	0	0	0	0	0	0	0	0
3.1	0	0	0	0	0	0	0	0	0	0	0	0	0	0	0
3.1	0	0	0	0	0	0	0	0	0	0	0	0	0	0	0
3.1	0	0	0	0	0	0	0	0	0	0	0	0	0	0	0
3.1	0	0	0	0	0	0	0	0	0	0	0	0	0	0	0
3.1	0	0	0	0	0	0	0	0	0	0	0	0	0	0	0
5.1	0	0	0	0	0	0	0	0	0	0	0	0	0	0	0
5.1	0	0	0	0	0	0	0	0	0	0	0	0	0	0	0
5.1	0	0	0	0	0	0	0	0	0	0	0	0	0	0	0
5.1	0	0	0	0	0	0	0	0	0	0	0	0	0	0	0
5.1	0	0	0	0	0	0	0	0	0	0	0	0	0	0	0
10.2	0	0	0	0	0	0	0	0	0	0	0	0	0	0	0
10.2	0	0	0	0	0	0	0	0	0	0	0	0	0	0	0
10.2	0	0	0	0	0	0	0	0	0	0	0	0	0	0	0
10.2	0	0	0	0	0	0	0	0	0	0	0	0	0	0	0
10.2	0	0	0	0	0	0	0	0	0	0	0	0	0	0	0
51.1	0	0	0	0	0	0	0.1	2	0.002	0.1	2	0.002	0.1	2	0.002
51.1	0	0	0	0	0	0	0.1	2	0.002	0.1	2	0.002	0.1	2	0.002
51.1	0	0	0	0	0	0	0.1	2	0.002	0.1	2	0.002	0.1	2	0.002
51.1	0	0	0	0	0	0	0.1	2	0.002	0.1	2	0.002	0.1	2	0.002
51.1	0	0	0	0	0	0	0.1	2	0.002	0.1	2	0.002	0.1	2	0.002
102.0	0.1	1	0.001	0.1	1	0.001	0.1	1	0.001	0.1	1	0.001	0.1	1	0.001
102.0	0.1	1	0.001	0.1	1	0.001	0.1	1	0.001	0.1	1	0.001	0.1	1	0.001
102.0	0.1	1	0.001	0.1	1	0.001	0.1	1	0.001	0.1	1	0.001	0.1	1	0.001
102.0	0.1	1	0.001	0.1	1	0.001	0.1	1	0.001	0.1	1	0.001	0.1	1	0.001
102.0	0.1	1	0.001	0.1	1	0.001	0.1	1	0.001	0.1	1	0.001	0.1	1	0.001
153.0	0.1	0.7	0.0007	0.1	0.7	0.0007	0.2	1.3	0.0013	0.2	1.3	0.0013	0.2	1.3	0.0013
153.0	0.1	0.7	0.0007	0.1	0.7	0.0007	0.2	1.3	0.0013	0.2	1.3	0.0013	0.2	1.3	0.0013
153.0	0.1	0.7	0.0007	0.1	0.7	0.0007	0.2	1.3	0.0013	0.2	1.3	0.0013	0.2	1.3	0.0013
153.0	0.1	0.7	0.0007	0.1	0.7	0.0007	0.2	1.3	0.0013	0.2	1.3	0.0013	0.2	1.3	0.0013
153.0	0.1	0.7	0.0007	0.1	0.7	0.0007	0.2	1.3	0.0013	0.2	1.3	0.0013	0.2	1.3	0.0013
340.0	0.3	0.9	0.0009	0.4	1.2	0.0012	0.4	1.2	0.0012	0.4	1.2	0.0012	0.4	1.2	0.0012
340.0	0.3	0.9	0.0009	0.4	1.2	0.0012	0.4	1.2	0.0012	0.4	1.2	0.0012	0.4	1.2	0.0012
340.0	0.3	0.9	0.0009	0.4	1.2	0.0012	0.4	1.2	0.0012	0.4	1.2	0.0012	0.4	1.2	0.0012
340.0	0.3	0.9	0.0009	0.4	1.2	0.0012	0.4	1.2	0.0012	0.4	1.2	0.0012	0.4	1.2	0.0012
340.0	0.3	0.9	0.0009	0.4	1.2	0.0012	0.4	1.2	0.0012	0.4	1.2	0.0012	0.4	1.2	0.0012
511.0	0.7	1.4	0.0014	0.6	1.2	0.0012	0.7	1.4	0.0014	0.7	1.4	0.0014	0.7	1.4	0.0014

Table C. 17 continued

Shear Rate [1/s]	Shear Stress [Pa]	Viscosity [cP]	Viscosity [Pa·s]	Shear Stress [Pa]	Viscosity [cP]	Viscosity [Pa·s]	Shear Stress [Pa]	Viscosity [cP]	Viscosity [Pa·s]	Shear Stress [Pa]	Viscosity [cP]	Viscosity [Pa·s]	Shear Stress [Pa]	Viscosity [cP]	Viscosity [Pa·s]
511.0	0.7	1.4	0.0014	0.7	1.4	0.0014	0.7	1.4	0.0014	0.7	1.4	0.0014	0.7	1.4	0.0014
511.0	0.7	1.4	0.0014	0.7	1.4	0.0014	0.7	1.4	0.0014	0.7	1.4	0.0014	0.7	1.4	0.0014
511.0	0.7	1.4	0.0014	0.7	1.4	0.0014	0.7	1.4	0.0014	0.7	1.4	0.0014	0.7	1.4	0.0014
511.0	0.7	1.4	0.0014	0.7	1.4	0.0014	0.7	1.4	0.0014	0.7	1.4	0.0014	0.7	1.4	0.0014
1021.0	1.5	1.5	0.0015	1.4	1.4	0.0014	1.5	1.5	0.0015	1.5	1.5	0.0015	1.5	1.5	0.0015
1021.0	1.5	1.5	0.0015	1.4	1.4	0.0014	1.5	1.5	0.0015	1.5	1.5	0.0015	1.5	1.5	0.0015
1021.0	1.5	1.5	0.0015	1.4	1.4	0.0014	1.5	1.5	0.0015	1.5	1.5	0.0015	1.5	1.5	0.0015
1021.0	1.5	1.5	0.0015	1.5	1.5	0.0015	1.5	1.5	0.0015	1.5	1.5	0.0015	1.5	1.5	0.0015
1021.0	1.5	1.5	0.0015	1.5	1.4	0.0014	1.5	1.5	0.0015	1.5	1.5	0.0015	1.5	1.5	0.0015

Table C. 18 *Salt water and particles, volume fraction 0.0029 measured data - 5 repetitions*

Shear Rate [1/s]	Shear Stress [Pa]	Viscosity [cP]	Viscosity [Pa·s]	Shear Stress [Pa]	Viscosity [cP]	Viscosity [Pa·s]	Shear Stress [Pa]	Viscosity [cP]	Viscosity [Pa·s]	Shear Stress [Pa]	Viscosity [cP]	Viscosity [Pa·s]	Shear Stress [Pa]	Viscosity [cP]	Viscosity [Pa·s]
1.5	0	0	0	0	0	0	0	0	0	0	0	0	0	0	0
1.5	0	0	0	0	0	0	0	0	0	0	0	0	0	0	0
1.5	0	0	0	0	0	0	0	0	0	0	0	0	0	0	0
1.5	0	0	0	0	0	0	0	0	0	0	0	0	0	0	0
1.5	0	0	0	0	0	0	0	0	0	0	0	0	0	0	0
3.1	0	0	0	0	0	0	0	0	0	0	0	0	0	0	0
3.1	0	0	0	0	0	0	0	0	0	0	0	0	0	0	0
3.1	0	0	0	0	0	0	0	0	0	0	0	0	0	0	0
3.1	0	0	0	0	0	0	0	0	0	0	0	0	0	0	0
3.1	0	0	0	0	0	0	0	0	0	0	0	0	0	0	0
5.1	0	0	0	0	0	0	0	0	0	0	0	0	0	0	0
5.1	0	0	0	0	0	0	0	0	0	0	0	0	0	0	0
5.1	0	0	0	0	0	0	0	0	0	0	0	0	0	0	0
5.1	0	0	0	0	0	0	0	0	0	0	0	0	0	0	0
5.1	0	0	0	0	0	0	0	0	0	0	0	0	0	0	0
10.2	0	0	0	0	0	0	0	0	0	0	0	0	0	0	0
10.2	0	0	0	0	0	0	0	0	0	0	0	0	0	0	0
10.2	0	0	0	0	0	0	0	0	0	0	0	0	0	0	0
10.2	0	0	0	0	0	0	0	0	0	0	0	0	0	0	0
10.2	0	0	0	0	0	0	0	0	0	0	0	0	0	0	0
51.1	0	0	0	0.1	2	0.002	0.1	2	0.002	0.1	2	0.002	0.1	2	0.002
51.1	0	0	0	0.1	2	0.002	0.1	2	0.002	0.1	2	0.002	0.1	2	0.002
51.1	0	0	0	0.1	2	0.002	0.1	2	0.002	0.1	2	0.002	0.1	2	0.002
51.1	0	0	0	0.1	2	0.002	0.1	2	0.002	0.1	2	0.002	0.1	2	0.002
51.1	0	0	0	0.1	2	0.002	0.1	2	0.002	0.1	2	0.002	0.1	2	0.002

Table C. 18 continued

Shear Rate [1/s]	Shear Stress [Pa]	Viscosity [cP]	Viscosity [Pa·s]	Shear Stress [Pa]	Viscosity [cP]	Viscosity [Pa·s]	Shear Stress [Pa]	Viscosity [cP]	Viscosity [Pa·s]	Shear Stress [Pa]	Viscosity [cP]	Viscosity [Pa·s]	Shear Stress [Pa]	Viscosity [cP]	Viscosity [Pa·s]
102.0	0.1	1	0.001	0.1	1	0.001	0.1	1	0.001	0.1	1	0.001	0.1	1	0.001
102.0	0.1	1	0.001	0.1	1	0.001	0.1	1	0.001	0.1	1	0.001	0.1	1	0.001
102.0	0.1	1	0.001	0.1	1	0.001	0.1	1	0.001	0.1	1	0.001	0.1	1	0.001
102.0	0.1	1	0.001	0.1	1	0.001	0.1	1	0.001	0.1	1	0.001	0.1	1	0.001
102.0	0.1	1	0.001	0.1	1	0.001	0.1	1	0.001	0.1	1	0.001	0.1	1	0.001
153.0	0.1	0.7	0.0007	0.1	0.7	0.0007	0.2	1.3	0.0013	0.2	1.3	0.0013	0.2	1.3	0.0013
153.0	0.1	0.7	0.0007	0.1	0.7	0.0007	0.2	1.3	0.0013	0.2	1.3	0.0013	0.2	1.3	0.0013
153.0	0.1	0.7	0.0007	0.1	0.7	0.0007	0.2	1.3	0.0013	0.2	1.3	0.0013	0.2	1.3	0.0013
153.0	0.1	0.7	0.0007	0.2	1.3	0.0013	0.2	1.3	0.0013	0.2	1.3	0.0013	0.2	1.3	0.0013
153.0	0.1	0.7	0.0007	0.2	1.3	0.0013	0.2	1.3	0.0013	0.2	1.3	0.0013	0.2	1.3	0.0013
340.0	0.4	1.2	0.0012	0.5	1.5	0.0015	0.5	1.5	0.0015	0.5	1.5	0.0015	0.5	1.5	0.0015
340.0	0.4	1.2	0.0012	0.5	1.5	0.0015	0.5	1.5	0.0015	0.5	1.5	0.0015	0.5	1.5	0.0015
340.0	0.4	1.2	0.0012	0.5	1.5	0.0015	0.5	1.5	0.0015	0.5	1.5	0.0015	0.5	1.5	0.0015
340.0	0.4	1.2	0.0012	0.5	1.5	0.0015	0.5	1.5	0.0015	0.5	1.5	0.0015	0.5	1.5	0.0015
340.0	0.4	1.2	0.0012	0.5	1.5	0.0015	0.5	1.5	0.0015	0.5	1.5	0.0015	0.5	1.5	0.0015
511.0	0.7	1.4	0.0014	0.7	1.4	0.0014	0.8	1.6	0.0016	0.8	1.6	0.0016	0.8	1.6	0.0016
511.0	0.7	1.4	0.0014	0.7	1.5	0.0015	0.8	1.6	0.0016	0.8	1.6	0.0016	0.8	1.6	0.0016
511.0	0.7	1.4	0.0014	0.8	1.6	0.0016	0.8	1.6	0.0016	0.8	1.6	0.0016	0.8	1.6	0.0016
511.0	0.7	1.4	0.0014	0.8	1.6	0.0016	0.8	1.6	0.0016	0.8	1.6	0.0016	0.8	1.6	0.0016
511.0	0.7	1.4	0.0014	0.8	1.6	0.0016	0.8	1.6	0.0016	0.8	1.6	0.0016	0.8	1.6	0.0016
1021.0	1.6	1.6	0.0016	1.6	1.6	0.0016	1.6	1.6	0.0016	1.6	1.6	0.0016	1.6	1.6	0.0016
1021.0	1.6	1.6	0.0016	1.6	1.6	0.0016	1.6	1.6	0.0016	1.6	1.6	0.0016	1.6	1.6	0.0016
1021.0	1.6	1.6	0.0016	1.6	1.6	0.0016	1.6	1.6	0.0016	1.6	1.6	0.0016	1.6	1.6	0.0016
1021.0	1.6	1.6	0.0016	1.6	1.6	0.0016	1.6	1.6	0.0016	1.6	1.6	0.0016	1.6	1.6	0.0016
1021.0	1.6	1.6	0.0016	1.6	1.6	0.0016	1.6	1.6	0.0016	1.6	1.6	0.0016	1.6	1.6	0.0016

Table C. 19 *Salt water and particles, volume fraction 0.0058 measuring data - 5 repetitions*

Shear Rate [1/s]	Shear Stress [Pa]	Viscosity [cP]	Viscosity [Pa·s]	Shear Stress [Pa]	Viscosity [cP]	Viscosity [Pa·s]	Shear Stress [Pa]	Viscosity [cP]	Viscosity [Pa·s]	Shear Stress [Pa]	Viscosity [cP]	Viscosity [Pa·s]	Shear Stress [Pa]	Viscosity [cP]	Viscosity [Pa·s]
1.5	0	0	0	0	0	0	0	0	0	1.5	0	0	0	0	0
1.5	0	0	0	0	0	0	0	0	0	1.5	0	0	0	0	0
1.5	0	0	0	0	0	0	0	0	0	1.5	0	0	0	0	0
1.5	0	0	0	0	0	0	0	0	0	1.5	0	0	0	0	0
1.5	0	0	0	0	0	0	0	0	0	1.5	0	0	0	0	0
3.1	0	0	0	0	0	0	0.1	33.3	0.0333	3.1	0	0	0	0	0
3.1	0	0	0	0	0	0	0.1	33.3	0.0333	3.1	0	0	0	0	0
3.1	0	0	0	0	0	0	0.1	33.3	0.0333	3.1	0	0	0	0	0
3.1	0	0	0	0	0	0	0.1	33.3	0.0333	3.1	0	0	0	0	0
3.1	0	0	0	0	0	0	0.1	33.3	0.0333	3.1	0	0	0	0	0

Table C. 19 continued

Shear Rate [1/s]	Shear Stress [Pa]	Viscosity [cP]	Viscosity [Pa·s]	Shear Stress [Pa]	Viscosity [cP]	Viscosity [Pa·s]	Shear Stress [Pa]	Viscosity [cP]	Viscosity [Pa·s]	Shear Stress [Pa]	Viscosity [cP]	Viscosity [Pa·s]	Shear Stress [Pa]	Viscosity [cP]	Viscosity [Pa·s]
5.1	0	0	0	0	0	0	0.1	20	0.02	5.1	0	0	0	0	0
5.1	0	0	0	0	0	0	0.1	20	0.02	5.1	0	0	0	0	0
5.1	0	0	0	0	0	0	0.1	20	0.02	5.1	0	0	0	0	0
5.1	0	0	0	0	0	0	0.1	20	0.02	5.1	0	0	0	0	0
5.1	0	0	0	0	0	0	0.1	20	0.02	5.1	0	0	0	0	0
10.2	0	0	0	0	0	0	0.1	10	0.01	10.2	0	0	0	0	0
10.2	0	0	0	0	0	0	0.1	10	0.01	10.2	0	0	0	0	0
10.2	0	0	0	0	0	0	0.1	10	0.01	10.2	0	0	0	0	0
10.2	0	0	0	0	0	0	0.1	10	0.01	10.2	0	0	0	0	0
10.2	0	0	0	0	0	0	0.1	10	0.01	10.2	0	0	0	0	0
51.1	0	0	0	0.1	2	0.002	0.2	3.9	0.0039	51.1	0	0	0	0.1	2
51.1	0	0	0	0.1	2	0.002	0.2	3.9	0.0039	51.1	0	0	0	0.1	2
51.1	0	0	0	0.1	2	0.002	0.2	3.9	0.0039	51.1	0	0	0	0.1	2
51.1	0	0	0	0.1	2	0.002	0.2	3.9	0.0039	51.1	0	0	0	0.1	2
51.1	0	0	0	0.1	2	0.002	0.1	2.3	0.0023	51.1	0	0	0	0.1	2
102.0	0.1	1	0.001	0.2	2	0.002	0.2	2	0.002	102.0	0.1	1	0.001	0.2	2
102.0	0.1	1	0.001	0.2	2	0.002	0.2	2	0.002	102.0	0.1	1	0.001	0.2	2
102.0	0.1	1	0.001	0.2	2	0.002	0.2	2	0.002	102.0	0.1	1	0.001	0.2	2
102.0	0.1	1	0.001	0.2	2	0.002	0.2	2	0.002	102.0	0.1	1	0.001	0.2	2
102.0	0.1	1	0.001	0.2	2	0.002	0.2	2	0.002	102.0	0.1	1	0.001	0.2	2
153.0	0.2	1.2	0.0012	0.3	1.8	0.0018	0.3	1.9	0.0019	153.0	0.2	1.2	0.0012	0.3	1.8
153.0	0.2	1.2	0.0012	0.3	1.8	0.0018	0.3	1.8	0.0018	153.0	0.2	1.2	0.0012	0.3	1.8
153.0	0.2	1.2	0.0012	0.3	1.8	0.0018	0.3	1.8	0.0018	153.0	0.2	1.2	0.0012	0.3	1.8
153.0	0.2	1.2	0.0012	0.3	1.8	0.0018	0.3	1.8	0.0018	153.0	0.2	1.2	0.0012	0.3	1.8
153.0	0.2	1.2	0.0012	0.3	1.8	0.0018	0.3	1.8	0.0018	153.0	0.2	1.2	0.0012	0.3	1.8
340.0	0.5	1.5	0.0015	0.6	1.8	0.0018	0.7	2.1	0.0021	340.0	0.5	1.5	0.0015	0.6	1.8
340.0	0.5	1.5	0.0015	0.6	1.8	0.0018	0.6	1.9	0.0019	340.0	0.5	1.5	0.0015	0.6	1.8
340.0	0.5	1.5	0.0015	0.6	1.8	0.0018	0.6	1.8	0.0018	340.0	0.5	1.5	0.0015	0.6	1.8
340.0	0.5	1.5	0.0015	0.6	1.8	0.0018	0.6	1.8	0.0018	340.0	0.5	1.5	0.0015	0.6	1.8
340.0	0.5	1.5	0.0015	0.6	1.8	0.0018	0.6	1.8	0.0018	340.0	0.5	1.5	0.0015	0.6	1.8
511.0	0.7	1.4	0.0014	0.9	1.8	0.0018	1	2	0.002	511.0	0.7	1.4	0.0014	0.9	1.8
511.0	0.7	1.4	0.0014	0.9	1.8	0.0018	1	2	0.002	511.0	0.7	1.4	0.0014	0.9	1.8
511.0	0.8	1.6	0.0016	0.9	1.8	0.0018	1	2	0.002	511.0	0.8	1.6	0.0016	0.9	1.8
511.0	0.8	1.6	0.0016	0.9	1.8	0.0018	1	2	0.002	511.0	0.8	1.6	0.0016	0.9	1.8
511.0	0.8	1.6	0.0016	0.9	1.8	0.0018	1	2	0.002	511.0	0.8	1.6	0.0016	0.9	1.8
1021.0	1.7	1.7	0.0017	1.8	1.8	0.0018	1.9	1.9	0.0019	1021.0	1.7	1.7	0.0017	1.8	1.8
1021.0	1.7	1.7	0.0017	1.8	1.8	0.0018	1.9	1.9	0.0019	1021.0	1.7	1.7	0.0017	1.8	1.8
1021.0	1.7	1.7	0.0017	1.8	1.8	0.0018	1.9	1.9	0.0019	1021.0	1.7	1.7	0.0017	1.8	1.8
1021.0	1.7	1.7	0.0017	1.8	1.8	0.0018	1.9	1.9	0.0019	1021.0	1.7	1.7	0.0017	1.8	1.8
1021.0	1.7	1.7	0.0017	1.8	1.8	0.0018	1.9	1.9	0.0019	1021.0	1.7	1.7	0.0017	1.8	1.8

Table C. 20 *Salt water and particles, volume fraction 0.0087 measuring data - 3 repetitions*

Shear Rate [1/s]	Shear Stress [Pa]	Viscosity [cP]	Viscosity [Pa·s]	Shear Stress [Pa]	Viscosity [cP]	Viscosity [Pa·s]	Shear Stress [Pa]	Viscosity [cP]	Viscosity [Pa·s]
1.5	0	0	0	0.1	100	0.1	0	0	0
1.5	0	0	0	0.1	100	0.1	0	14.6	0.0146
1.5	0	0	0	0.1	100	0.1	0.1	100	0.1
1.5	0	0	0	0.1	100	0.1	0.1	100	0.1
1.5	0	0	0	0.1	100	0.1	0.1	100	0.1
3.1	0	0	0	0.2	61.1	0.0611	0.1	33.3	0.0333
3.1	0	0	0	0.1	33.3	0.0333	0.1	33.3	0.0333
3.1	0	0	0	0.1	33.3	0.0333	0.1	33.3	0.0333
3.1	0	0	0	0.1	33.3	0.0333	0.1	33.3	0.0333
3.1	0	0	0	0.1	33.3	0.0333	0.1	33.3	0.0333
5.1	0	0	0	0.2	40	0.04	0.1	20	0.02
5.1	0	0	0	0.2	40	0.04	0.1	20	0.02
5.1	0	0	0	0.2	40	0.04	0.1	20	0.02
5.1	0	0	0	0.1	23.6	0.0236	0.1	20	0.02
5.1	0	0	0	0.1	20	0.02	0.1	20	0.02
10.2	0.1	10	0.01	0.2	20	0.02	0.2	20	0.02
10.2	0.1	10	0.01	0.2	20	0.02	0.2	20	0.02
10.2	0.1	10	0.01	0.2	20	0.02	0.2	20	0.02
10.2	0.1	10	0.01	0.2	20	0.02	0.1	10	0.01
10.2	0.1	10	0.01	0.2	20	0.02	0.1	10	0.01
51.1	0.2	3.9	0.0039	0.4	8.4	0.0084	0.3	6.3	0.0063
51.1	0.1	2	0.002	0.3	5.9	0.0059	0.2	4.1	0.0041
51.1	0.1	2	0.002	0.3	5.9	0.0059	0.2	3.9	0.0039
51.1	0.1	2	0.002	0.3	5.9	0.0059	0.2	3.9	0.0039
51.1	0.1	2	0.002	0.3	5.9	0.0059	0.2	3.9	0.0039
102.0	0.2	2	0.002	0.5	5.1	0.0051	0.4	4	0.004
102.0	0.2	2	0.002	0.5	4.5	0.0045	0.4	3.9	0.0039
102.0	0.2	2	0.002	0.4	3.9	0.0039	0.4	3.9	0.0039
102.0	0.2	2	0.002	0.4	3.9	0.0039	0.4	3.9	0.0039
102.0	0.2	2	0.002	0.4	3.9	0.0039	0.4	3.9	0.0039
153.0	0.4	2.1	0.0021	0.7	3.9	0.0039	0.6	3.5	0.0035
153.0	0.3	1.8	0.0018	0.6	3.5	0.0035	0.5	3	0.003
153.0	0.3	1.8	0.0018	0.6	3.5	0.0035	0.5	2.9	0.0029
153.0	0.3	1.8	0.0018	0.6	3.5	0.0035	0.5	2.9	0.0029
153.0	0.3	1.8	0.0018	0.6	3.5	0.0035	0.5	2.9	0.0029
340.0	0.7	2.1	0.0021	1.1	3.3	0.0033	1.1	3.1	0.0031
340.0	0.7	2.1	0.0021	1	2.9	0.0029	1	2.9	0.0029
340.0	0.7	2.1	0.0021	1	2.9	0.0029	1	2.9	0.0029
340.0	0.7	2.1	0.0021	1	2.9	0.0029	1	2.9	0.0029
340.0	0.7	2.1	0.0021	1	2.8	0.0028	1	2.9	0.0029
511.0	1.1	2.1	0.0021	1.3	2.6	0.0026	1.4	2.7	0.0027
511.0	1	2	0.002	1.3	2.5	0.0025	1.3	2.5	0.0025

Table C. 20 continued

Shear Rate [1/s]	Shear Stress [Pa]	Viscosity [cP]	Viscosity [Pa·s]	Shear Stress [Pa]	Viscosity [cP]	Viscosity [Pa·s]	Shear Stress [Pa]	Viscosity [cP]	Viscosity [Pa·s]
511.0	1	2	0.002	1.3	2.5	0.0025	1.3	2.5	0.0025
511.0	1	2	0.002	1.2	2.4	0.0024	1.3	2.5	0.0025
511.0	1	2	0.002	1.2	2.4	0.0024	1.3	2.5	0.0025
1021.0	2	2	0.002	2.4	2.4	0.0024	2.4	2.4	0.0024
1021.0	2	2	0.002	2.4	2.4	0.0024	2.4	2.4	0.0024
1021.0	2.1	2.1	0.0021	2.4	2.4	0.0024	2.4	2.4	0.0024
1021.0	2.2	2.2	0.0022	2.4	2.4	0.0024	2.4	2.4	0.0024
1021.0	2.2	2.2	0.0022	2.5	2.4	0.0024	2.5	2.4	0.0024

Table C. 21 *Salt water and particles, volume fraction 0.0116 measuring data - 3 repetitions*

Shear Rate [1/s]	Shear Stress [Pa]	Viscosity [cP]	Viscosity [Pa·s]	Shear Stress [Pa]	Viscosity [cP]	Viscosity [Pa·s]	Shear Stress [Pa]	Viscosity [cP]	Viscosity [Pa·s]
1.5	0	0	0	0.1	100	0.1	0.1	100	0.1
1.5	0	0	0	0.1	100	0.1	0.1	100	0.1
1.5	0	0	0	0.1	148.3	0.1483	0.1	116.7	0.1167
1.5	0	0	0	0.2	200	0.2	0.2	200	0.2
1.5	0	0	0	0.2	200	0.2	0.2	200	0.2
3.1	0	0	0	0.2	66.7	0.0667	0.3	100	0.1
3.1	0	0	0	0.2	66.7	0.0667	0.3	100	0.1
3.1	0	0	0	0.2	66.7	0.0667	0.3	100	0.1
3.1	0	0	0	0.2	66.7	0.0667	0.3	100	0.1
3.1	0	0	0	0.2	66.7	0.0667	0.3	100	0.1
5.1	0	0	0	0.3	58	0.058	0.4	80	0.08
5.1	0	0	0	0.2	40	0.04	0.3	60	0.06
5.1	0	0	0	0.2	40	0.04	0.3	60	0.06
5.1	0	0	0	0.2	40	0.04	0.3	60	0.06
5.1	0	0	0	0.2	40	0.04	0.3	60	0.06
10.2	0	0	0	0.3	30	0.03	0.6	60	0.06
10.2	0	0	0	0.3	30	0.03	0.5	52	0.052
10.2	0	0	0	0.3	30	0.03	0.5	50	0.05
10.2	0	0	0	0.3	30	0.03	0.5	50	0.05
10.2	0	0	0	0.3	30	0.03	0.4	41.5	0.0415
51.1	0.2	3.9	0.0039	0.5	9.7	0.0097	1.2	23.6	0.0236
51.1	0.2	3.9	0.0039	0.4	7.8	0.0078	0.9	17.9	0.0179
51.1	0.2	3.9	0.0039	0.4	7.8	0.0078	0.8	15.7	0.0157
51.1	0.2	3.9	0.0039	0.4	7.8	0.0078	0.7	14.6	0.0146
51.1	0.2	3.9	0.0039	0.3	6.4	0.0064	0.7	13.7	0.0137
102.0	0.3	2.9	0.0029	0.7	6.5	0.0065	1.2	11.6	0.0116
102.0	0.3	2.9	0.0029	0.5	4.9	0.0049	1	10	0.01
102.0	0.3	2.9	0.0029	0.5	4.9	0.0049	1	9.8	0.0098

Table C. 21 continued

Shear Rate [1/s]	Shear Stress [Pa]	Viscosity [cP]	Viscosity [Pa·s]	Shear Stress [Pa]	Viscosity [cP]	Viscosity [Pa·s]	Shear Stress [Pa]	Viscosity [cP]	Viscosity [Pa·s]
102.0	0.3	2.9	0.0029	0.4	3.9	0.0039	0.9	8.8	0.0088
102.0	0.3	2.9	0.0029	0.4	3.9	0.0039	0.9	8.8	0.0088
153.0	0.4	2.4	0.0024	0.7	4.3	0.0043	1.3	7.5	0.0075
153.0	0.4	2.4	0.0024	0.7	4.1	0.0041	1.2	7.1	0.0071
153.0	0.4	2.4	0.0024	0.7	4.1	0.0041	1.1	6.5	0.0065
153.0	0.4	2.4	0.0024	0.7	4.1	0.0041	1.1	6.5	0.0065
153.0	0.4	2.4	0.0024	0.7	3.9	0.0039	1.1	6.5	0.0065
340.0	0.7	2.1	0.0021	1.1	3.2	0.0032	1.7	4.9	0.0049
340.0	0.7	2.1	0.0021	1	2.9	0.0029	1.5	4.4	0.0044
340.0	0.7	2.1	0.0021	1	2.9	0.0029	1.4	4.1	0.0041
340.0	0.7	2.1	0.0021	1	2.9	0.0029	1.3	3.8	0.0038
340.0	0.7	2.1	0.0021	1	2.9	0.0029	1.3	3.8	0.0038
511.0	1	2	0.002	1.3	2.5	0.0025	1.8	3.5	0.0035
511.0	1	2	0.002	1.3	2.5	0.0025	1.7	3.3	0.0033
511.0	1	2	0.002	1.3	2.5	0.0025	1.6	3.1	0.0031
511.0	1	2	0.002	1.3	2.5	0.0025	1.5	2.9	0.0029
511.0	1	2	0.002	1.3	2.5	0.0025	1.5	2.9	0.0029
1021.0	2.1	2.1	0.0021	2.4	2.4	0.0024	2.8	2.7	0.0027
1021.0	2.1	2.1	0.0021	2.4	2.4	0.0024	2.8	2.7	0.0027
1021.0	2.1	2.1	0.0021	2.4	2.4	0.0024	2.8	2.7	0.0027
1021.0	2.2	2.2	0.0022	2.5	2.4	0.0024	2.8	2.7	0.0027
1021.0	2.2	2.2	0.0022	2.6	2.5	0.0025	2.9	2.8	0.0028

Table C. 22 *Salt water and particles, volume fraction 0.0144 measuring data - 3 repetitions*

Shear Rate [1/s]	Shear Stress [Pa]	Viscosity [cP]	Viscosity [Pa·s]	Shear Stress [Pa]	Viscosity [cP]	Viscosity [Pa·s]	Shear Stress [Pa]	Viscosity [cP]	Viscosity [Pa·s]
1.5	0	0	0	0	0	0	0	0	0
1.5	0	0	0	0.1	71.7	0.0717	0	7.1	0.0071
1.5	0.1	82.9	0.0829	0.1	100	0.1	0.1	100	0.1
1.5	0.1	100	0.1	0.1	100	0.1	0.1	100	0.1
1.5	0.1	100	0.1	0.1	100	0.1	0.1	100	0.1
3.1	0.2	66.7	0.0667	0.2	66.7	0.0667	0.1	33.3	0.0333
3.1	0.1	33.3	0.0333	0.2	66.7	0.0667	0.2	55.6	0.0556
3.1	0.1	33.3	0.0333	0.2	66.7	0.0667	0.2	66.7	0.0667
3.1	0.1	33.3	0.0333	0.2	66.7	0.0667	0.2	66.7	0.0667
3.1	0.1	33.3	0.0333	0.2	66.7	0.0667	0.2	66.7	0.0667
5.1	0.2	40	0.04	0.2	40	0.04	0.3	60	0.06
5.1	0.2	40	0.04	0.2	40	0.04	0.3	60	0.06
5.1	0.2	40	0.04	0.2	40	0.04	0.3	60	0.06
5.1	0.2	40	0.04	0.2	40	0.04	0.3	60	0.06

Table C. 22 continued

Shear Rate [1/s]	Shear Stress [Pa]	Viscosity [cP]	Viscosity [Pa·s]	Shear Stress [Pa]	Viscosity [cP]	Viscosity [Pa·s]	Shear Stress [Pa]	Viscosity [cP]	Viscosity [Pa·s]
5.1	0.2	40	0.04	0.2	40	0.04	0.3	60	0.06
10.2	0.2	20	0.02	0.5	50	0.05	0.7	70	0.07
10.2	0.2	20	0.02	0.5	50	0.05	0.7	70	0.07
10.2	0.2	20	0.02	0.4	39.2	0.0392	0.6	60	0.06
10.2	0.2	20	0.02	0.3	30	0.03	0.6	60	0.06
10.2	0.2	20	0.02	0.3	30	0.03	0.6	60	0.06
51.1	0.6	12.4	0.0124	1.2	23.1	0.0231	1.6	30.8	0.0308
51.1	0.3	5.9	0.0059	0.8	15.1	0.0151	0.9	18.1	0.0181
51.1	0.3	5.9	0.0059	0.7	13.3	0.0133	0.7	13.7	0.0137
51.1	0.3	5.9	0.0059	0.6	11.8	0.0118	0.7	13.7	0.0137
51.1	0.3	5.9	0.0059	0.6	11.8	0.0118	0.7	13.7	0.0137
102.0	0.6	5.9	0.0059	0.9	8.8	0.0088	1.1	10.7	0.0107
102.0	0.6	5.9	0.0059	0.8	7.6	0.0076	1	9.8	0.0098
102.0	0.5	4.9	0.0049	0.7	6.9	0.0069	1	9.8	0.0098
102.0	0.5	4.9	0.0049	0.7	6.9	0.0069	1	9.8	0.0098
102.0	0.5	4.9	0.0049	0.7	6.9	0.0069	1	9.8	0.0098
153.0	0.7	4.1	0.0041	1	5.9	0.0059	1.4	7.9	0.0079
153.0	0.6	3.8	0.0038	0.9	5.3	0.0053	1.2	7	0.007
153.0	0.6	3.5	0.0035	0.9	5.3	0.0053	1.1	6.5	0.0065
153.0	0.6	3.5	0.0035	0.9	5.3	0.0053	1.1	6.5	0.0065
153.0	0.6	3.5	0.0035	0.9	5.3	0.0053	1.1	6.5	0.0065
340.0	1	2.9	0.0029	1.4	4.2	0.0042	2	6	0.006
340.0	0.9	2.6	0.0026	1.3	3.8	0.0038	1.7	5.1	0.0051
340.0	0.9	2.6	0.0026	1.2	3.5	0.0035	1.7	5	0.005
340.0	0.9	2.6	0.0026	1.2	3.5	0.0035	1.6	4.7	0.0047
340.0	0.9	2.6	0.0026	1.2	3.5	0.0035	1.5	4.4	0.0044
511.0	1.2	2.4	0.0024	1.7	3.3	0.0033	2.1	4.2	0.0042
511.0	1.2	2.4	0.0024	1.6	3.1	0.0031	2	3.9	0.0039
511.0	1.2	2.4	0.0024	1.5	3	0.003	1.9	3.6	0.0036
511.0	1.2	2.4	0.0024	1.5	2.9	0.0029	1.8	3.5	0.0035
511.0	1.2	2.4	0.0024	1.5	2.9	0.0029	1.8	3.5	0.0035
1021.0	2.6	2.5	0.0025	3	2.9	0.0029	3.4	3.3	0.0033
1021.0	2.6	2.5	0.0025	3	2.9	0.0029	3.4	3.3	0.0033
1021.0	2.6	2.6	0.0026	3	2.9	0.0029	3.4	3.3	0.0033
1021.0	2.7	2.6	0.0026	3	2.9	0.0029	3.4	3.3	0.0033
1021.0	2.7	2.6	0.0026	3.1	3	0.003	3.5	3.4	0.0034

Table C. 23 *Salt water and particles, volume fraction 0.0182 measuring data - 3 repetitions*

Shear Rate [1/s]	Shear Stress [Pa]	Viscosity [cP]	Viscosity [Pa·s]	Shear Stress [Pa]	Viscosity [cP]	Viscosity [Pa·s]	Shear Stress [Pa]	Viscosity [cP]	Viscosity [Pa·s]
1.5	0.1	100	0.1	0.3	301.7	0.3017	0.1	100	0.1
1.5	0.1	100	0.1	0.4	400	0.4	0.1	145	0.145
1.5	0.1	100	0.1	0.5	463.3	0.4633	0.2	215.8	0.2158
1.5	0.1	100	0.1	0.5	500	0.5	0.3	332.5	0.3325
1.5	0.1	100	0.1	0.5	500	0.5	0.5	515	0.515
3.1	0.2	66.7	0.0667	0.7	236.4	0.2364	0.8	266.7	0.2667
3.1	0.2	66.7	0.0667	0.7	233.3	0.2333	0.8	266.7	0.2667
3.1	0.2	66.7	0.0667	0.6	214.4	0.2144	0.8	266.7	0.2667
3.1	0.2	66.7	0.0667	0.6	205.6	0.2056	0.8	266.7	0.2667
3.1	0.2	66.7	0.0667	0.6	200	0.2	0.8	266.7	0.2667
5.1	0.2	40	0.04	0.7	140	0.14	1	190.8	0.1908
5.1	0.2	40	0.04	0.7	140	0.14	0.9	180	0.18
5.1	0.2	40	0.04	0.7	140	0.14	0.9	180	0.18
5.1	0.2	40	0.04	0.7	140	0.14	0.9	180	0.18
5.1	0.2	40	0.04	0.7	140	0.14	0.9	180	0.18
10.2	0.2	22	0.022	0.9	88.2	0.0882	1.4	139.9	0.1399
10.2	0.2	20	0.02	0.8	80	0.08	1.3	128	0.128
10.2	0.2	20	0.02	0.8	80	0.08	1.2	120	0.12
10.2	0.2	20	0.02	0.8	80	0.08	1.2	117	0.117
10.2	0.2	20	0.02	0.8	80	0.08	1.1	110	0.11
51.1	0.6	11.7	0.0117	1.7	33.6	0.0336	3.4	66.2	0.0662
51.1	0.5	9.8	0.0098	1.1	22.3	0.0223	2.6	51.4	0.0514
51.1	0.4	7.8	0.0078	1	19.3	0.0193	2.1	42.1	0.0421
51.1	0.4	7.8	0.0078	0.9	17.6	0.0176	1.8	34.7	0.0347
51.1	0.4	7.8	0.0078	0.9	17.6	0.0176	1.5	29.5	0.0295
102.0	0.6	5.9	0.0059	1.2	11.8	0.0118	2.3	22.3	0.0223
102.0	0.5	4.9	0.0049	1.1	10.5	0.0105	1.4	13.9	0.0139
102.0	0.5	4.9	0.0049	1	9.8	0.0098	1.2	11.8	0.0118
102.0	0.5	4.9	0.0049	1	9.8	0.0098	1.2	11.8	0.0118
102.0	0.5	4.9	0.0049	1	9.8	0.0098	1.2	11.8	0.0118
153.0	0.7	4.1	0.0041	1.4	8.2	0.0082	1.9	11.2	0.0112
153.0	0.7	4.1	0.0041	1.3	7.6	0.0076	1.9	11.2	0.0112
153.0	0.7	4.1	0.0041	1.3	7.6	0.0076	1.9	11.2	0.0112
153.0	0.7	4.1	0.0041	1.2	7.1	0.0071	1.9	11.2	0.0112
153.0	0.7	4.1	0.0041	1.2	7.1	0.0071	1.9	11.2	0.0112
340.0	0.9	2.6	0.0026	2.2	6.6	0.0066	3.4	10	0.01
340.0	0.9	2.6	0.0026	1.9	5.6	0.0056	3.2	9.5	0.0095
340.0	0.8	2.4	0.0024	1.8	5.3	0.0053	3.1	9.2	0.0092
340.0	0.8	2.4	0.0024	1.7	4.9	0.0049	3	8.9	0.0089
340.0	0.8	2.4	0.0024	1.6	4.7	0.0047	3	8.8	0.0088
511.0	1	2	0.002	2.2	4.3	0.0043	3.7	7.2	0.0072

Table C. 23 continued

Shear Rate [1/s]	Shear Stress [Pa]	Viscosity [cP]	Viscosity [Pa·s]	Shear Stress [Pa]	Viscosity [cP]	Viscosity [Pa·s]	Shear Stress [Pa]	Viscosity [cP]	Viscosity [Pa·s]
511.0	1	2	0.002	2	4	0.004	3.5	6.8	0.0068
511.0	0.9	1.8	0.0018	1.7	3.4	0.0034	3.3	6.5	0.0065
511.0	0.9	1.8	0.0018	1.6	3.2	0.0032	3.2	6.3	0.0063
511.0	0.9	1.8	0.0018	1.6	3.1	0.0031	3.1	6.1	0.0061
1021.0	1.9	1.9	0.0019	3.1	3.1	0.0031	5.2	5.3	0.0053
1021.0	2	1.9	0.0019	3	2.9	0.0029	4.9	4.8	0.0048
1021.0	2	2	0.002	3	2.9	0.0029	4.6	4.5	0.0045
1021.0	2.1	2.1	0.0021	3.1	3	0.003	4.5	4.4	0.0044
1021.0	2.2	2.2	0.0022	3.1	3	0.003	4.6	4.5	0.0045

Table C. 24 *Salt water and particles, volume fraction 0.0201 measuring data - 3 repetitions*

Shear Rate [1/s]	Shear Stress [Pa]	Viscosity [cP]	Viscosity [Pa·s]	Shear Stress [Pa]	Viscosity [cP]	Viscosity [Pa·s]	Shear Stress [Pa]	Viscosity [cP]	Viscosity [Pa·s]
1.5	0	0	0	0	0	0	0.1	94.6	0.0946
1.5	0	20	0.02	0.1	64.2	0.0642	0.1	100	0.1
1.5	0.1	100	0.1	0.1	100	0.1	0.1	100	0.1
1.5	0.2	193.8	0.1938	0.2	176.7	0.1767	0.2	182.1	0.1821
1.5	0.3	305	0.305	0.3	312.8	0.3128	0.3	278.8	0.2788
3.1	0.6	202.8	0.2028	0.6	207.2	0.2072	0.5	168.9	0.1689
3.1	0.6	200	0.2	0.7	233.3	0.2333	0.6	200	0.2
3.1	0.6	200	0.2	0.7	240.8	0.2408	0.7	233	0.233
3.1	0.6	200	0.2	0.8	266.7	0.2667	0.8	255.8	0.2558
3.1	0.7	232.2	0.2322	0.8	266.7	0.2667	0.8	268.9	0.2689
5.1	0.8	160	0.16	1	200	0.2	1.1	220	0.22
5.1	0.8	160	0.16	1	200	0.2	1.1	220	0.22
5.1	0.8	160	0.16	1	200	0.2	1.1	222.8	0.2228
5.1	0.8	160	0.16	1	200	0.2	1.2	238.4	0.2384
5.1	0.8	160	0.16	1	200	0.2	1.2	240	0.24
10.2	1.1	111.5	0.1115	1.6	163.5	0.1635	1.9	190	0.19
10.2	1	103.8	0.1038	1.5	154.5	0.1545	1.8	180	0.18
10.2	1	100	0.1	1.5	150	0.15	1.8	177	0.177
10.2	1	98	0.098	1.4	140	0.14	1.7	170	0.17
10.2	0.9	90	0.09	1.4	140	0.14	1.7	167.8	0.1678
51.1	2.5	49.3	0.0493	4.2	81.5	0.0815	5.1	100.9	0.1009
51.1	1.9	37.1	0.0371	3.1	60.5	0.0605	4.1	79.5	0.0795
51.1	1.7	32.4	0.0324	2.6	50.2	0.0502	3.5	67.9	0.0679
51.1	1.5	29.4	0.0294	2.3	45.4	0.0454	3	58.5	0.0585
51.1	1.4	28.3	0.0283	2.1	40.9	0.0409	2.8	54.5	0.0545
102.0	2.3	22.3	0.0223	3.3	32.4	0.0324	4.3	42.4	0.0424

Table C. 24 continued

Shear Rate [1/s]	Shear Stress [Pa]	Viscosity [cP]	Viscosity [Pa·s]	Shear Stress [Pa]	Viscosity [cP]	Viscosity [Pa·s]	Shear Stress [Pa]	Viscosity [cP]	Viscosity [Pa·s]
102.0	2	20	0.02	2.5	24.8	0.0248	3.9	38.2	0.0382
102.0	1.9	18.6	0.0186	1.6	16.1	0.0161	3.5	34.2	0.0342
102.0	1.8	17.6	0.0176	1.4	14	0.014	2.9	28.6	0.0286
102.0	1.8	17.6	0.0176	1.4	13.7	0.0137	2.5	24.5	0.0245
153.0	2.5	14.6	0.0146	2.1	12.4	0.0124	2.6	15.3	0.0153
153.0	2.3	13.5	0.0135	2.1	12.4	0.0124	2.1	12.1	0.0121
153.0	2.2	12.9	0.0129	2.2	12.9	0.0129	1.9	11.2	0.0112
153.0	2.1	12.4	0.0124	2.2	12.9	0.0129	1.9	11.2	0.0112
153.0	2	11.8	0.0118	2.2	12.9	0.0129	2	11.8	0.0118
340.0	3.5	10.3	0.0103	4.1	12	0.012	3.9	11.5	0.0115
340.0	2.3	6.8	0.0068	3.9	11.5	0.0115	3.9	11.5	0.0115
340.0	2	5.8	0.0058	3.8	11.2	0.0112	3.8	11.2	0.0112
340.0	1.9	5.6	0.0056	3.7	10.8	0.0108	3.8	11.2	0.0112
340.0	1.9	5.6	0.0056	3.6	10.6	0.0106	3.8	11.2	0.0112
511.0	2.7	5.3	0.0053	4.6	9	0.009	5	9.8	0.0098
511.0	2.6	5.1	0.0051	4.4	8.6	0.0086	4.8	9.4	0.0094
511.0	2.5	4.9	0.0049	4.3	8.4	0.0084	4.7	9.2	0.0092
511.0	2.4	4.7	0.0047	4.1	8	0.008	4.6	9	0.009
511.0	2.3	4.5	0.0045	4	7.8	0.0078	4.5	8.8	0.0088
1021.0	4.1	4	0.004	6.2	6.3	0.0063	7.7	7.6	0.0076
1021.0	3.8	3.8	0.0038	4.5	4.4	0.0044	5.4	5.2	0.0052
1021.0	3.7	3.6	0.0036	4.5	4.4	0.0044	5.4	5.3	0.0053
1021.0	3.7	3.6	0.0036	4.6	4.5	0.0045	5.6	5.5	0.0055
1021.0	3.7	3.6	0.0036	4.6	4.5	0.0045	5.7	5.6	0.0056

Appendix D – Matlab Script

```
ndata = xlsread ('file destination.xls')

A = ndata(:,1);
A = size(A)
A = a(1,1)
B = ndata(:,3);
B = size(B)
B = b(1,1)

j0=1;
for i=1:5:a
    j=j0;
    A_m = A(i:(i+4),1);
    A_mean(i,1) = mean(A_m);
    B_m = B(i:(i+4),1);
    B_mean(i,1) = mean(B_m);

j0=j+1;
    A_mean_c(j,1) = A_mean(i,1);
    B_mean_c(j,1) = B_mean(i,1);

end
A_mean_c
B_mean_c

a = axes('…');
plot(A_mean_c,B_mean_c,'ob')
grid on
h = legend('…');
set(h,'Interpreter','none');
xlabel('…');
ylabel('…');
title('…');
```